

THE WAKES OF CYLINDRICAL BLUFF BODIES AT LOW REYNOLDS NUMBER

BY J. H. GERRARD

Department of the Mechanics of Fluids, University of Manchester, Manchester M13 9PL, U.K.

(Communicated by Sir James Lighthill, F.R.S. – Received 15 March 1977)

[Plates 1–14]

CONTENTS

	PAGE
1. INTRODUCTION	352
(a) Definitions	353
2. APPARATUS AND METHOD	353
3. AN OVERALL VIEW OF THE REYNOLDS NUMBER RANGE	356
4. Re_{osc} AND THE WAKE AT $Re < Re_{osc}$	361
5. $Re_{osc} < Re < Re_{vs}$	364
6. CIRCULAR CYLINDER WAKES IN THE Re RANGE FROM Re_{vs} TO ABOUT 140	366
7. THE WAKES OF CIRCULAR CYLINDERS IN THE RANGE $140 < Re < 500$	370
8. TRANSITION WAVES, CIRCULAR CYLINDER AT $Re > 350$	374
9. FLOW PAST BLUFF BODIES OTHER THAN CIRCULAR CYLINDERS	376
(a) Variation of frequency with Re for cylinders of various cross sectional shapes	376
(b) The effect of splitter plates on the flow past a circular cylinder	377
10. CONCLUSIONS	379
REFERENCES	381

The wakes of bluff bodies have been investigated by means of flow visualization, with dye washed from the rear of the cylinders, at Reynolds numbers less than 2000. Observations were made in a towing tank which, for most of the measurements, had been treated to produce minimal background motions. The majority of the work concerns the flow past circular cylinders, but some measurements have been made on cylinders of square and diamond section as well as on a flat plate towed broadside on. The effect of splitter plates in the wakes of circular cylinders has also been investigated.

The principal investigations have been concerned with the separation bubble behind bodies at very low Reynolds number; the Reynolds number (Re_{osc}) above which oscillations are always found; the wake frequency; the mode of formation and the motion of the wake vortices; the transition to turbulence and with details of the flow in certain ranges of Reynolds number.

The range is divided into the following régimes:

$Re < Re_{osc}$	Steady flow; standing eddies.
$Re_{osc} < Re < Re_{vs}$	Wavy wake, no accumulation of dye into vortices.

$Re_{vs} < Re < 100$	Vortex street wake; remnants of the standing eddies still present; diffusion of vorticity important.
$100 < Re < 140$	Increased efficiency of convective mass transfer behind the body; an accelerating phase of vortex motion present up to $Re = 500$.
$140 < Re < 500$	Fingers of dye moving back towards the body from the wake; vortex strength irregular; more nearly two-dimensional flow; transition to turbulent vortex cores downstream.
$250 < Re < 400$	Transition to high Re type of vortex shedding.
$350 < Re < 2000 +$	Transition waves in the separated layers and transition to turbulence in the vortex cores on formation.

1. INTRODUCTION

Experiments on the near wake of a cylinder will be described in an attempt to present a coherent picture of the events encountered as the Reynolds number increases from small values up to values of a few thousand. Much work on this subject has already been done, but there are gaps in our description of these flows as well as more fundamental deficiencies in our understanding of them. The subject has been reviewed several times and most recently by Berger & Wille (1972) whose paper covers much of the ground that will be discussed again here. The present work may be regarded as built upon this latest review. I remember with gratitude many helpful discussions with the late Rudolph Wille who contributed so much to this subject.

The investigation has concentrated on circular cylinders, but the wakes of bluff cylinders of different cross sectional shapes have also been observed. Bluff cylinders in general are considered in §§4 and 5, together with the effect of splitter plates on circular cylinders in §9. The experiments concern, almost exclusively, flow visualization of the wakes by means of dye washed from the bodies. The patterns of dye observed are, therefore, filament line representations of the flow leaving the separation lines on the body. It must be stressed that the dye does not make visible the vorticity bearing fluid because at low Reynolds number, vorticity diffuses considerably more rapidly than does dye. The ratio of the molecular diffusivity of momentum to that of mass of dye is of the order of 100.

In the range of Reynolds number considered the flow past a circular cylinder exhibits a series of régimes of flow. These régimes are not in the main separated by abrupt transitions but merge gradually into one another. In the transition regions the flow makes erratic changes between one régime of flow and the other. In these situations the frequency of wake oscillation is not well defined. Even at Reynolds numbers away from a transition, the cycles of oscillation are never of constant duration nor are the main dimensions of the wake constant. Morkovin (1964) aptly described the bluff body wake flow as 'a kaleidoscope of challenging fluid phenomena'. An intriguing mixture of facts present themselves which are further complicated by the appearance of transition to turbulence at low Reynolds number which adds to the inconstancy of the appearance and of the frequency in the wake. The flow is sensitive to disturbances and in particular to conditions at the ends of the cylinder. The results of bluff body experiments are never free from the effects of the environment and the conclusions we draw must be related to the particular experimental arrangement. The ratio of the length to

the transverse dimension of the cylinders used in the present work is not very large, ranging from 14 to 55. The effect of finite cylinder length is taken into account in the following discussions.

The present work is different from previous investigations in several respects: (a) the background disturbances are reduced to a minimum, (b) flow visualization is exclusively used and (c) a wide range of Reynolds number is covered. The idea behind this approach was to link up with previous work at Reynolds numbers greater than 1000. A review of the subject revealed more gaps in our knowledge at low Reynolds number. Two basic mechanisms which occur in the low Reynolds number range are transition to turbulence in the wake and, as Reynolds number increases, the diminution of the effect of diffusion of vorticity which dominates the flow at very low Reynolds number. The mode of vortex formation at low Reynolds numbers has not been investigated before. Though much work still remains to be done some progress is reported here. The wide view over a broad Reynolds number range has been an advantage in this respect. The work involves a reconsideration of previous work by Roshko (1954*a*), Tritton (1959, 1971), Berger (1964*a, b*) and Gaster (1969, 1971). A review of the main conclusions and the division of the flow into Reynolds number regions is given in the concluding §10 and a brief outline in the abstract. In the sections which follow the subject is divided into Reynolds number ranges.

(a) Definitions

The principal parameter of incompressible viscous flow is the Reynolds number. There seems to be no alternative to repeating the words 'Reynolds number' every few sentences: it will, therefore, be abbreviated to *Re*. $Re = Ud/\nu$ where *U* is the speed at which the cylinder is towed in the stationary water, *d* is the maximum transverse dimension and ν is the kinematic viscosity of the water. It is useful to employ the symbol *Re* with subscripts: thus, Re_{osc} is used to signify the *Re* above which oscillations in the wake are always observed. Re_{vs} signifies the *Re* above which a vortex street is observed with the present method of flow visualization.

It is found that Nd^2/ν , where *N* is the wake frequency, is an indispensable parameter. This combination of variables, which is equal to *Re* times Strouhal number, does not have a name. Kohan & Schwarz (1973) call it the Roshko number, recognizing the fact that it was Roshko who introduced it to the subject of bluff body wakes. The parameter is, however, of much wider significance and use. I should like to call it the Stokes number, *St*. The number is of physical significance in oscillating flows at low *Re* and is a measure of the importance of the diffusion of vorticity. \sqrt{St} is proportional to the ratio of the characteristic length, *d*, to the distance vorticity diffuses in one period of the oscillation. The quantity is generally called α in oscillating pipe flow but in that subject also has not been given a name. (There is a possible confusion with the Stokes number used in two-phase flow to denote the ratio of relaxation time of a solid particle to the time taken by a neighbouring fluid particle to make an excursion from a steady state of motion.)


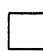


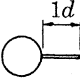
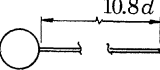
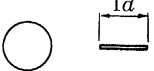
2. APPARATUS AND METHOD

Experiments have been made by using flow visualization in a towing tank. The tank which is 4 m long \times 750 mm wide \times 460 mm deep and was usually filled with water to a depth of 360 mm has been described elsewhere by Anagnostopoulos & Gerrard (1976). A weightily

constructed carriage was towed on rails along the top of the tank support frame at speeds continuously variable between 1.2 and 110 mm/s. Cylindrical models were attached to the carriage with their axes vertical. Visual and photographic observation was possible from above, through the end walls and through the side walls at a central section 1 m in length.

It was initially discovered that there were motions in the tank due to thermal convection. Most of the results presented here were obtained after treatment of the tank to considerably reduce these motions as described in the paper cited above. The tank was housed in a temperature controlled room and was insulated at the sides and bottom. The water surface was covered with oil to prevent evaporation. In order to subdue the remaining convection currents, the water was made thermally stratified by heating (of amount 38 W) by means of 10 wires stretched along the length of the tank at about 10 mm below the water surface. With these modifications the temperature difference between the bottom of the water and a level some 20 mm below the heating wires was about 1 °C. Finally the background velocities were negligible over the central 200 mm of the depth. In surface layers at the top and bottom, each of about 80 mm thickness the maximum velocities were about 0.02 mm/s.

TABLE 1

model shape	transverse dimension, d /mm
	25.4, 12.65, 10.3, 6.3, 4.7
	6.325
	8.763
	12.50
	10.0
	10.0
	12.65

Model submerged lengths 350 mm

All measurements have been taken from flow visualization by using I.C.I. Edicol food dye. A very strong aqueous solution of the dye was painted onto the cylinders and allowed to dry. The cylinders were immersed, with as little disturbance as possible, just before a run. The dye eroded into the wake as the cylinder moved. The dye forward of the separation points soon washed off but that initially to the rear of the separation points lasted for the whole traverse of the tank at the speeds used in these experiments and with the current model sizes. In some experiments a cloud of dyed water was injected into the wake just behind the cylinder while it was in motion.

Photographs were taken with a camera mounted on a tripod at the side of the tank by looking through the transparent section towards a white sheet attached to the opposite wall inside the tank. This sheet was ruled with vertical lines at 100 mm spacing and horizontal rows of dots at the same spacing: these as well as transparent scales on the outside of the tank can be seen in some of the photographs presented. On other occasions the camera was mounted on the carriage looking vertically downwards. Calibration photographs of scales in the wake position were taken. Measurements were made by projecting the images of the negatives onto a screen. When measuring the speeds of the vortices or waves in the wake, exposures were made at known time intervals.

Each model was mounted on the slide of the vertical optical bench attached to the carriage so that it could be immersed with the minimum of disturbance. Table 1 shows the cylinder cross sectional shapes and sizes used in the main experiments. The size of the cross section is designated by d which is the maximum transverse dimension of the body.

The same model was used for the square and diamond section cylinders which were rotated through 45° about their axes to produce the other configuration. The corner radius of the square was 0.09 mm. The flat plate thickness was 3.175 mm, the sides were angled at 45° and a flat of 0.38 mm was machined at the edges so presenting a square corner to the flow. The splitter plates on the last three models were 1.0 mm thick.

Generally the cylinders were clamped above the water line and passed through the surface. In order to view the region close behind the cylinder from above, an alternative mounting by means of a cranked rod was sometimes used so that the top of the cylinder lay just below the surface which was therefore not disturbed.

The choice of the size of the model is important. Obviously the length must be much larger than the transverse dimension if end effects are not to dominate the appearance of the wake. When the transverse dimension is small (some models with $d = 2$ mm were used), the dye on the cylinder produces a departure from the cylindrical shape with attendant three-dimensionalities in the wake. A compromise must be made between reducing end effects and obtaining an effectively smooth cylinder. The smoothness of the cylinder is also related to the scale of disturbances in the relative motion of the body and the water. Various devices aimed at reducing end effects were tried without any noticeable change in the appearance of the wake. It was invariably found, for example, that the critical Reynolds number, Re_{osc} , for the start of wake oscillations was lower at the bottom end of a cylinder than it was higher up the body. Reference to the work of Coutanceau & Bouard (1977) suggests that in the present experiments, the ratio of diameter to width of tank is small enough for the wall not to affect the near wake.

The determination of the size of the model enters in another way. At low Reynolds numbers the distance moved by the cylinder before steady oscillations are observed, increases as the Reynolds number decreases towards Re_{osc} . Measurements made with a circular cylinder of 25 mm diameter revealed that the 4 m length of the tank was insufficient at low Reynolds numbers for the study of the steady wake. Honji & Taneda (1969) have published values of what amounts to the distance travelled after the impulsive start of a circular cylinder before the steady wake bubble breaks down. The present measurements at Reynolds number less than 80 lie at distances which sometimes agree with Honji & Taneda's values but at other times the length of run before shedding becomes visible is very much longer. The indication of the present work is that shedding is almost instantaneous at Reynolds numbers above 100, that is, as soon as the dye gets into the wake it rolls up into a vortex. Results will thus depend on the

time required for dye to get into the wake which will be a function of velocity and cylinder diameter rather than the Reynolds number. This effect is not sufficient to account for the scatter of the starting lengths at lower Reynolds numbers. A private communication by Dr Honji reveals that at the higher Reynolds numbers the cylinder in their experiments was subject to large blockage effects which increased the distance travelled before shedding started.

These results are additional to those discussed in §7 where it is shown that in a particular Re range appreciable time is required for end conditions to affect the wake all along the cylinder. This suggests that the significant size ratio is that of the length of the body to the wake wavelength (or vortex spacing) which is some five times larger than the cylinder transverse dimension. In the present experiments the length to transverse dimension ratio was not large and varied for 14 to 55. The observations at high Re were for length/diameter = 14 only.

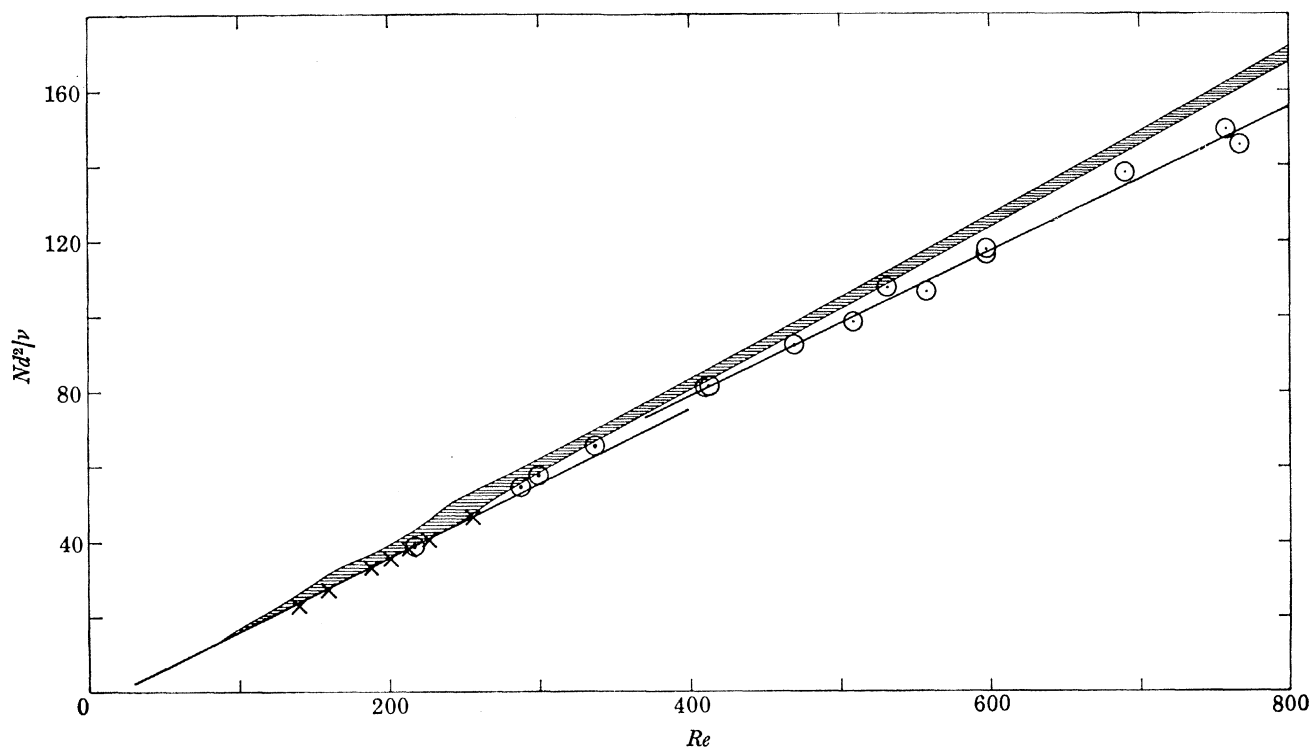


FIGURE 1. Stokes number as a function of Re for a circular cylinder, a comparison with the measurements of Roshko (1954*a*). \parallel Roshko; present measurements \circ $d = 25.4$ mm; \times $d = 12.65$ mm.

3. AN OVERALL VIEW OF THE REYNOLDS NUMBER RANGE

In a later section we shall briefly discuss the wakes of bluff bodies at Re low enough for the wake flow to be steady, but the main characteristic of bluff-body wakes is their oscillation. In this section we consider oscillating wakes of circular cylinders. The wake frequency is the easiest quantity to measure, yet its value at low Re has been in question in recent years. Different observers report different values of the Stokes number at the same Re . Berger (1964*b*) showed that the frequency is sensitive to disturbances in the free stream and that oscillation of the cylinder predisposes the wake to take on the frequency of the disturbance-free mode of

oscillation. Gaster (1971) has shown that the frequency- Re relation is sensitive to three-dimensional effects in general and to end conditions in particular. It has become generally recognized that disturbances affect the Stokes number- Re relation as evidenced by the work of Kohan & Schwarz (1973) and Hussain & Ramjee (1976). Until recently the frequency measurements of Roshko (1954*a, b*) were regarded as definitive. Careful scrutiny of the frequency variation at those Re below 150 where the oscillations seemed to be reasonably constant and well defined has revealed a range of values and some controversy as explained by Tritton (1971) and Berger & Wille (1972). These other values of Tritton and Berger lie below the mean curve through Roshko's data. We, therefore, begin by presenting figure 1 which compares some of the present measurements with the envelope of the measurements of Roshko (1954*a*) and notice that the present results coincide with the lower boundary of Roshko's observations. The results shown in figure 1 were obtained by observing dye washed from the rear of the cylinder and counting cycles of near-wake oscillation in a time interval determined by a stop watch. This method is accurate to better than 1%. It is noteworthy that in the range $150 < Re < 300$ our observations do not exhibit the scatter detected by Roshko. Bloor (1964) has already shown that this range is disturbance sensitive. The points in figure 1 are scattered at Re greater than 500 due to an ill-defined process of vortex shedding as we shall see below (§8). In view of the evidence concerning the effect of disturbances, it is reasonable to suggest that the scatter of Roshko's results is due to free stream turbulence. His quoted turbulence level (0.03%) lies below the value (0.05%) which Berger (1964*b*) regards as critical, but the scale of the turbulence could be expected to be of significance.

Further comment on the frequency variation over the Re range must be in anticipation of what follows. We shall see that there are several different flow régimes in the Re range covered in figure 1. We have chosen to draw two straight lines on figure 1 because the departures from these two variations are small. Between the two lines is a major transition which occupies the range $250 < Re < 380$ in which the mode of vortex shedding changes. Above $Re = 380$ the shedding is changing towards that described by Gerrard (1966*a, b*) in which the balance of mass transfer to the interior of the formation region is maintained by the velocity field of the growing vortex. Below $Re = 250$ the vortex just shed is also involved in this mass balance and in the determination of the strength of the shed vortices. A fuller discussion follows in §6.

More detailed graphs of part of the Re range are shown in figures 2 and 3. Figure 3 is included following Tritton (1971), for ease of comparison of different results. The points on figure 2 were determined by direct counting of vortex shedding and also from the results of determining wavelength and vortex speed from photographs taken at known time intervals. The results generally refer to an average frequency over some 5 to 10 periods of oscillation. The scatter of the points is due to inconstancy of the frequency rather than inaccuracy of measurement. Even in figure 13, which shows a view of the wake in its most regular form, the wavelength generally fluctuates 4 to 5% and in places up to 10%. Though it is possible to obtain a smaller scatter by averaging over many periods (in a wind tunnel experiment, for example) there is, as Tritton's (1959) work shows, a danger of smoothing out the effects of the real existence of a dual frequency relation. Examination of figure 2 soon shows that the determination of the best fitting polynomial depends on the range of Re chosen. Kohan & Schwarz (1973), for example, fit two straight lines to their data by a choice which emphasizes a discontinuity at $Re \approx 80$ whereas a single straight line up to $Re \approx 100$ fits very well. Whether the discontinuity in the region of $Re = 80$ exists at all is not clear from their results as presented in the paper cited. It seems

clear that the division of the Re range into separate regions must be made in the light of additional information. At much higher Re the effect of turbulence on the frequency is slight even when it has a profound effect on other parameters of the flow (Gerrard 1965). As we shall see later, there is a major transition in flow pattern in the range $55 < Re < 70$ which is not reflected in any change in the frequency relation.

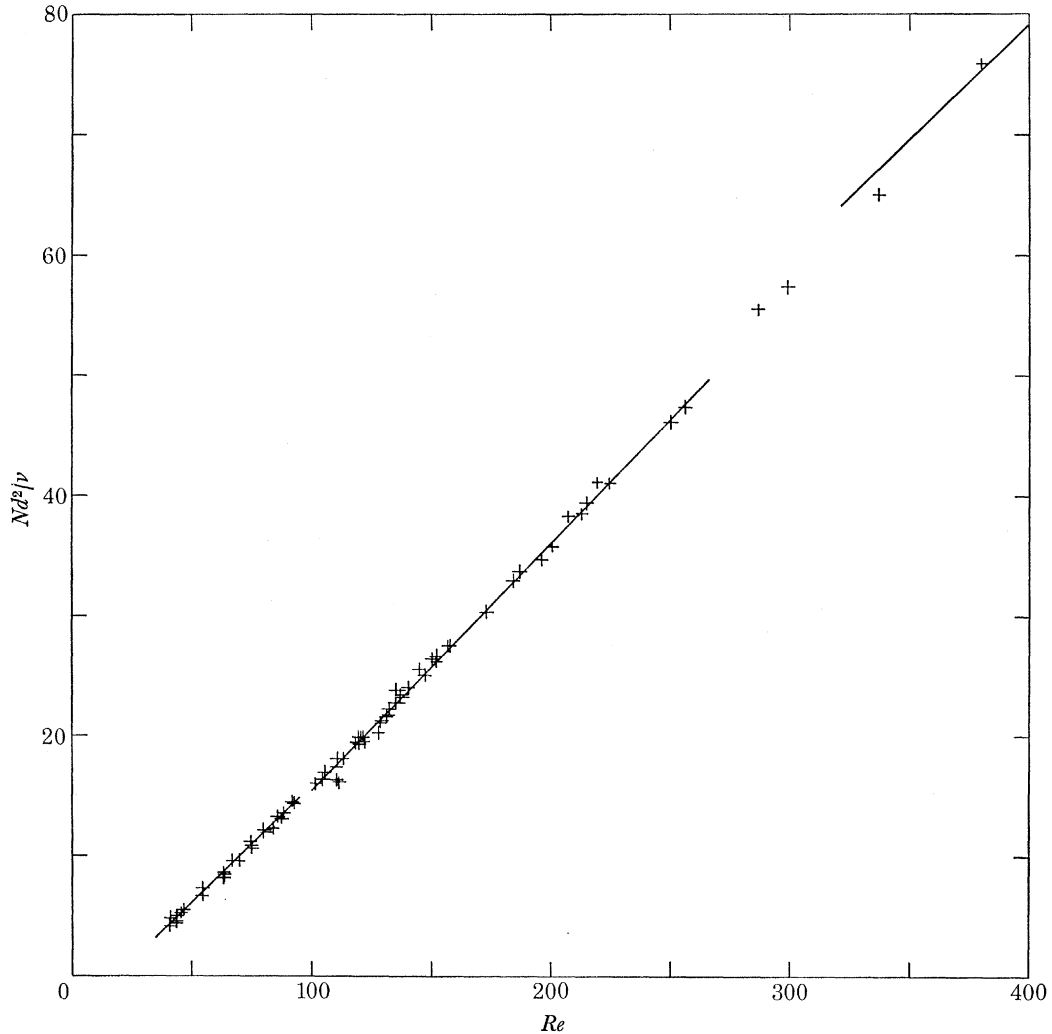


FIGURE 2. Stokes number as a function of Re for a circular cylinder showing all the experimental observations except in the region $100 < Re < 150$ in which only points obtained late in the cylinder run are included. Curves indicated in table 2.

The results of curve fitting are listed in table 2. Also shown there are the symbols used in figure 3 and the number of points used in the determination of the equations. The r.m.s. deviation of the points from the curves are also quoted. A second degree equation can be fitted to all the points up to $Re = 380$. This curve is not shown in figure 3 because it is not believed to have physical significance. The Re range has been divided at $Re = 100$, 256 and 380. The transition in the range 256 to 380 has already been referred to. In the region of $Re = 100$ there is a peculiarity in the relationship between Stokes number and Re which has been discussed at length by Tritton (1959, 1971), Berger (1964*a, b*), Gaster (1969, 1971) and Berger & Wille

(1972). In the present experiments the existence of two modes at the same Re was originally found in the range $100 < Re < 150$. These findings are depicted by the dashed double curves in figure 3. It was later discovered that the higher curve was only obtained at the beginning of the motion of the cylinder through the water. These ‘transient’ points are omitted from figure 2 in which the ‘best’ curves for Re below and above 100 are straight lines which intersect at $Re = 130$. The discontinuity at $Re = 100$ is a product of the curve fitting. The points lie just as close (i.e. within the r.m.s. deviation) to the other curves which have no discontinuity.

TABLE 2. THE RESULTS OF FITTING POLYNOMIALS TO THE FREQUENCY VARIATIONS WITH REYNOLDS NUMBER FOR CIRCULAR CYLINDER WAKES

symbols on figures			expression for $St = Nd^2/\nu$	r.m.s. deviation	Re	no. of points	reference
1	2	3					
—			$0.2013 Re - 4.167$	0.314	41-93	34	
			$2.584 \times 10^{-5} Re^2 + 0.1942 Re - 3.822$	0.303	152-256		
—	—	—	$0.1913 Re + 2.791$	2.09	380-767	12	
			$6.148 \times 10^{-5} Re^2 + 0.185 Re - 3.424$	0.407	41-380	71	
—	—	—	$0.1959 Re - 3.811$	0.269	41-93	25	
—	—	—	$0.2064 Re - 5.173$	0.450	101-256	42	
	---		$2.586 \times 10^{-4} Re^2 + 0.1619 Re - 2.784$	0.235	41-137	30	
	—		$0.212 Re - 4.5$		50-150		Roshko (1954a)
	—		$0.212 Re - 2.7$		300-2000		Roshko (1954a)
	---		$4.1 \times 10^{-4} Re^2 + 0.144 Re - 2.1$		50-105		Tritton (1959). Low speed mode
-----			$0.224 Re - 6.70$		80-150		Tritton (1959)
					115-155		Berger (1964a, b). High speed mode
-----			$1.625 \times 10^{-4} Re^2 + 0.164 Re - 2.55$		50-170		Berger (1964a, b). Low speed mode
-----			$0.220 Re - 7.4$		130-160		Berger (1964a, b). Basic mode

The conclusion from observation of flow visualization, which will be described, is that there are changes in the mode of vortex formation at $Re = 100$. This suggests that the discontinuity could be real. The present values of frequency lie closest to those of Berger (1964) in which there was a smooth transition from his low speed mode to his basic mode. It is worth pointing out that where Berger found a jump from low to high speed mode (at higher turbulence levels of the free stream) the jump was to higher Stokes numbers. Tritton’s discontinuity from low to high speed mode was a transition to lower Stokes numbers. At Re greater than 150 the frequency is more stable. Further discussion of these ranges is postponed to later sections.

Before discussing the Re ranges in detail we present data for the whole range for another important property. The ‘length of the formation region’ is shown in figure 4. A curve is included which shows the position of the end of the ‘bubble’ enclosing the two standing vortices (Taneda 1956). Also shown is the median value of the formation region length as defined by Bloor (1964). In view of the difference in the mode of vortex shedding at low and high Re it needs to be stressed that ‘formation region’ is a term which was coined in conjunction with the high Re mode of shedding. Bloor showed that the formation region length could be defined in three alternative and mutually compatible ways. The points plotted in figure 4 are based on an adaptation of the definition that the end of the formation region is the point

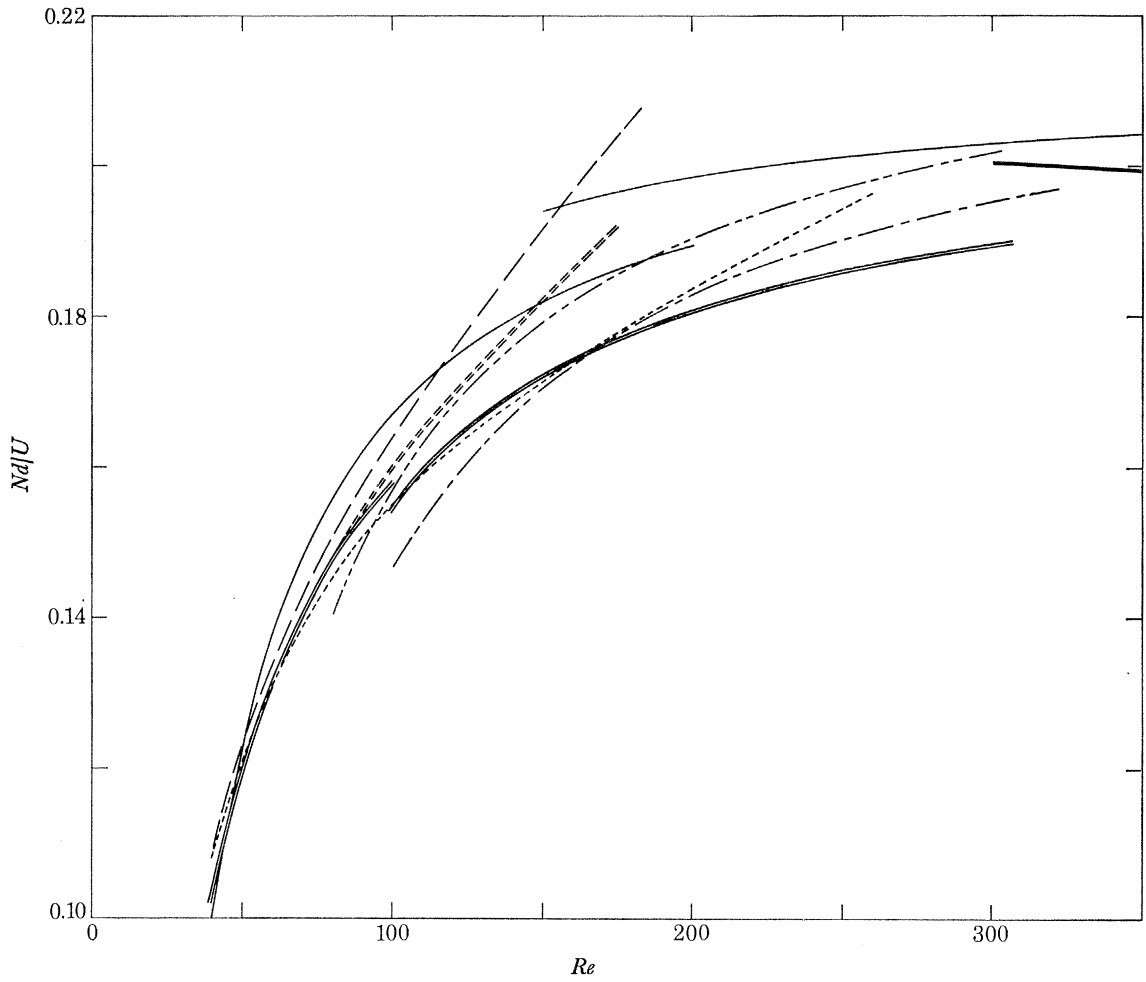


FIGURE 3. Comparison of results of frequency measurement. Strouhal number as a function of Re .
Key to symbols in table 2.

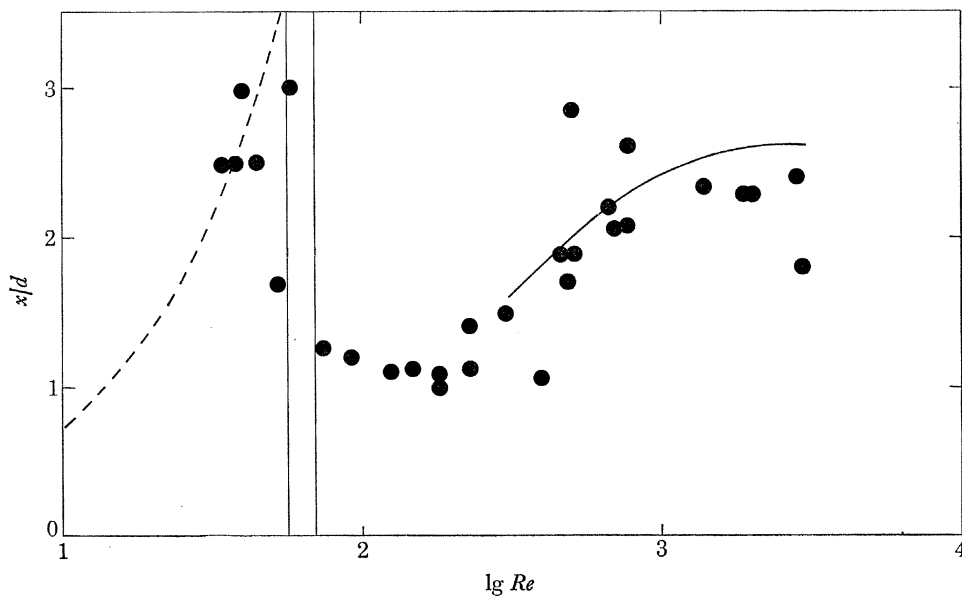


FIGURE 4. Length of the formation region as a function of Re : Bloor (1964) —; Taneda (1965) ----. Points from present observations, ●, show the positions from which the vortices roll up.

closest to the cylinder at which irrotational fluid crosses the wake centre line. At low Re the fluid entering the region at the rear of the body is not irrotational and approaches from the downstream direction rather than from the side as at high Re . The detail of the low Re flow will be discussed below in connection with figure 20. The closest approach to the rear of the body of the tongues of undyed fluid in their first thrust towards the body is the basis on which figure 4 was compiled. The undyed fluid approaches closer to the body in subsequent half cycles. This method of defining formation region length does not possess high accuracy but shows a general trend and agrees with the measurements of Bloor. The most striking feature of figure 4 is the discontinuity in the range $55 < Re < 70$ which is indicated on the figure. This range separates a wake with a waving oscillation at low Re from a wake which develops into a vortex street at higher Re . Within the range the wake of a circular cylinder may be observed in either configuration. For the circular cylinder the $Re = Re_{vs}$ of this transition is not well defined. It is noteworthy that the change in the wake appearance is not reflected in the variation of Stokes number with Re . A more precise determination of formation region length by Griffin & Votaw (1972), in terms of the position of maximum velocity fluctuation as a function of downstream distance, gives 3.2 diameters for the x value of the end of the vortex formation at $Re = 144$. This implies a region of rapid decrease in x/d at some higher Re . The variation of x/d depicted in figure 4 had the same shape as the variation of the base pressure coefficient with Re which is shown in figure 24.

4. Re_{osc} AND THE WAKE AT $Re < Re_{osc}$

The wake of a circular cylinder at very low Re has already been thoroughly investigated experimentally, principally by Taneda (1963) and more recently by Coutanceau & Bouard (1977) who review the published experimental and numerical work. In this section we will present experimental and computed results for cylinders of various cross sectional shapes and conclude by suggesting some ideas about the Reynolds number, Re_{osc} , above which oscillations are always present in the wake.

It has been shown by Taneda (1963) that close behind a cylinder, the wake can be made to oscillate by oscillating the cylinder even at Reynolds numbers as low as unity. In view of the sensitivity to disturbances any determination of the Reynolds number for what might be called the spontaneous onset of oscillations is likely to be inaccurate and a function of the particular experimental arrangement. This Re_{osc} for the beginning of oscillations needs to be defined. There are alternative statements of the definition even when attention is restricted to flow visualization methods. Dye shed from the body ahead of the separation points finds itself concentrated along the wake centre line at low Reynolds numbers. At $Re = Re_{osc}$ this dye line is seen to be wavy. Taneda (1955) suggests that 'gathers', which progress down the boundary of the separation bubble behind the body, are observed at $Re = Re_{osc}$. When dye is applied to the body only behind the separation points, this will not be found in the wake outside the separation bubble at $Re < Re_{osc}$. The small amount which escapes by diffusion may be neglected. When oscillation begins dye is shed into the wake from the separation bubble.

In the present experiments all these methods have been used and seem to give the same value for Re_{osc} . Coutanceau & Bouard (1977) determine Re_{osc} as that Re at which asymmetry of the standing vortices is first apparent. They obtain $Re_{osc} = 34$ for a circular cylinder which is of vanishingly small diameter compared with the tank width. We found no systematic variation of Re_{osc} with cylinder diameter in the range $4.7 \text{ mm} < d < 25.4 \text{ mm}$.

The results for different bodies are shown in figure 5 which principally shows the variation of the length of the separation bubble as a function of Re . It is seen that, to a good approximation, Re_{osc} is equal to that Re at which the length of the bubble is two body widths. Figure 6, plate 1, shows the typical appearance of the wake bubble at Re just greater than Re_{osc} . The gathers which Taneda describes are only just visible. Figure 7, plate 1, shows the gathers more clearly.

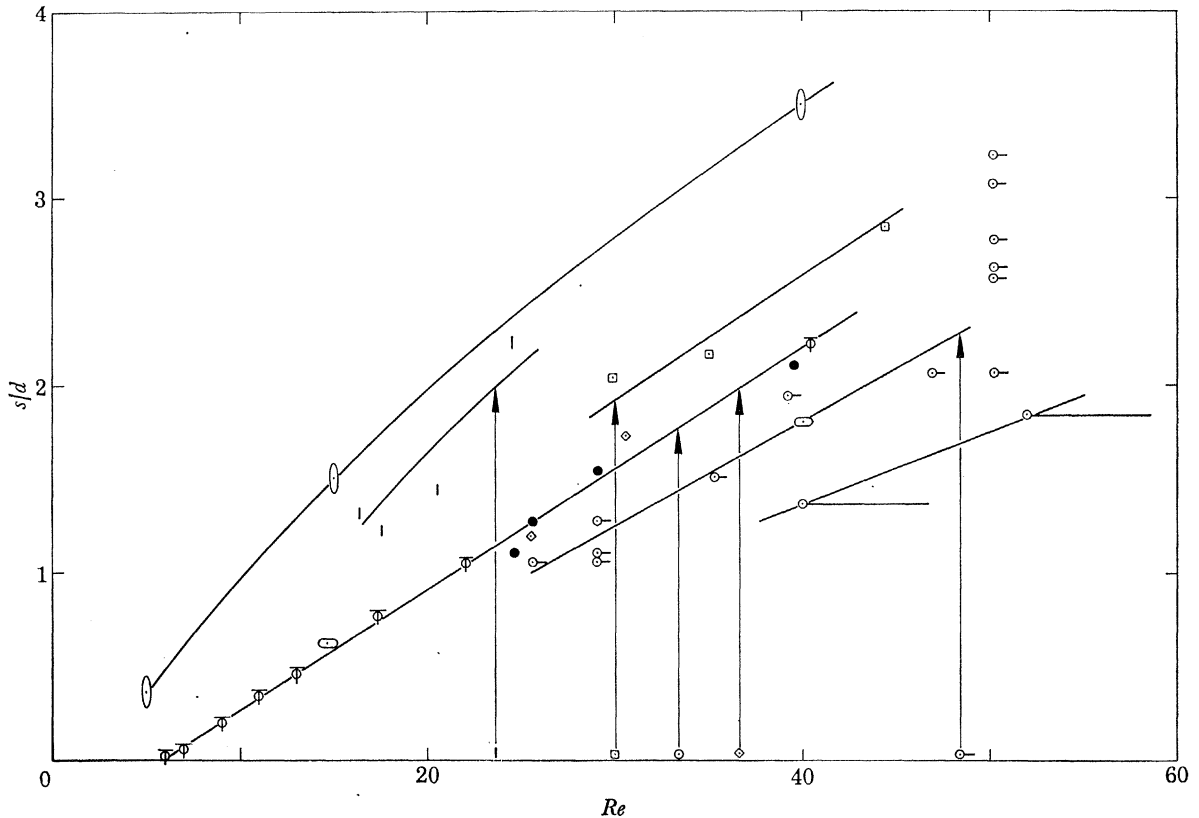


FIGURE 5. Variation with Re of the length of the separation bubble containing the standing eddies. This length is defined as the distance from the rear of the body to the end of the bubble. d is the maximum transverse dimension of the body cross section. $\uparrow Re_{osc}$ for the section indicated. Φ Experimental values for circular cylinder, Taneda (1955). \circ 5:1 Ellipse broadside on, calculations of Masliyah & Epstein (1971). \odot 2:1 Ellipse edge-on, calculations of Masliyah & Epstein (1971).

The gather is Z shaped: the downstream spike elongates downstream, the one pointing into the bubble behind the body likewise elongates, travels towards the body and executes a circulating motion around the attached vortex. The arm of the gather which passes downstream, at low Re , folds back towards the wake centre line and the double layer oscillates but does not develop into a vortex street. This folding back is visible in figure 8, plate 1. It must be stressed that the dye in the photographs indicates filament lines and in no way represents the spread of the wake. Vorticity diffuses considerably at these Re . It is obvious from the photographs that the dye diffuses very little. When a long splitter plate is employed gathers are still noticeable and become drawn out in the stream direction, but oscillation cannot occur. The behaviour of the wake can be different on the two sides as is seen in figure 9, plate 1.

When end plates were placed on circular cylinders so that the 'length to diameter' ratio was

small, no significant increase in Re_{osc} was observed. This is in disagreement with the findings of Nishioka & Sato (1974) which show significant increases when the separation of their comparatively much larger plates reduced the ratio of length to diameter to below 20. The author has also observed the quenching of vortex shedding in a wind tunnel at high Reynolds number when end plates were used to produce a small ratio of length to diameter. In this case the shedding could be resurrected by irradiation with sound at the transition wave frequency. It is possible that the disturbances in the present experimental arrangement are of just the right frequency to promote vortex shedding. Because it was considered that at the rear of the body spanwise fluid motion, which is certainly present, may produce a reduction of Re_{osc} , some experiments were made in a different tank filled with a density stratified salt solution. In a stratified liquid, significant vertical motion is inhibited. No appreciable increase in Re_{osc} was observed. The towing arrangement, which was not designed for our purposes, produced a somewhat non-uniform model speed.

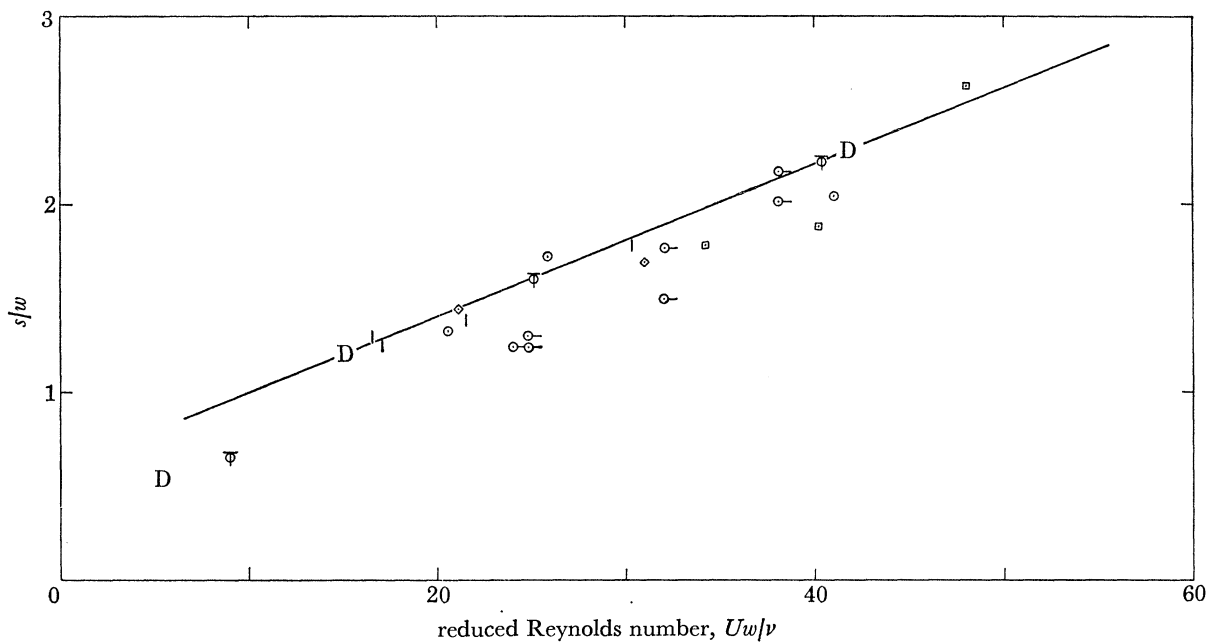


FIGURE 10. Length of the steady separation bubble as a function of Re when the maximum width, w , of the bubble is used as the characteristic length. Φ Experimental values for circular cylinder, Taneda (1955). D Computed values for circular cylinder, Dennis & Chang (1970).

Reference has already been made to figure 5 which shows the variation with Re of the length of the region just behind the cylinder which contains the two standing eddies. The length of this 'bubble' is measured from the rearmost point of the basic body to the end of the bubble. The presence of a splitter plate is ignored in defining the rearmost point of the body. From the data available it appears that the length of the bubble is the same for the circular and diamond section cylinders. Bodies which are more bluff have a higher value of s/d . At the higher Re the scatter of the points increases especially when oscillations are present. In any case it is not easy to assign an accurate value to the length s as can be seen even in a clear and steady photograph.

Great simplification results when the length of the bubble is compared with its width. This ratio is shown as a function of Reynolds number based on bubble width in figure 10. As far as

experimental inaccuracy allows we conclude from this figure that a universal function is obtained when the bubble maximum width w is used as the characteristic dimension. It may be noted that the points for the square cylinder and for the circular cylinder with a splitter plate one diameter long, lie some 10% below the other points. The circular cylinder with a long splitter plate has s/w values which are scattered but systematically further reduced and which lie at about one half of the values shown. Though a straight line has been drawn on the graph the variation is certainly curved convex upwards when viewed over a wider Re range through the computed results of Dennis & Chang (1970).

It has been asserted, for example by Tritton (1959), that the wavy wake is the result of a wake instability in which the only rôle of the body is to produce the velocity profile. This, however, is superseded by the discovery by Taneda (1963) that Re_{osc} is attended by the appearance of gathers on the bubble boundary which suggests a near wake or bubble instability. Some additional comments may be made on this point.

The bubble boundary is the stagnation streamline across which there is no flux of mass. The bubble is fed by diffusion with circulation from the separating boundary layer. It must lose circulation at the same rate and it does this by diffusion across the centre line of the bubble (oppositely signed vorticity diffusion in opposite directions). In the case of the body with a splitter plate the circulation balance must be maintained by production of circulation by the back flow along the splitter plate. When the bubble reaches a great enough length ($= 2d$) it becomes unstable, gathers appear and these carry away circulation into the wake. The periodic appearance of gathers results in the wavy wake. Once one gather appears at one side the other side becomes more likely to shed one. When the balance of circulation within the bubble can no longer be maintained by diffusive transfer, circulation is removed from the bubble by the convective action of the gathers. A numerical experiment to investigate these ideas suggests itself. Computer solutions, however, seem to produce stable bubbles at high Re from which realistic wake flows are only produced when a disturbance initiates the oscillation. It thus appears that the instability does not have the mechanistic interpretation suggested but the results of a numerical experiment would be interesting.

5. $Re_{osc} < Re < Re_{vs}$

There is a range of Re in which the wake oscillations produce filament lines which are sinuous and no vortex street is observed. At the high Re end of this range ($Re = Re_{vs}$) the waving filament line rolls up into a vortex street some distance downstream. At Re smaller than Re_{osc} when the cylinder is oscillated transversely to the direction of uniform motion of the body a similar wavy wake is produced. In this low Re case, however, the amplitude of the filament line which marks the centre of the wake dies away to zero. At Re greater than Re_{osc} the amplitude stabilizes and remains of constant amplitude for long distances downstream. In this sense the range is a continuation of the flows existing at $Re < Re_{osc}$. We have already seen in §4 and figure 8 that the wavy wake results when gathers fold back to the wake centre line. A photograph of the flow visualization produced by injecting dye into the wake is shown in figure 11, plate 1. In this range we find, as did Tritton (1959), that dye is swept from the wake into the attached vortices and that it remains there for many cycles of oscillation.

For the circular cylinder the end of this range is not clearly defined but is found to lie anywhere in the range $55 < Re_{vs} < 70$. This range is indicated in figure 4. Vortex streets are

sometimes observed at $Re = 55$ and sometimes the filament lines remain wavy and do not roll up into a vortex street even at $Re = 70$.

In one series of measurements the Stokes number was determined from photographs taken at known time intervals. From the photographs the vortex speed U_v and the wave length λ (vortex spacing) were determined. Thus

$$St = Nd^2/\nu = Re S = Re (1 - U_v/U)/(\lambda/d),$$

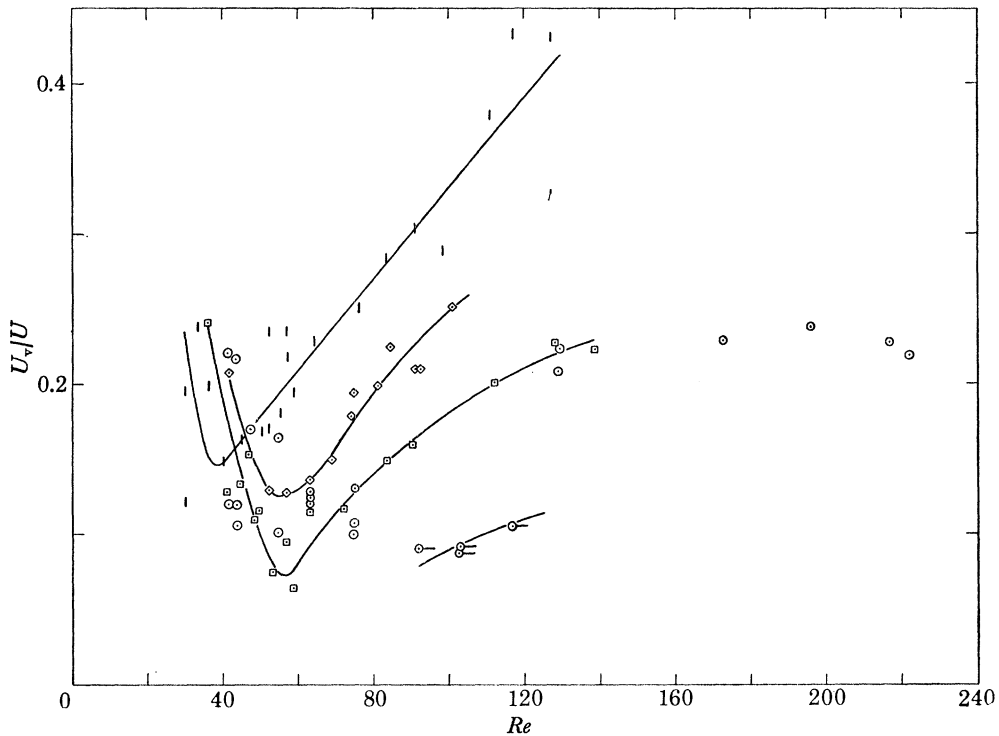


FIGURE 12. Vortex speed as a function of Re for body cross sections of the shape indicated by the symbols.

where U is the cylinder speed. Measurements were made within about 10 wavelengths of the body. There was a slight increase in λ with downstream distance but this was ignored. In this range of Re the $St-Re$ relation is a straight line as we saw in figure 2. In figure 12 values of U_v/U for different body cross sectional shapes are shown. The curves have been drawn so that their minima lie at $Re = Re_{vs}$ at which there is a change in the appearance of the wake. No curve has been drawn through the points for the circular cylinders because there is no well defined Re_{vs} : the points also show no well defined minimum. The values of U_v/U for the flat plate do not lie well on the curve drawn but the square and diamond section cylinders possess a well defined minimum of U_v/U at the same Re as Re_{vs} . In general, the wakes of the square and diamond section cylinders are more organized than those of circular cylinders. The frequencies measured in the wakes of cylinders of cross section other than circular are discussed in §9.

6. CIRCULAR CYLINDER WAKES IN THE Re RANGE FROM Re_{vs} TO ABOUT 140

On the basis of the variation of Stokes number with Re which is shown in figure 2 this present range may be divided at $Re \approx 100$. The frequency varies linearly with Re below $Re \approx 100$ but when higher Re are included a curvature is noticed. There may even be a discontinuity at $Re \approx 100$. If we include measurements taken during the unsteady region in the earlier part of the traverse of the towing tank there are two frequency relations in the range $100 < Re < 140$. Flow visualization reveals some systematic changes but the main characteristics of the flow are common to the whole range $70 < Re < 140$.

The dual frequency relation may be connected with the observations of Tritton (1959) and Berger (1964*a, b*). Tritton concedes that his finding of a dual frequency relation at Re in the range 80 to 105 could well be the same phenomenon as that observed by Berger in the range $115 < Re < 160$. In his repeat measurements, Tritton (1971) found a discontinuity at $Re = 110$. These dual relations remain unexplained as far as detail is concerned. We will allude to the possible effect of vibrations in the next section. Berger remarked that from observations with one hot wire it is not possible to distinguish between high and low speed modes from the appearance of the oscillograms. With two hot wires instability of the phase difference of the signals was apparent in the high speed mode only. Tritton (1959) relates his high and low speed modes to the appearance of flow visualization in a water channel.

Consider first the view of the wake from the side in which the dye is concentrated in the vortex cores which appear as lines more or less parallel to the cylinder axis. Some examples are seen in figures 13 to 16, plates 2 and 3. The main characteristic of the vortices in this range is that they are hardly ever straight or parallel to the cylinder axis. In figure 13 we see the vortices in their most regular form. Straight and parallel vortices occur only transiently. Initially it was found that dual frequencies were observed in the range $100 < Re < 140$, as shown in figure 3. Considerable effort was expended in trying to discover what, if any, was the difference in the mode of flow between the high and low frequencies. The main conclusion is that the higher frequency only occurred in the first phase of the cylinder's motion: for distances travelled less than *ca.* $200d$, (though it may be a distance in terms of cylinder length which is significant). Vortices were generally more or less parallel to the body axis in the initial phase only, and then usually only at the beginning of this. In this condition, detail of the process of vortex formation is visible in views of flow visualization from above as in figures 18 to 20, plates 5 and 6. When the vortices are inclined, detail is obscured because the dye is inevitably spread over at least one diameter of the cylinder's length and one sees different phases of the oscillation superimposed. After the initial phase of the motion the vortices were always bowed as in figure 14. The amplitude of the bow at its peak varied from 1 to 4 wavelengths but was always of the same form. This finding was independent of the direction of travel of the body and so could not be associated with slight residual motions in the water. These experiments were made after the background motions had been minimized. The vortices must curve towards the body at the ends. The bowing of the vortices is considered to be due to the end effects. It was not determined whether the bowing eventually remained constant: sometimes it did and sometimes not in the present experiments. The amount of bowing was not found to depend systematically on the ratio of length to diameter of the cylinder. While the shape of the vortices is changing, the frequency of the wake oscillation must be changing. If the frequency is different at different stations along the span when the vortices are bowed then the amount of

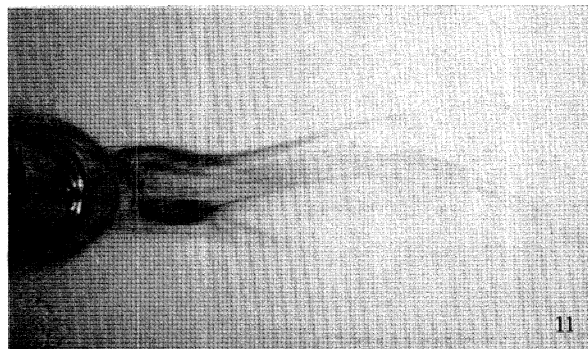
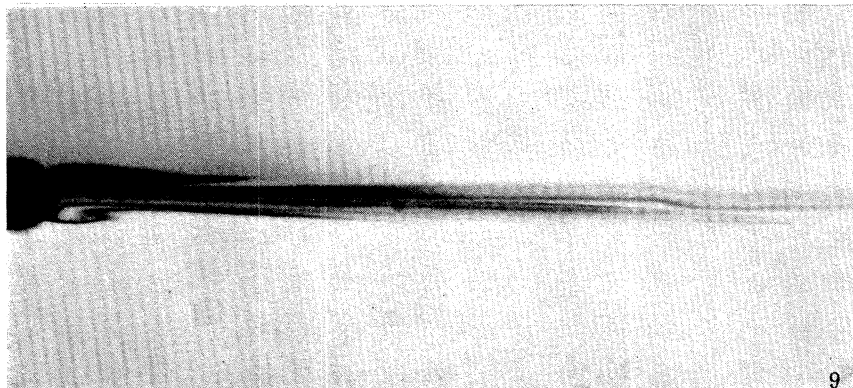
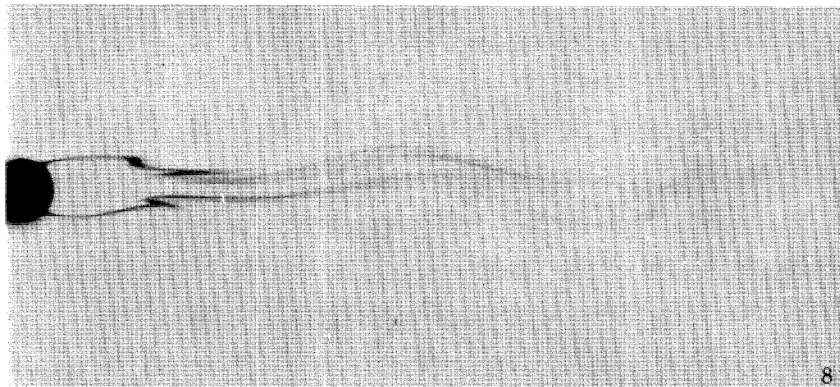
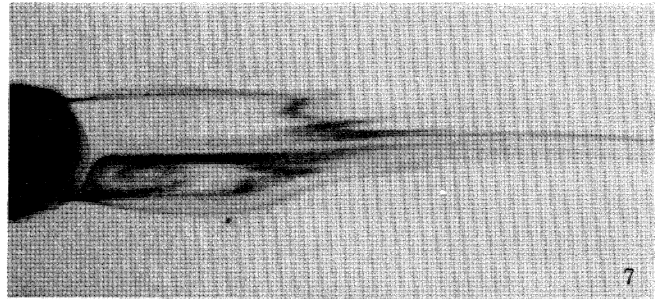
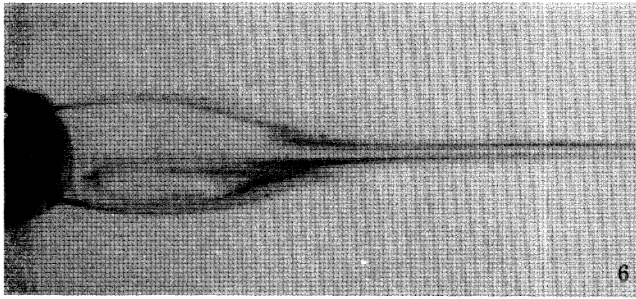


FIGURE 6. Wake of a circular cylinder at $Re = 37.8$.

FIGURE 7. Wake of a circular cylinder at $Re = 44.4$.

FIGURE 8. Wake of a circular cylinder at $Re = 39.6$ showing gathers folding on to sinuous wake.

FIGURE 9. Wake of a circular cylinder with a splitter plate 10.8 diameters in length. $Re = 40.2$.

FIGURE 11. Elongated gathers and a sinuous wake at $Re = 52.5$. Dye injected into the wake.

(Facing p. 366)

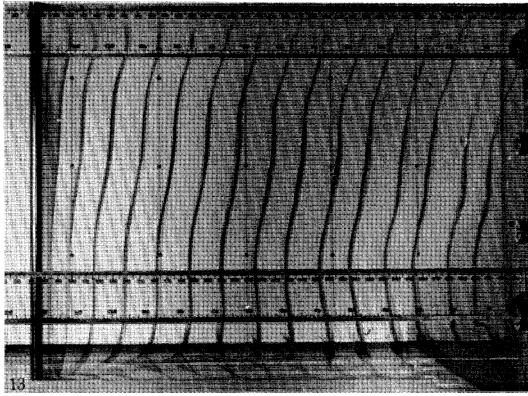


FIGURE 13. Vortex street in its most regular appearance $Re = 75$.

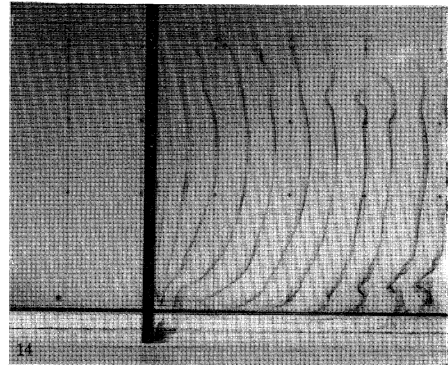


FIGURE 14. The usual bowed appearance of vortices when they attain their established form.

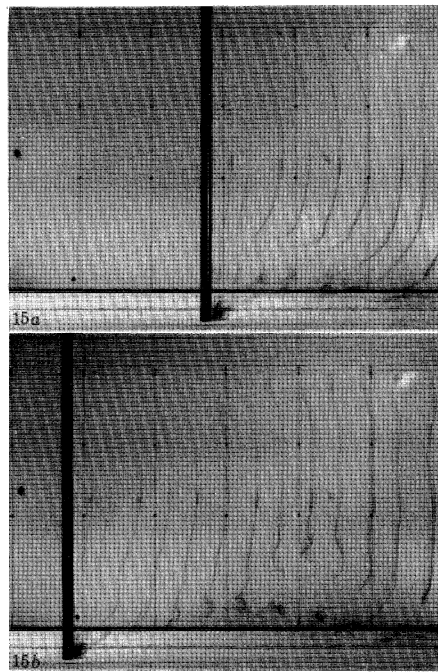


FIGURE 15. Two photographs obtained in the same run showing the appearance of a 'knot' near to the lower end. The water in the tank has minimal background motion. $Re = 120$.

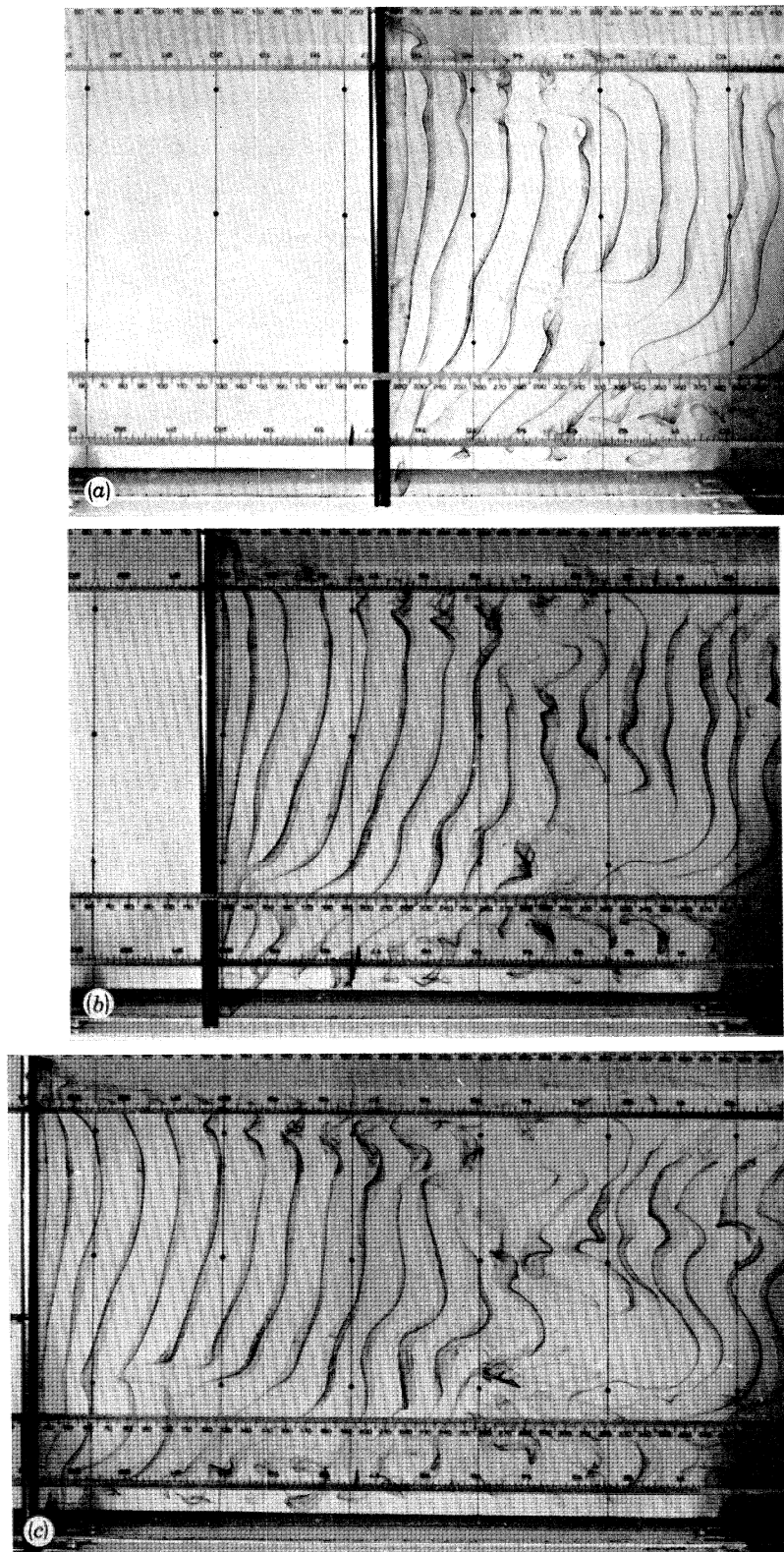


FIGURE 16. The appearance of knots when there are background motions of about 0.2 mm/s. Knots appear at regular intervals. $Re = 129$.

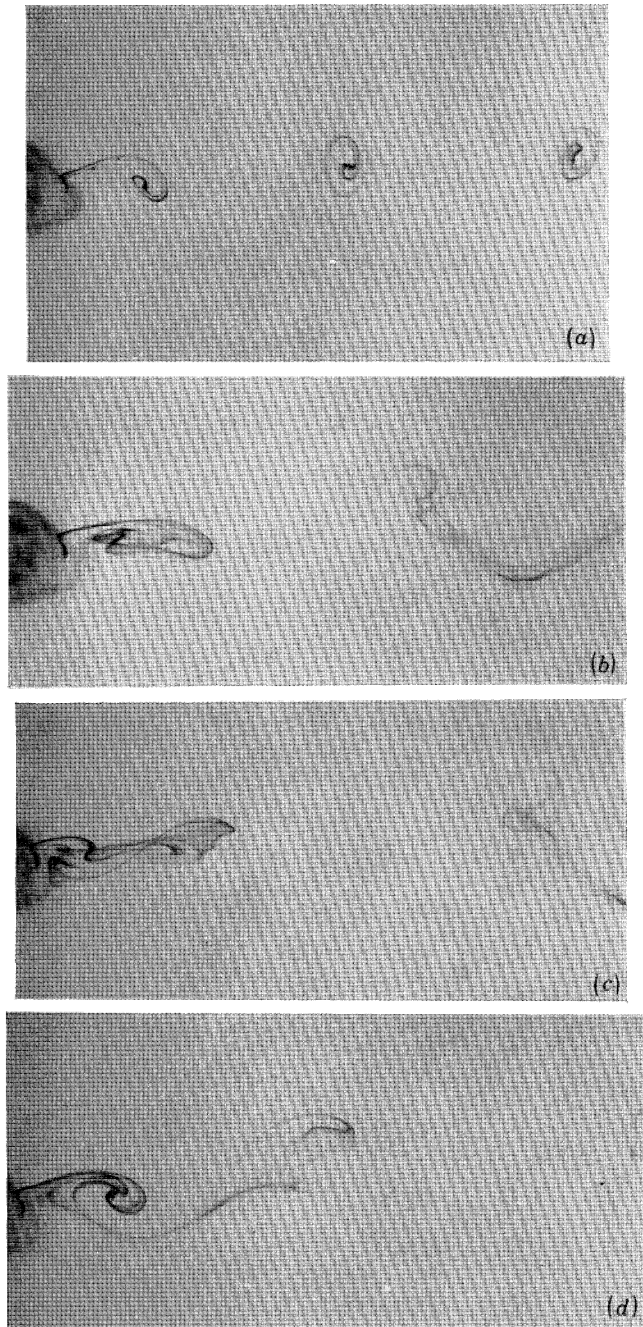


FIGURE 17. The appearance of a knot from above. Wake of a flat plate with a 2% step in its width. Re above and below the step 73.1 and 71.7. Dye on one side of the cylinder only. (a) Wake appearance with no knot present; (b), (c) and (d) Consecutive photographs showing the vortex core linking with the next vortex of the same sign.

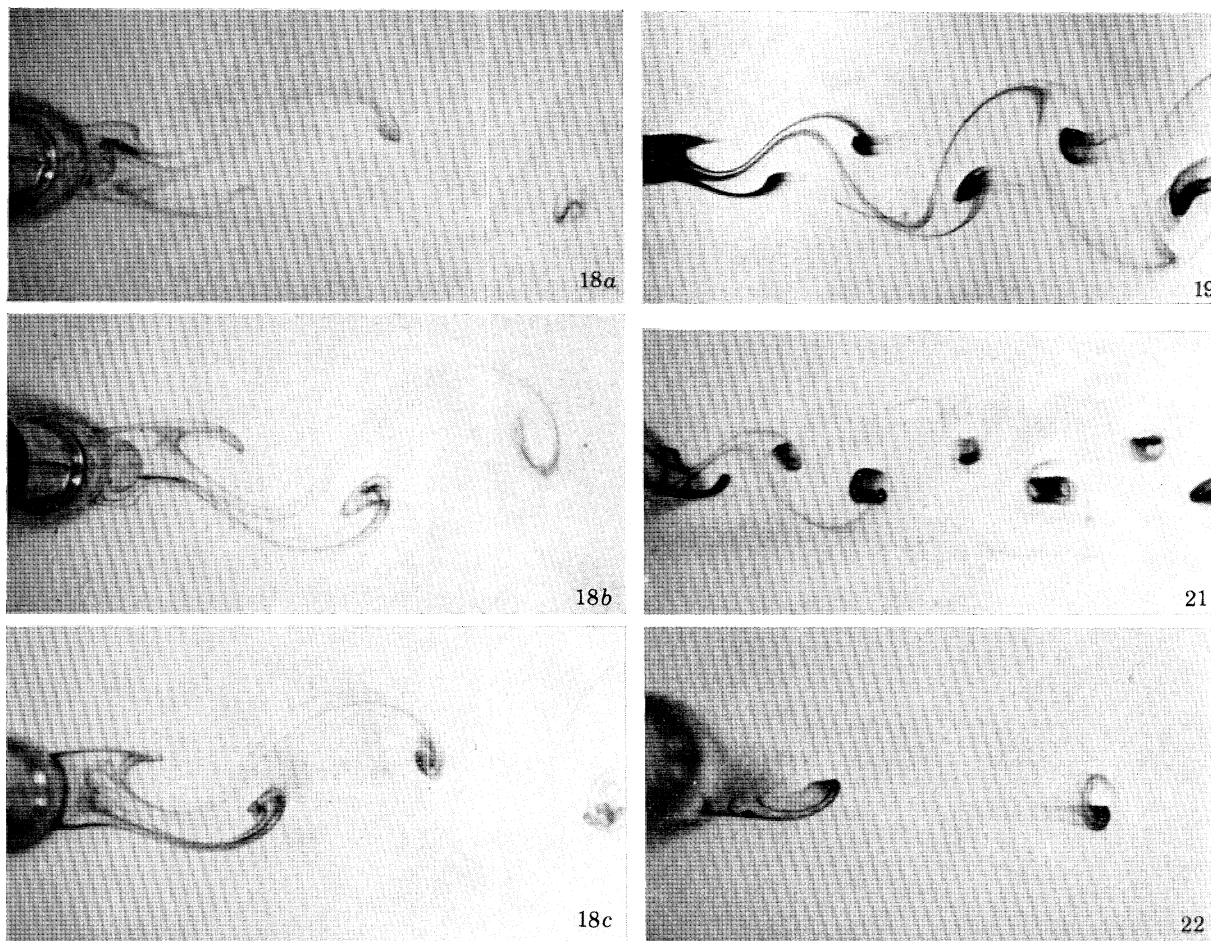


FIGURE 18. Views of the wake produced by injection of dyed water into the wake showing the steadily oscillating pattern resulting after the cloud of dye has been left behind. (a) $Re = 91$, (b) $Re = 124$, (c) $Re = 150$.

FIGURE 19. Circular cylinder wake at $Re = 77$. The region behind the body is filled with dyed fluid.

FIGURE 21. Circular cylinder wake at $Re = 106$. The absence of an accumulation of dyed fluid behind the body is apparent.

FIGURE 22. Circular cylinder wake at $Re = 109$. Dye on one side of the rear of the body. Two filaments of dye are visible close behind the body.

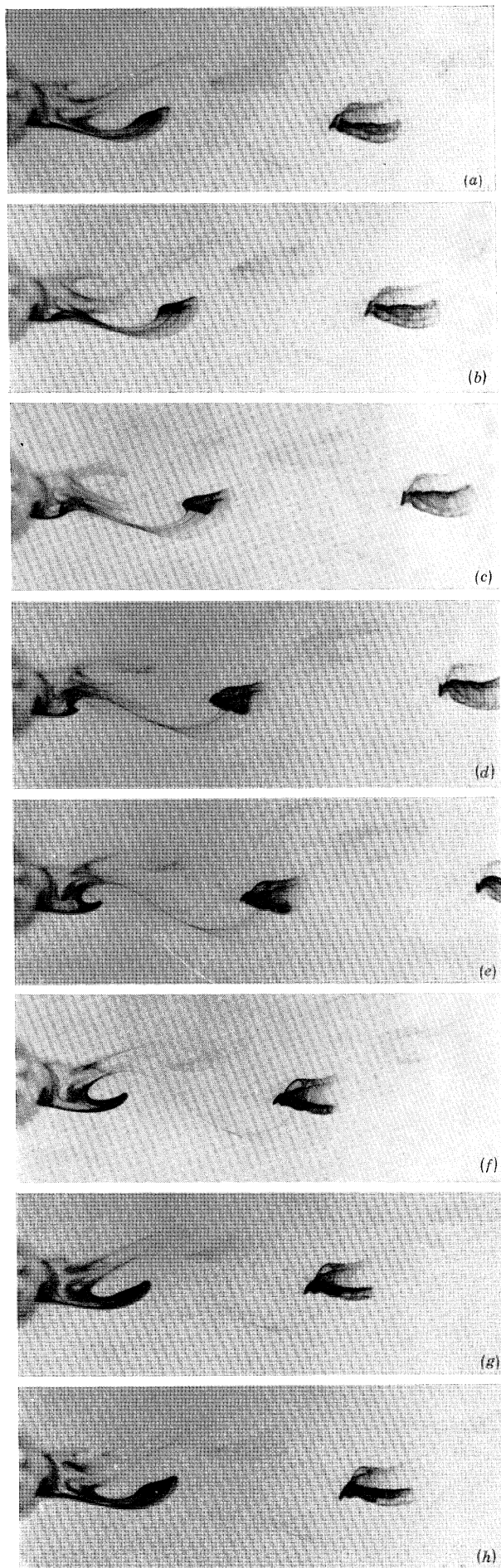


FIGURE 20. Consecutive views of the wake of a circular cylinder at $Re = 93$. Time intervals between exposures = 0.135 period.

bowing would change. It is conceivable that end effects also affecting the frequency could produce a stable bowed configuration. With end effects the straight configuration is not a stable state. It is found that vortices which are bowed on formation may become straight as they pass downstream; this is seen in figures 14 and 15.

Differences between the beginning and end of the cylinder's motion along the tank are attributed to the effects of the end constraints spreading along the span. This suggests that the frequency measured early in the run may correspond to that of an infinitely long cylinder; the vortices are more often straight and parallel to the body axis at this stage. In Tritton's (1959) experiments the length/diameter ratio was very large but so also was that in Berger's (1964) work in which the same frequency variation was not observed.

Another phenomenon common to the whole range of Re and which Tritton (1959) also observed is visible in figures 15 and 16. These we have chosen to call 'knots' because their occurrence and development when viewed from the side is as if the dye filaments had become tied to the cylinder at one point along the span from which, at any instant, they travel downstream before turning up and down into the general vortex core direction. These knots only ever occur when the number of vortices above and below them are different. They do not move along the cylinder span. Gaster (1971) noted that cells of coherent vortex production migrated along the span of a cylinder as the free stream speed changed and that these could be anchored by the use of end plates. It has been noticed in the present work that sometimes vortices are produced with a step in them when seen in side view near to the beginning of the motion. These steps move along the span in successive vortices and become more rounded: the step in streamwise position changes to a similar position difference, spread along the whole span. The knot seen in figure 16*a*, *b* and *c* was observed before the background motions were minimized. In this condition knots are noticed at all spanwise stations. In the quiescent tank condition, knots only appeared near the ends of the body and usually near to the bottom free end. In the minimal background motion condition, there remained small motions near to the surface and bottom and thus one expects to find different frequencies in these positions. When the vortices become sufficiently far out of step, the distortion relaxes in the formation of a knot. This process was discussed by Gerrard (1966*a*) in a paper on three-dimensional effects. In figure 17*b*, *c* and *d*, plate 4, taken sequentially from above the cylinder, one can see the filaments linking round to the next vortex on its own side of the wake as explained by Gerrard (1966*a*). Figure 17*a*, plate 4, shows the same wake in the absence of a knot. These photographs are of the wake of a flat plate which had a 2% step in its transverse dimension at about mid-span. In this way the knots occur at a fixed position along the span. The same process has been observed behind the circular cylinder but the taking of photographs was not possible because when the vortices are inclined and the dye is spread along the span it is difficult to see what is happening in this view. With one spot of dye the probability of the knot appearing at just the right spanwise position is too small.

Photographs typical of this range are shown in figure 18. These patterns were produced by injecting dye into the wake. From views like this in which there is no control of the amount of dye the appearance depends on the time since the injection of the dye. One concludes from figure 18 that the general appearance of the wake is essentially the same at all Re in the range. When dye is painted in a thick patch on each side of the rear of the cylinder, as in figures 19 to 21, plate 5, the differences in the rate of ablation of dye at different Re are determined solely by the flow processes close behind the body. In these figures a change is noticeable at $Re = 100$.

The contrast between figures 19 and 21 in the region close behind the body is typical of all the present experiments. At Re less than 100 there is an accumulation of dyed fluid behind the cylinder. At higher Re the dye remains close behind the body for a much shorter time and only one or two strands of dye filament are seen. This is more clearly visible in figure 22, plate 5, in which dye was only deposited on one side of the body. A similar observation was made by Tritton (1959) who ascribed the change to the difference between the high and low speed modes of oscillation. We will return to this phenomenon after discussing the mode of vortex formation for which we refer to figure 20.

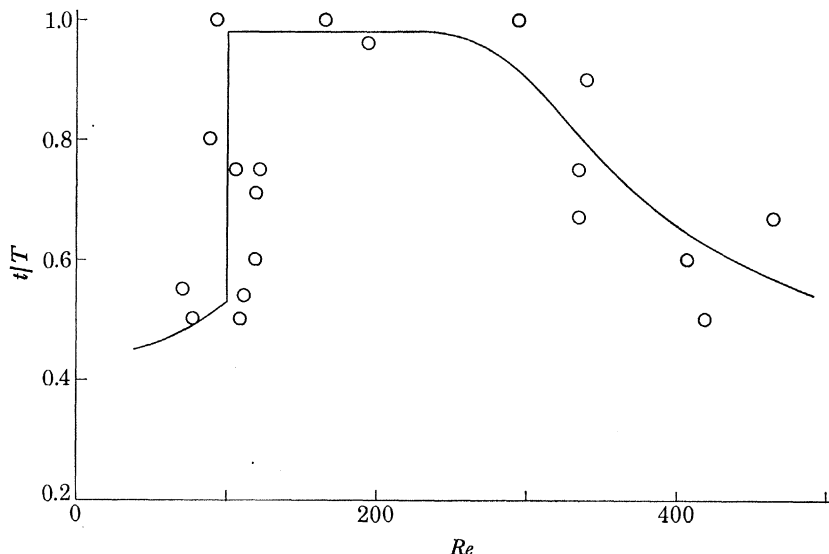


FIGURE 23. The time during which the vortex accelerates. t = the time from the first appearance of a vortex to the instant at which it begins to move with constant speed. T = the period of oscillation.

Figure 20 shows consecutive photographs separated by 0.135 of a period of the oscillation, and mounted so that they are evenly spaced. It is apparent from the photographs that the vortices are slightly inclined to the vertical line of sight. Consider first the paths of the rolling-up dye filaments. It is evident from figure 20 that the vortex first appears as a wave in the filament line, as in (*b*), that the wave develops into a kink (*c* and *d*) and then rolls up as it moves downstream. The vortex made visible in this way moves relative to the cylinder with a speed which increases to a constant value. The acceleration period varies with Re and the results of investigations of this over a range of Re are shown in figure 23. This graph indicates a transition in the region of $Re = 100$. The times measured in the region of $Re = 100$ are very scattered, indicating that the transition Re is not well defined. At low Re (and early in the run) the vortices rapidly attain their constant speed but at Re between 100 and 300 the acceleration period is approximately constant at about one period of oscillation, after which there is a decrease, as Re increases, to approach one half period at high Re as expected. An alternative representation of the accelerating phase is shown in figure 33 which is discussed in the next section.

Before discussing the $Re = 100$ transition further, it is necessary to describe the mode of vortex formation in this Re range. Referring to figures 18 to 20 and particularly to figure 20 one sees that in the rolling-up process some undyed fluid is trapped between the dye filament

and the sinuous wake centre line. Most of this fluid is carried downstream with the vortex but some, separated by a dye filament, is thrust back towards the cylinder along the centre of the wake once in each half cycle at both sides of the wake. It may not be presumed that some irrotational fluid is similarly transported, for vorticity diffuses much more rapidly than the dye. This statement is certainly true at the low Re in this range but perhaps not at Re greater than 100. The photographs of Zdravkovich (1969), at Re about 100, show that little irrotational fluid finds its way into the region close behind the body. The fluid thrust back towards the body is seen to execute a circulatory motion on its own side of the wake to be scavenged in succeeding

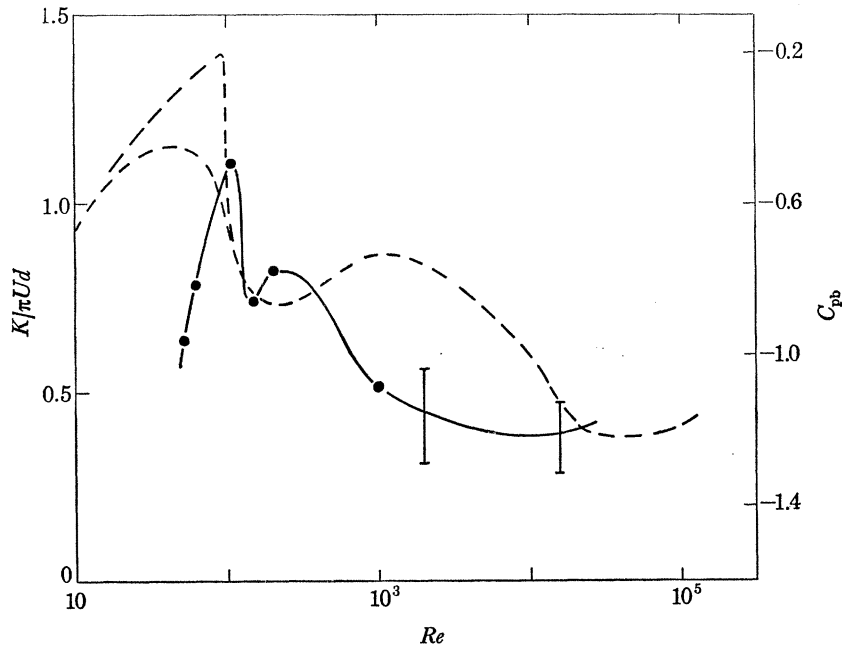


FIGURE 24. Vortex strength and base pressure variation. --- C_{pb} ; — $K/\pi Ud$.

cycles as it is drawn into the separating filament line. At Re less than 100, fluid is trapped behind the cylinder; the standing eddies of lower Re are seen to be still present in some form. That the fluid remains on its own side of the wake is in disagreement with the interpretation of Zdravkovich (1969) of the findings of Nayler & Frazer (1917). These measurements were rather rudimentary and also concerned flow about a short tapered body. At Re greater than 100, essentially the same process seems to take place, except that the scavenging of fluid from the rear of the cylinder is much more energetic. There is no accumulation of dye and the single dye filaments do not remain for more than one period of oscillation. At these Re , both greater and smaller than 100, the fluid which is left behind in the interior of the wake when the dye filament rolls up, sooner or later finds its way into a vortex on its own side of the wake. At the lower Re the vorticity bearing fluid which returns towards the rear of the cylinder remains long enough for its circulation to be depleted by diffusion cancellation from the opposite side of the wake. The diffusion effect decreases as Re increases and so one expects that the non-dimensional vortex strength will increase as Re increases.

In figure 24, vortex strength and base pressure coefficient are shown as functions of Re . The vortex strength, K , is abstracted from the paper of Bloor & Gerrard (1966), the base pressure

coefficient values are reproduced from a private communication from A. Roshko and are principally the work of Weidman, a student of his. The alternative possibilities for C_{pb} near $Re = 100$ are Weidman's idea. Both curves in figure 24 are tentative at low Re so that all one can say with certainty is that C_{pb} may well indicate a transition at $Re = 100$. Measurement of C_{pb} at low Re is not easy but might well be very illuminating. There is evidence that the vortex strength has a maximum at $Re = 100$ after which it rapidly decreases as Re increases. Similarly the base suction increases rapidly at $Re = 100$. This requires explanation. At Re greater than 100 almost all the fluid returning towards the cylinder is removed by the next vortex which is an indication that convection is taking precedence over diffusion near to the body. That the base suction increases corresponds to the increased scavenging of the base region. At low Re where diffusion of vorticity is large the dye does not mark the vorticity bearing fluid. Hama (1962) has shown that in a shear flow a dye filament does not by its rolling up indicate that there is a vorticity concentration. One must be careful in interpreting dye filament line patterns at low Re in the present work. If diffusion ceases to be significant at $Re \approx 100$ the dye more nearly indicates where the vorticity is located. The appearance of figure 21 suggests that the vortex strength could decrease because of entrainment, by a vortex, of fluid of oppositely signed vorticity from the other side of the wake during the unsteady vortex motion represented in figure 23. This variation of vortex strength remains to be investigated.

The initial perturbation of the separated shear layer is similar at low and high Re in the range we are considering. The perturbation which is followed by a rolling up of the filament line represents a concentration of vorticity at the higher Re . At the lower Re there is not necessarily such concentration. More work suggests itself on the development of an initial disturbance on narrow and wide shear layers.

In conclusion it is suggested that the transition at $Re \approx 100$ is real. One is tempted to suggest that the transition marks the end of the Re range in which diffusion of vorticity plays a primary rôle in the determination of vortex strength and hence of frequency. The $Re = 100$ marks the end of the range in which there is any remnant of the standing eddies behind the cylinder as Tritton originally suggested.

7. THE WAKES OF CIRCULAR CYLINDERS IN THE RANGE $140 < Re < 500$

The transition range discovered by Roshko (1954*a*) is generally recognized (see Berger & Wille 1972) as extending over the Re range 150–200 to 300–400. Bloor (1964) showed that the range is not associated with transition to turbulence in the free shear layers before they roll up into vortices and since then no explanation has existed which adequately describes the flow in this transition.

Flow visualization shows that the character of the wake changes when this Re range is entered. We have seen that, with the exception of the occurrence of knots, the vortices are tightly and uniformly rolled up when seen in side view as in figures 13 and 16. Side views of the dye washed from a circular cylinder into the wake are shown in figures 25 to 28, plate 7, at values of Re of 200 to 344. The notable feature of all these views is that the vortices do not extend along the whole length of the cylinder in the tightly rolled up form. Fingers of dye extend from the vortex just formed and point towards the cylinder. Hama (1957) has published photographs showing these fingers in the same Re range but he offered no explanation of their

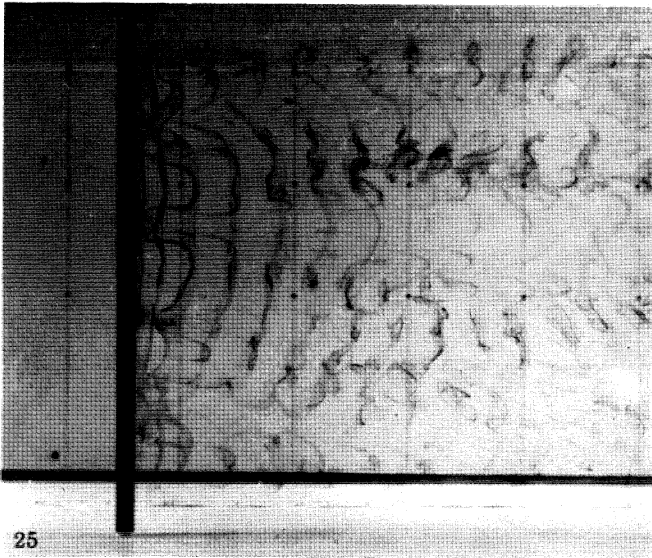


FIGURE 25. Side view of the wake of a circular cylinder at $Re = 200$.

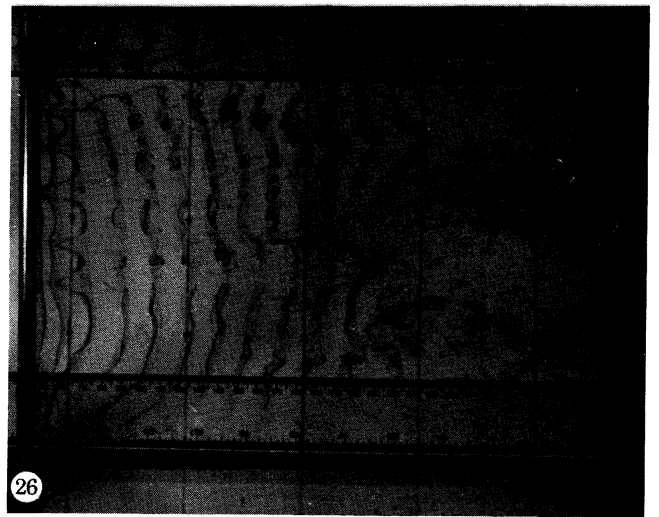


FIGURE 26. Side view of the wake of a circular cylinder at $Re = 217$.

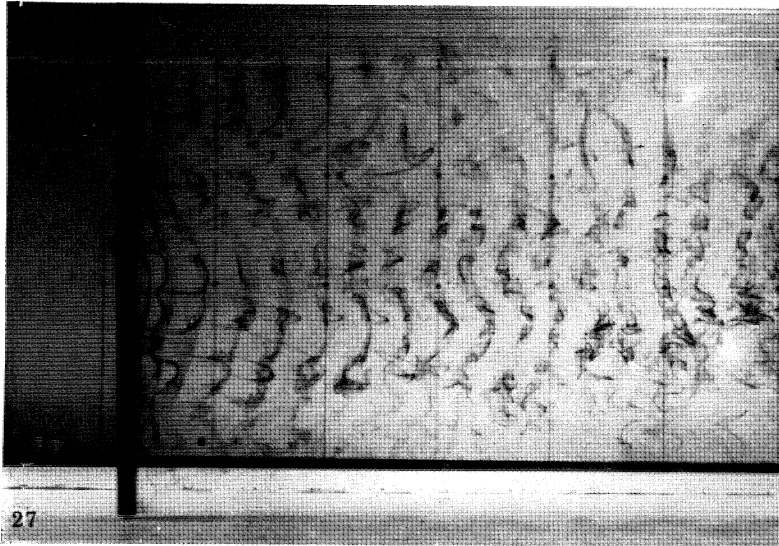


FIGURE 27. Side view of the wake of a circular cylinder at $Re = 232$.



FIGURE 28. Side view of the wake of a circular cylinder at $Re = 344$.

(Facing p. 370)

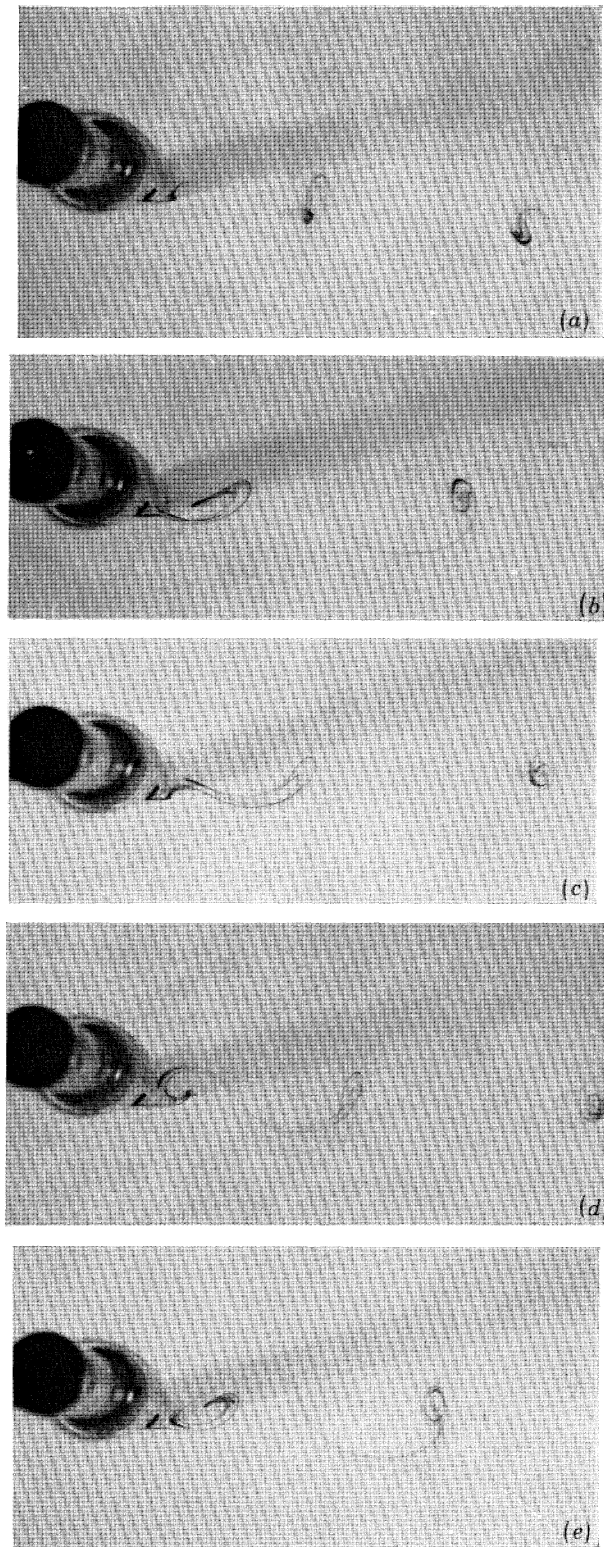


FIGURE 29. Wake of a circular cylinder at $Re = 180$ showing a minor form of finger. Dye on one side only of the rear of the body. (a) Appearance in the absence of a finger. (b)–(e) Consecutive instants during which dye is drawn back from a vortex into the next vortex on the same side of the wake.

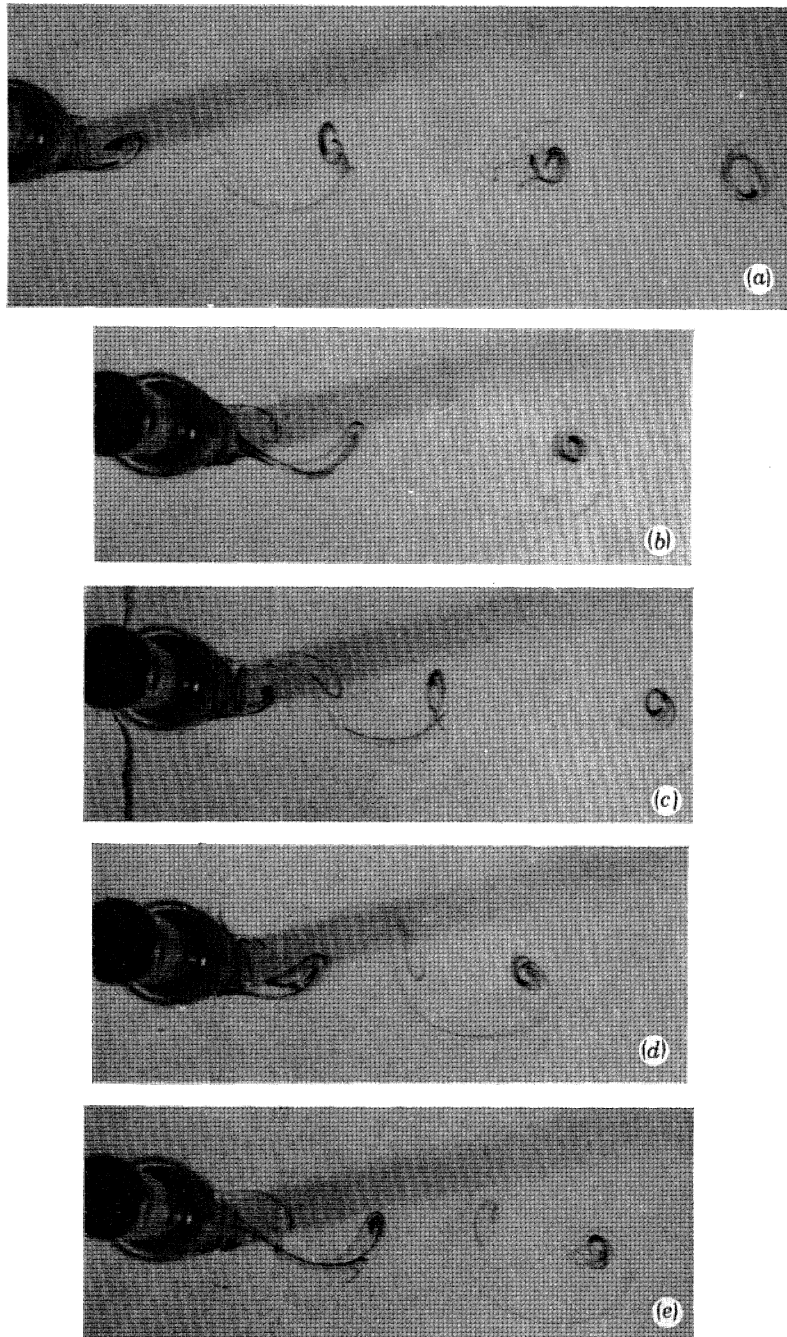


FIGURE 30. Wake of a circular cylinder at $Re = 230$ showing the sequence of events in the formation of a finger. Dye is drawn back from a vortex to the rear of the body and thence into the opposite side of the vortex street.

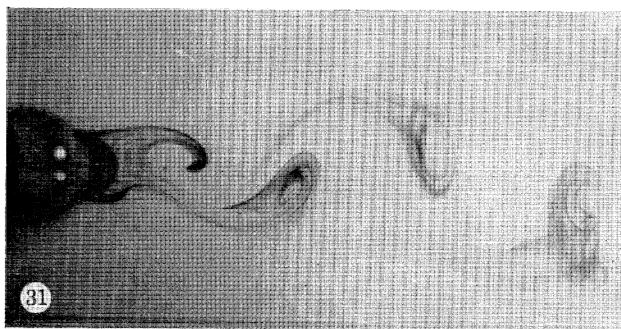


FIGURE 31. Wake of a circular cylinder at $Re = 188$.

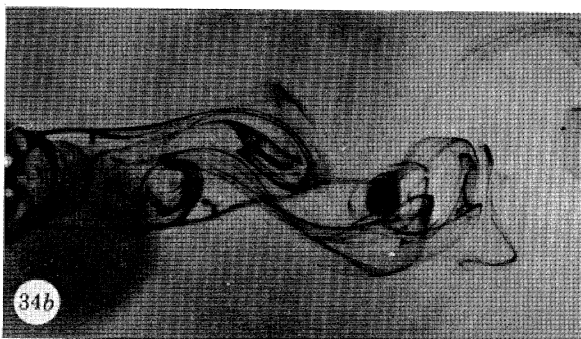
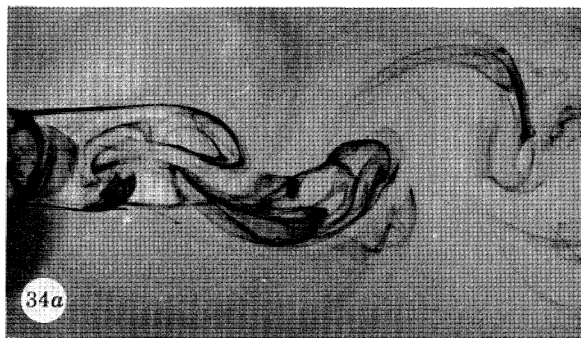


FIGURE 34. The wake of a circular cylinder at $Re = 334$. Consecutive views at separation 0.22 period of oscillation.

presence. The fingers appear at randomly disposed spanwise positions but follow each other in succession at the same spanwise position. At each end of the range fingers persist for 2 or 3 cycles. In the centre of the range at $Re \approx 250$ the fingers appear more frequently at each position and occur in clumps of larger numbers.

At the beginning of the transition range ($Re = 180$ to 200), the wake hot wire traces of Bloor (1964) show occasional slight increases in velocity amplitude and more frequent drastic diminutions in amplitude. Viewing dye from above shows how this occurs. Figures 29 and 30, plates 8 and 9, show the patterns produced by dye washed from one spot on one side of the rear of the cylinder. Figure 29*a* relates to the usual situation below and at the lower Re end of the range. Dye leaves the cylinder at the separation point, rolls into the vortex as it forms and principally remains in the core of the vortex as it moves downstream. A fine trail of dye is swept across the wake between the vortices: close to the cylinder it does not enter the core of the vortex of opposite sign but marks out the sinuous wake centre line. The wake centre line is seen more clearly when more dye is present as in figure 31, plate 10. In the wake regions from which fingers are absent the appearance of the wake from above is similar to that at $Re < 140$. Thus the lower range of Re merges into the present one.

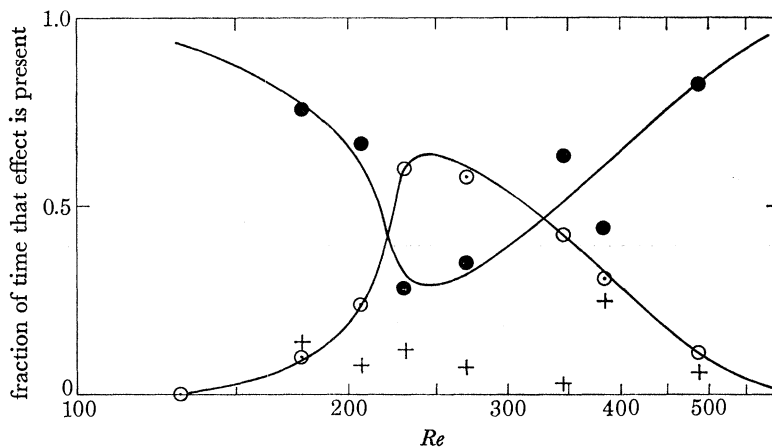


FIGURE 32. The frequency of occurrence of fingers. ● Dye drawn into a single vortex on its own side of the wake and the dye staying in that vortex (as figure 29*a*). + Dye drawn back from the vortex into the next one of the same sign (as figure 29*b-e*). ○ Dye drawn back from the vortex, back to the cylinder and into the next vortex of opposite sign (as figure 30).

In the finger, dye is drawn back along the sinuous wake centre line from the core of a vortex after it has left the cylinder. Infrequently, but particularly at the lower Re , this dye rolls up into the next vortex of the same sign: the dye stays in its own side of the wake. This motion of vorticity bearing fluid corresponds to an increase in the strength of the vortex which is fed in this way. Sometimes the drawing back is more energetic: the dye enters the region close behind the cylinder and most of it enters the next but one vortex which is of opposite sign. This corresponds to a decrease in strength of that vortex. Figure 29 shows dye being drawn back into the next vortex of the same sign whereas figure 30 shows the dye going across into the vortex at the other side of the wake. The frequency of occurrence, at one spanwise station, of this energetic drawing back increases with Re to reach a maximum at $Re \approx 230$. At this Re , 60% of the vortices exhibit the occurrence. The results of observations of the wake are shown in

figure 32. At Re greater than 230 there is a decrease in the occurrence of this effect to reach almost zero at $Re \approx 500$. We seem to come to the surprising conclusion that Roshko's transition range is not, as expected, a change which as Re increases affects an increasingly larger proportion of the vortices, but rather is a mechanism which is absent above and below this range of Re and has its maximum in the middle of the range. There is, however, a transition from one state to another which starts within this range and which accompanies the disappearance of the fingers. We have seen (in § 6) that at lower Re , fluid enters the region close behind the cylinder from the downstream direction. The same general pattern is still present in the fingers we have described. Between Re of about 250 to 500 there is a transition to a different

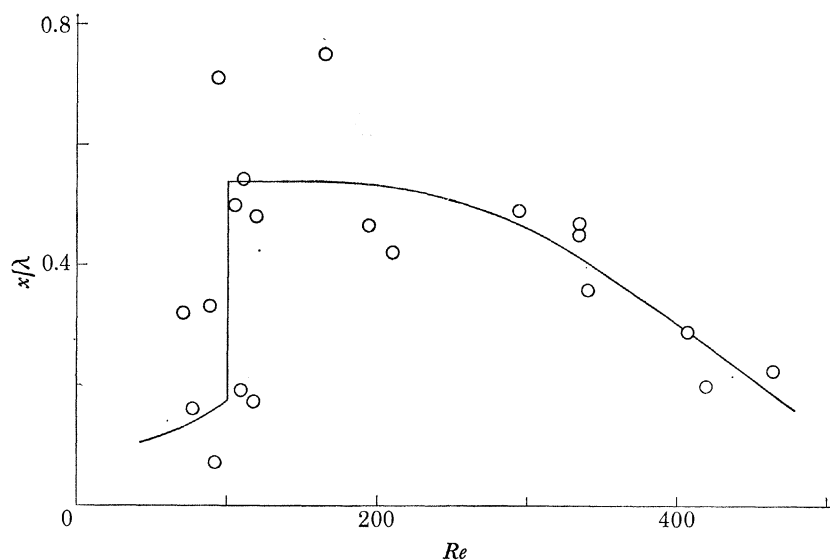


FIGURE 33. Motion of the vortex while accelerating. x = distance moved by the vortex relative to the cylinder from its first appearance to the position where its speed becomes constant. λ = longitudinal spacing of vortices on one side of the wake (the wake wavelength).

mode of shedding of vortices which is similar to that described by Gerrard (1966*b*) and which is fully operative at Re of about 10^4 . In the towing tank the high Re mode of vortex formation is interrupted over a range of Re in the manner we shall describe in the next section. The high Re mode involves the growth of a vortex in a stationary position for half a period of oscillation until it is strong enough to cut itself off from the cylinder by inducing a cross flow between itself and the cylinder. We have seen in figure 23 that at Re between 140 and 300 the vortex accelerates for more than half a period before it moves with constant speed. An alternative representation is given in figure 33 which shows the distance the vortex moves before travelling with constant speed. Above $Re = 300$ the distance travelled by the growing vortex falls with increasing Re to reach zero in the region of $Re = 500$.

At $Re = 100$ and below, both Zdravkovich (1969) and Tritton (1959) showed that there was a transverse flow between the vortices at some distance downstream from the cylinder. This flow can be seen in figures 18, 19, 21 and 31. It appears that the position of appreciable transverse flow approaches the cylinder as Re increases. At $Re = Re_{vs}$ the cross flow is very far downstream. In figure 34, plate 10, we see that there is transverse flow in the low Re position, that is, in a region separated from the cylinder by at least one vortex. In figure 35, plate 11,

the downstream development is more clearly visible. The transverse flow is greatest where the vortices are accelerating. At $Re = 407$ in figure 36, plate 11, we see the same process occurring in a position closer to the cylinder. When this transverse flow is present, fingers must be absent. Figure 36 shows the more common appearance of the wake at $Re = 407$ but the appearance is sometimes as in figure 37, plate 11, in which one sees transverse flow between the growing vortex and the cylinder at the same time as the next vortex starts to grow. This is the more common pattern at $Re = 464$ at which figure 37 was observed. At the higher Re in this range, the flow is often indistinguishable from the high Re mode of shedding but, the evidence is not conclusive because the transition to the flow, to be described in the next section, is intermittently present.

We return now to the subject with which we opened this section, namely, the transition to turbulent vortices. Figures 34–37 clearly show turbulent motion within the vortices even though the vortex rolling up next to the cylinder appears to be laminar. The figures 29 and 30 which illustrated the finger mechanism show that the finger itself does not produce a turbulent vortex. The views from the side of the wake in figures 25–28 do give the appearance of turbulence, especially at some distance behind the body. This appearance is different from the contortion of the vortex cores downstream, as in figure 16*c*, which is caused by knots. The conclusion to be drawn from figures 34–37, which cover the Re range from 334 to 464, is that turbulent vortices are produced by the mixing with the induced transverse flow. It is clear that the fingers accompany the appearance of Roshko's irregular vortices. The transition to turbulence follows at high Re . The fingers and the transverse mixing both seem to be responsible for the vortices being much more nearly straight and parallel to the cylinder at these Re . It is noticed, at the low Re end of this range where the occurrence of fingers is infrequent, that fingers are present in greater number at the start of the motion. The vortices become synchronized along the span through the action of the fingers. It is possible that the encroachment of the end effects towards the centre of the body is inhibited by both the finger and the transverse flow mixing. It is to be noted that when the vortices are turbulent their transverse separation is much less than for laminar vortices. Zdravkovich (1967) associated small transverse spacing with transition to turbulence in the wake some distance downstream from the body.

As far as transition to turbulence is concerned we conclude that both Bloor and Roshko were correct. In this range of Re the separated shear layer rolls up in a laminar vortex. By the time the vortex is moving at constant speed it has become turbulent. We will see in the next section that (in figures 39–41, plate 13) the flow at slightly higher Re becomes turbulent in the free shear layers before the appearance of the vortices which form the vortex street.

Before closing this section some remarks need to be made about the effects of transverse vibration of the cylinder. It would seem that such motion would reduce the Re at which high Re shedding is observed. Griffin & Ramberg (1974) have observed transverse flow between an oscillating cylinder and the nearest vortex at Re as low as 190. Koopman (1967) remarks on the opposite effects of vibration on the Strouhal number at high Re and at Re below 300.

One wonders to what extent cylinder motion affects the transition from the low to the high speed modes of Berger and Tritton, and whether transverse motion which is sporadic and in no way connected with the natural vortex shedding frequency may be important. Both these workers have used very slender cylinders which would respond to mechanical disturbances.

8. TRANSITION WAVES, CIRCULAR CYLINDER AT $Re > 350$

In the flow past a circular cylinder at Re of about 350 or a little higher the instability of the separated boundary layer is first manifested. At higher Re , Bloor (1969) discovered oscillations in the separated boundary layers and called them transition waves because they precede transition to turbulence in the free shear layers at Re greater than about 1000. Bloor's measurements did not cover Re less than 1000 but indicated that the transition wave frequency and the shedding frequency were approaching each other as Re decreased. It is interesting, therefore, to investigate those Re at which the two frequencies are equal. This range of Re is also of interest because it has been suggested by Gerrard (1967) from the results of numerical experiments that at Re of 1000 to 2000 the wake near to the body may cease to oscillate. This is associated with the extremely small fluctuating lift coefficient at these Re in a low disturbance stream. A symmetrical formation region has been reported by Papailou & Lykoudis (1974) in experiments on the wakes of bluff bodies towed through mercury. Observation of the dyed wake extends Bloor's results to lower Re and allows us to present a new interpretation of those results.

Photographs of the wake are presented in figures 38 to 41, plates 12 and 13. As Re increases transition waves first appear as undulations in the filament lines springing from the separation points. At all Re investigated, these waves are in phase on the two sides of the wake: thus, though they appear to be the same as those waves observed on a single shear layer by Sato (1956), it appears that in the bluff-body wake the two sets of waves are coupled. Surprising though it may seem, the coupling does not seem likely to be forcing by the main vortex shedding because as we shall see this is not always present. One of the characteristics of hot wire measurements in the wake is the appearance of low frequency modulation. The counterpart of this in the flow visualization studies is the observed inconstancy of the frequency of vortex production which is not so immediately obvious as the modulation of the hot wire traces. Toebe (1969) showed that the low frequency modulations at $Re = 10^5$ were equivalent to a pulsation of the near wake rather than a flapping or swinging motion. This is a similar motion to that produced by the transition waves: the origin of neither motion is yet explained.

At Re between 350 and 2000 (if not greater) there is an interaction between vortex formation and the transition waves. Figure 39 *a* and *b* shows two, well separated, instants in the same run. In figure 39 *b* the transition wave and the rolling-up vortex are superimposed while in figure 39 *a* two waves are seen on each side of the wake, and vortex shedding is temporarily inhibited. The interaction remains unexplained. The original suggestion by Gerrard (1967) was that in this region the free shear layers are at their widest transverse separation which inhibits their interaction. There is, however, no noticeable difference in the separation of the shear layers in figure 39 *a* and *b*.

As a consequence of interference like that illustrated, the vortex formation frequency is imprecise in this range of Re . Figure 41 shows a similar occurrence to that shown in figure 39 but at a higher Re at which the transition waves are strong enough to roll up into vortices. Again sometimes there is whole wake oscillation producing vortices and sometimes there is not. It may be remarked that if a vortex street is formed downstream rather than at a position close to the body the fluctuating lift is small because the transverse momentum flux may be balanced by fluid motions rather than by body forces.

Transition waves display a regularity which is absent in the oscillating wake at other Re or at these Re further downstream. Besides being in phase on the two sides of the wake the transition



FIGURE 37. The wake of a circular cylinder at $Re = 464$.

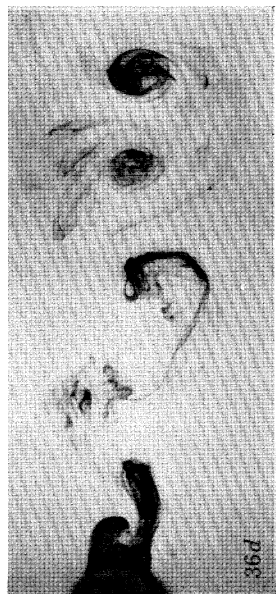
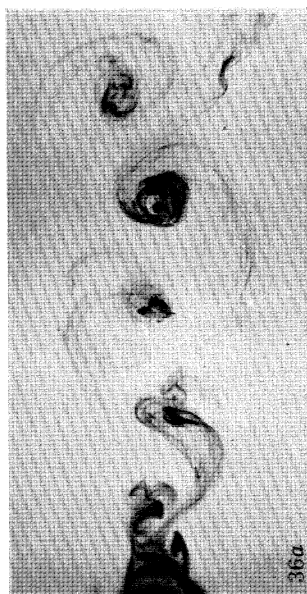


FIGURE 36. The wake of a circular cylinder at $Re = 407$.
Consecutive views separated by 0.55 period.

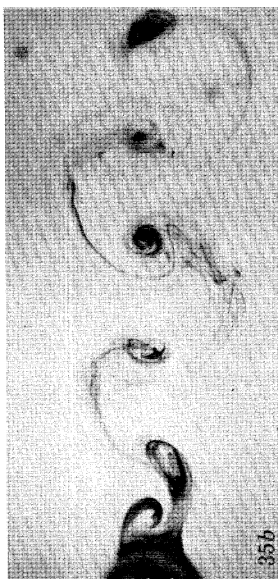


FIGURE 35. The wake of a circular cylinder at $Re = 340$.
Consecutive views separated by 0.41 period.

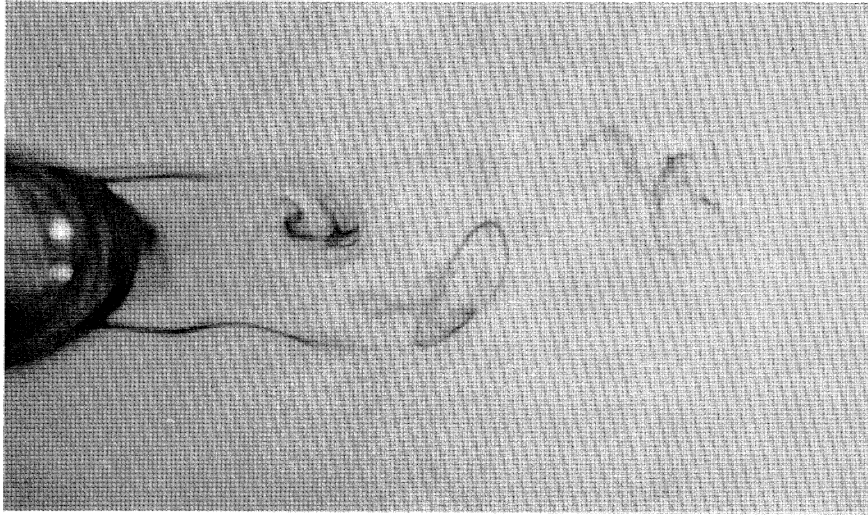


FIGURE 38. Transition waves at $Re = 488$.

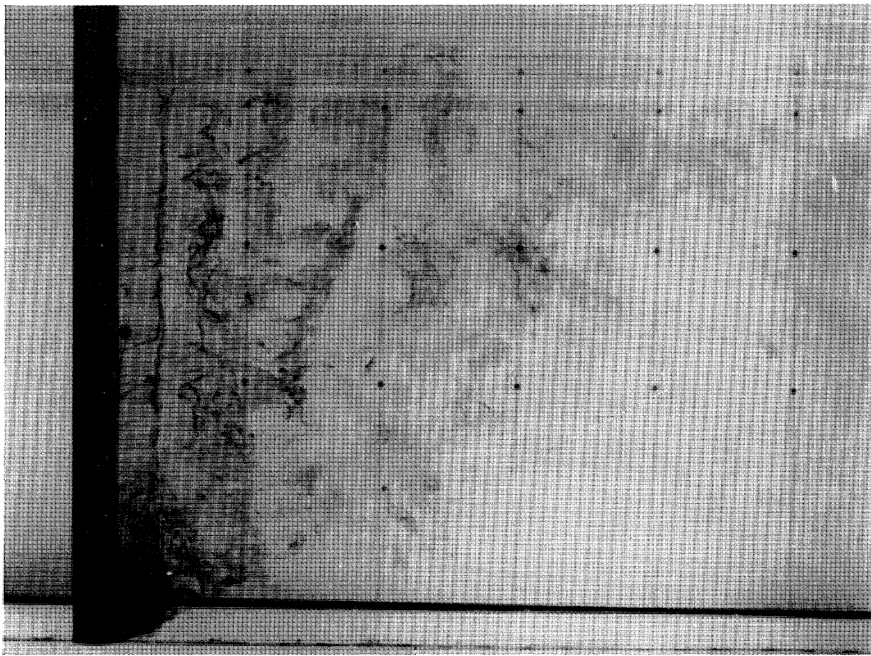


FIGURE 42. Side view of the wake at $Re = 1116$ showing the transition waves in phase along the span.

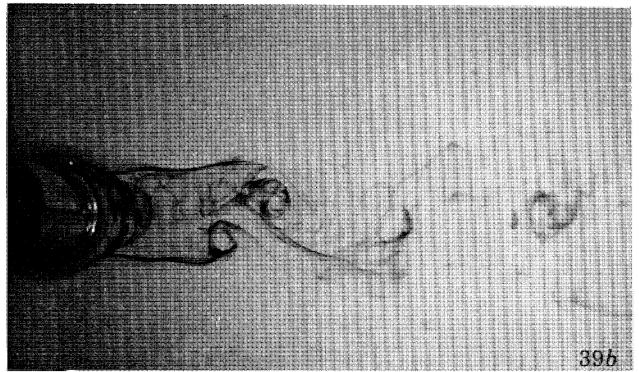
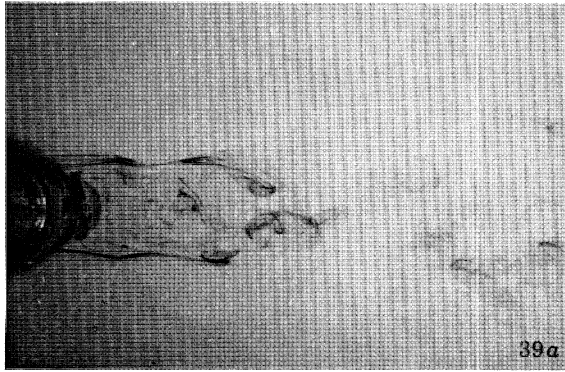


FIGURE 39. Transition waves at $Re = 682$.

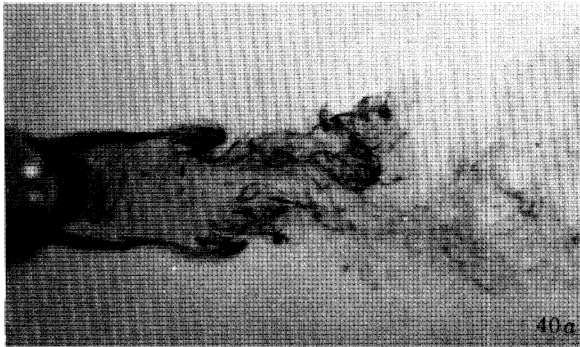


FIGURE 40. Transition waves at $Re = 1083$.

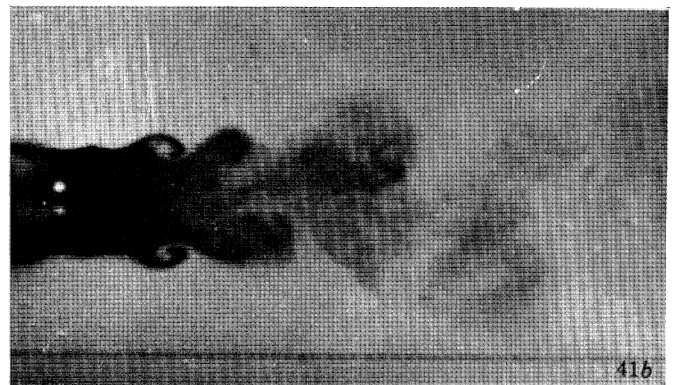
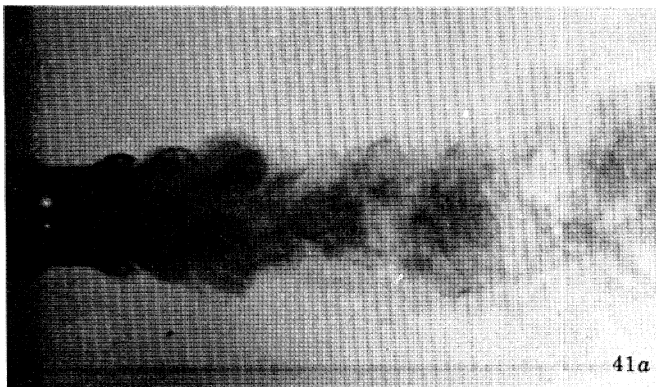


FIGURE 41. Transition waves at $Re = 1968$.

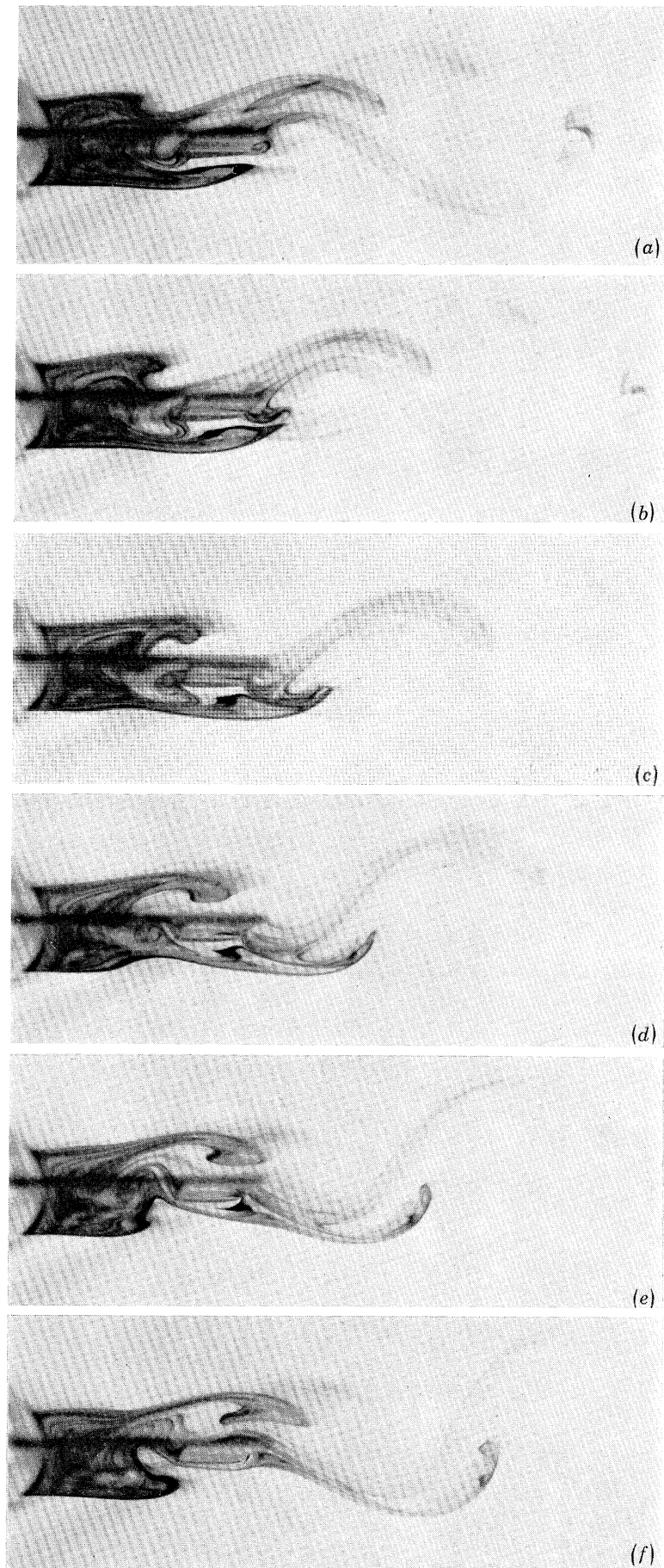


FIGURE 48. Consecutive equally spaced views of the wake of a circular cylinder with splitter plate with $g/d = 1.265$ at $Re = 166$.

waves are in phase along the length of the body. Figure 42, plate 12, shows a side view in which a transition wave in phase for the whole body length is visible. It is remarkable that this regular behaviour extends even to the ends of the cylinder.

The frequency of the transition waves as well as the shedding frequency have been measured by the direct method of counting and using a stop watch. The results are shown together with the results of Bloor in figure 43. It is interesting to note that the departure from a straight line relation, in the lg–lg plot of this figure, which Bloor discovered, does in fact disappear if one counts all the vortices (transition waves plus shed vortices) and not just the transition waves.

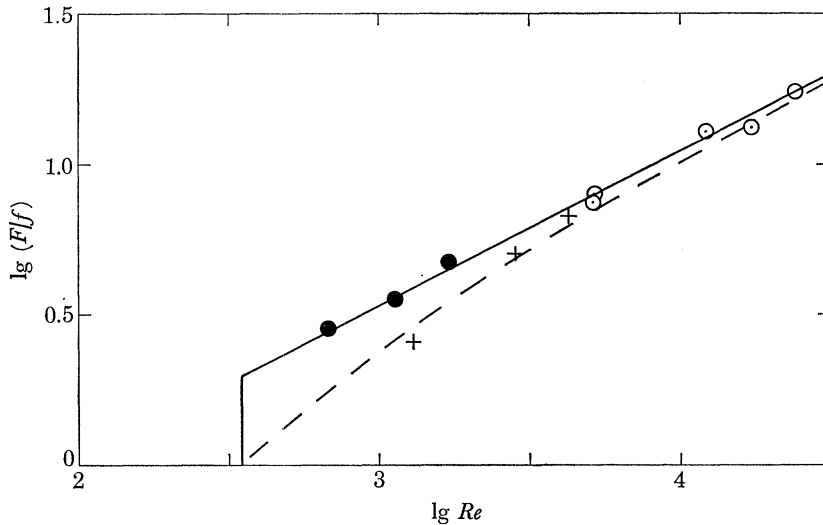


FIGURE 43. Frequency in the near wake as a function of Re . \circ + Bloor (1964); \bullet present measurements. — $F = f_T$ = 'total' frequency counting all vortices. --- $F = f_t$ = transition wave frequency.

The two curves in figure 43 are related by $f_T/f = 1 + f_t/f$ where f_T is the frequency of all the waves, f is the shedding frequency and f_t is the transition wave frequency. At the lower Re in this range it is reasonable to count all the waves because in some cases the transition wave and the shed vortex are indistinguishable. The lines drawn in figure 43 indicate why the value $Re = 350$ is chosen to mark the start of the range. Measurements near to $Re = 350$ are difficult because the transition waves are only intermittently present.

We can only conclude our remarks on transition waves by saying that their development and interaction with vortex shedding is not understood. There is some other work which further illuminates their formation. In flow started from rest Honji & Taneda (1969) discovered that at Re greater than 522 there existed a separation of the reversed flow behind the cylinder. In this way a triangular region bounded by the body and two separated boundary layers was formed. In a film on bluff bodies and vortex shedding made by Prandtl one can see transition waves produced from such a triangular region in what appears to be a shedding mechanism like the main vortex shedding at high Re but on a smaller scale.

9. FLOW PAST BLUFF BODIES OTHER THAN CIRCULAR CYLINDERS

The question which naturally arises from what has been written above is whether the flow régimes observed in the flow past a circular cylinder are different for bluff bodies of different cross sectional shape. At high Re the effect of splitter plates appended to the circular cylinder helped to elucidate the mechanism of the production of vortices. The results of some preliminary observations are presented in this section.

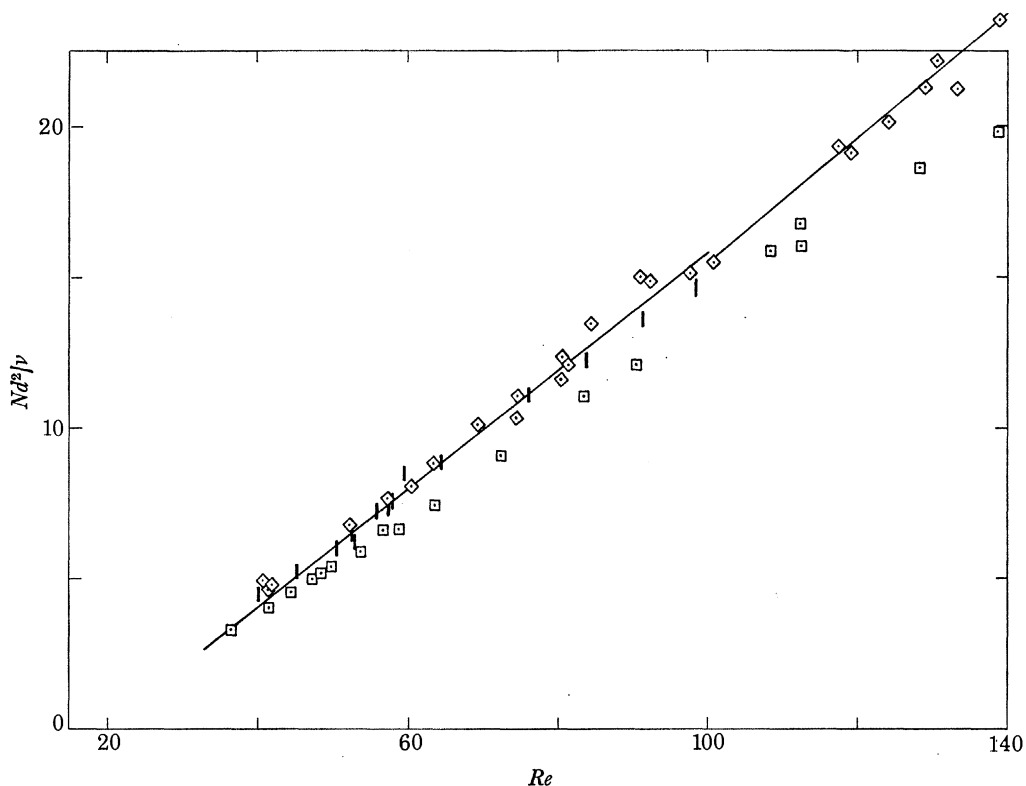


FIGURE 44. Stokes number as a function of Re for different cross section cylinders. — Circular cylinder as figure 2; | flat plate; \square square section; \diamond diamond section.

(a) *Variation of frequency with Re for cylinders of various cross sectional shape*

In figure 44 the variation of wake frequency with Re is presented for the same cross sectional shapes that were discussed at Re less than Re_{osc} in § 4. The Re is based on the maximum transverse dimension of the cross section. The frequency observed in the wake of the flat plate and the diamond-shaped cylinder are very little different from the circular cylinder results. The diamond has a just significantly higher frequency at Re less than 100. The frequency measured behind the square-section cylinder is significantly below that of the circular cylinder at the same value of Re . We shall see that a splitter plate, of length equal to the diameter, in the centre of the wake of a circular cylinder, reduces the frequency. The square-section cylinder is a flat plate with a wide splitter plate of length (and width) equal to the transverse dimension d . Comparison of figures 44 and 46 shows that the frequency reduction is approximately the same in these two cases at Re between 90 and 120.

(b) *The effect of splitter plates on the flow past a circular cylinder*

Measurements have been made with a splitter plate one diameter in length with a variable gap between the leading edge of the plate and the circular cylinder, as shown in figure 45. This figure shows a surprising result. The measurements made by Roshko (1954*b*) at $Re = 10^4$ were repeated here at $Re = 150$ by observing the effect on the wake frequency of the variation of the gap. The variation of frequency with gap size is essentially the same. From what has gone before we know that the mode of vortex production is not the same at these two Re . The effect of the splitter plate on the flow at high Re was described by the author (1966*b*), the different mechanism at low Re will be described here. It appears that the agreement between the two sets of results in figure 45 is fortuitous.

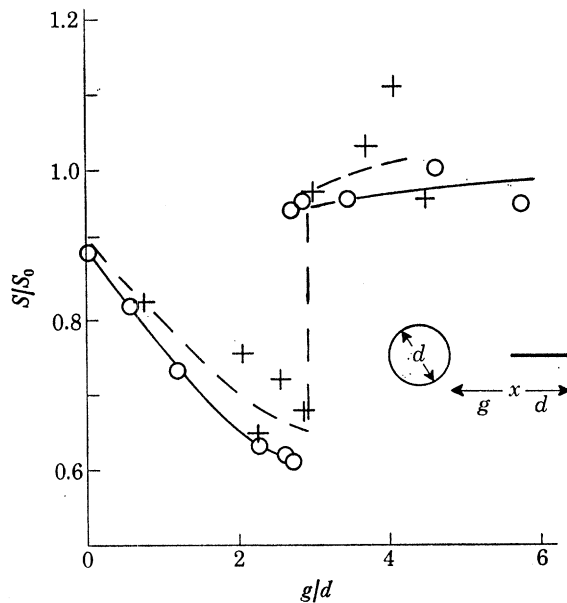


FIGURE 45. Ratio of wake frequency, expressed as Strouhal number, with a splitter plate to that of a plain circular cylinder. \circ Roshko (1954*b*) $Re = 10^4$. $+$ Present measurements, $Re = 150$.

Frequency has been measured for three gap sizes at various Re with the results shown in figure 46. The splitter plate has essentially the same effect at all Re of the range covered. The straight line drawn through the values corresponding to the largest gap size shows that there is no immediately obvious change at $Re = 100$. We have already seen however that there is no obvious change in the flow pattern at this Re either. It is possible that a change may become apparent at Re greater than 140 but measurements at Re greater than the values examined here would be necessary to investigate this effect. The insertion of a splitter plate shifts the frequency to a value corresponding to a lower Re but the effect is more complicated than this.

Values of the vortex speed have also been measured and are shown in figure 47. These results also indicate a shift to lower Re values. The points marked W, signifying a wavy wake (without vortices), lie at a value of Re at which the wake is in the form of a vortex street in the absence of the splitter plate. That the vortex speed is reduced by the splitter plate suggests that the vortices become weaker but there is also an effect of change in vortex disposition. As with the

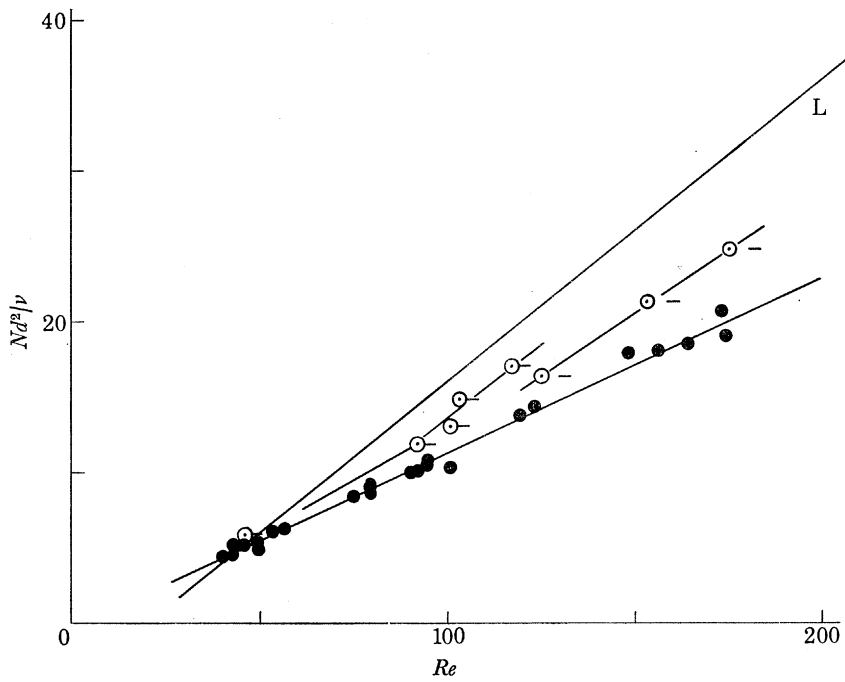


FIGURE 46. Stokes number as a function of Re for circular cylinders with and without splitter plates of the type shown in figure 45. L curve of figure 1 and table 2. \circ - $g/d = 0$, \circ - $g/d = 0.75$, \bullet $g/d = 2.25$.

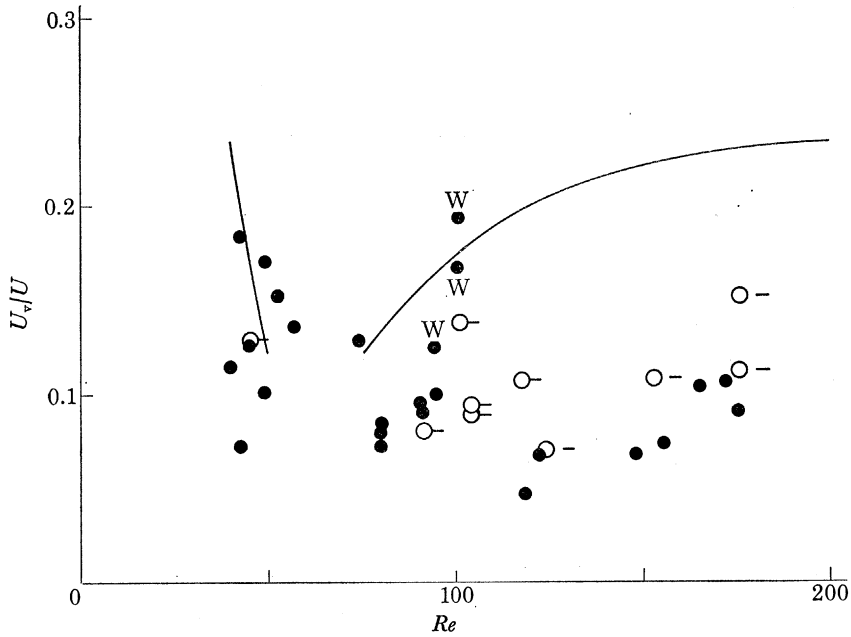


FIGURE 47. The effect of splitter plates on vortex speed in circular cylinder wakes. — Plain cylinder as figure 12, \circ - $g/d = 0$, \circ - $g/d = 0.75$, \bullet $g/d = 2.25$, W $g/d = 2.25$ wake sinuous but no discrete vortices visible.

frequency, the splitter plate has less effect on the vortex speed at lower Re . It appears also that the variation of gap size has less effect on the vortex speed than on the frequency.

Figure 48, plate 14, shows flow visualization of the wake with a splitter plate. One notices, by comparison with figures 18 to 21, that the developing wake has the appearance of the much lower Re wake of a plain cylinder. It is clear that the vortices are weakened by mixing taking place round the splitter plate. One sees the transfer of dyed fluid across the wake at the leading and trailing edges of the splitter plate as the sinuous wake centre line plays between these positions. At large gap sizes the wake centre line and its attendant reversed flow will miss the splitter plate. As the gap is increased from small values a size will be reached at which plate interference and mixing across the wake will cease. This is attended by the abrupt return to the plain cylinder frequency. There is no transfer of fluid between the two sides of the wake in figures 18 to 21. We surmise that there is a transfer of circulation by diffusion at Re less than 100 in an amount similar to that induced by convection when a splitter plate is present. When a splitter plate is inserted into a wake at Re less than 100 it interferes with the diffusive transfer as well as producing convective transfer across the wake. The two effects will cancel each other to some extent: figures 46 and 47 indicate that the convective effect is the larger.

10. CONCLUSIONS

The wakes of bluff cylinders have been observed by means of flow visualization by dye. The dye has been painted on the rear of the bodies from where it was washed into the wake, making visible the filament lines springing from the separation lines. The majority of the findings relate to the motion through water with minimal background motion. The flow visualization is clearer in this condition but it is not considered that the main conclusions would be affected by the presence of some background motion though the effects would depend on the scale of the motion. The principal results will be summarized by describing the wake of a circular cylinder as the Re rises through the range with which we have been concerned.

At low Re (less than Re_{osc}) the flow possesses an internal and an external region. The internal flow consisting of two standing eddies is contained within the stagnation streamline boundary (the separation bubble) at the rear of the body. The bubble boundary exhibits gathers at $Re = Re_{osc}$. The value of Re_{osc} is difficult to define precisely, but occurs when the length of the bubble is approximately $2d$ for each of the cross sectional shapes investigated. The gathers are associated with the transfer of fluid into and out of the bubble at its downstream end and also with the oscillation of the wake. For the circular cylinder, $Re_{osc} = 34$; the Re_{osc} values for other cylinders are shown on figure 5. At Re below Re_{osc} the circulation of the attached eddies is maintained by a balance of the diffusion of vorticity. Convective transfer of circulation from the bubble begins at Re_{osc} but the effect of diffusion is of major importance up to Re in the region of 100. Between Re_{osc} and $Re = 100$, the Stokes number is given by

$$Nd^2/\nu = 0.1959 Re - 3.811.$$

At $Re = 100$ the vortex motion changes. From the instant of its first appearance as a wave in the dye filament, the vortex moves with constant speed at low Re . At Re greater than 100 there is an acceleration phase lasting for about one period in time and about one half wake wavelength in distance. The last remnants of the standing eddy pair are seen to disappear at $Re = 100$. There is some evidence that the vortex strength and the base pressure coefficient reflect these changes. It is suggested that at this Re the régime in which vorticity diffusion

dominates the vortex formation comes to an end. The general appearance of the wake as shown by flow visualization does not change at $Re = 100$ except in the detail of the disappearance of the mass of dye close behind the body. The interpretation of the flow visualization, however, may well change at this Re .

Between Re of 100 and 140, a dual frequency relation has been found. At the beginning of a run (and possibly at the centre of a very long cylinder) the Stokes number is found to be given by

$$Nd^2/\nu = 2.586 \times 10^{-4} Re^2 + 0.1619 Re - 2.784$$

whereas in the developed wake, where the effects of the ends have spread along the span,

$$Nd^2/\nu = 0.2064 Re - 5.173,$$

and this relation holds up to $Re = 250$. At Re smaller than 140, the vortices are roughly straight and parallel to the cylinder axis at the beginning of the run. As end effects encroach across the wake, the vortices become bowed.

At low Re the wake centre line is sinuous near to the cylinder. The dye in the near wake stays on its own side of this centre line. Fluid is removed from the back of the body by entrainment into the separating shear layers; replacement of fluid is along each side of the sinuous centre line from the downstream direction. At Re less than 100, vortex strength is reduced by diffusive cancellation of vorticity. At Re close to 100, there is evidence that the strength of the developed vortices undergoes a sharp decrease but this has not been investigated and is not at present understood. We see the involvement of the vortex which has already left the cylinder at Re above 140 where in the 'finger', dye which has rolled up into a vortex returns to the cylinder. These fingers are associated with Roshko's transition range in which the vortex strength changes from being approximately constant at lower Re to possessing irregular and continuous changes at higher Re . In this range the vortex strength decreases due to entrainment of fluid bearing oppositely signed vorticity from the region close behind the body. When the fingers appear, the vortex formation becomes more nearly in phase along the span of the cylinder. At all Re an induced flow takes place between the vortices. The region in which this transverse flow develops approaches the cylinder as Re increases. At Re above 250 the mode of vortex formation begins to change as this transverse flow occurs closer to the body. It seems that, if transition waves did not start to appear at Re above 350, the high Re mode of vortex formation described by Gerrard (1966*b*) would be fully operative at Re of about 500. The frequency of the vortex shedding undergoes a transition between Re of 250 and 400. Above $Re = 380$ the Stokes number is given by

$$Nd^2/\nu = 0.1913 Re + 2.791.$$

At Re above 350, transition waves begin to appear on the filament lines springing from the separation points. These waves have the same characteristics as the waves on the shear layer, leaving a rearward facing step, but are somehow coupled across the wake because they are in phase on the two shear layers and also in phase along the span of the cylinder. Transition waves intermittently interfere with the vortex shedding mechanism so that the wake is sometimes oscillating and sometimes turbulent. This is observed in the minimal background motion condition of the tank used in these experiments. Other work has suggested that their interference with vortex shedding only occurs in conditions of minimal disturbance.

Transition to turbulence in the wake commences as soon as the vortex street is formed, at

Re_{vs} , due to three-dimensional contortions of the vortices. This low Re effect is a consequence of the finite span of the cylinder or of non-uniformities in the motion such as the 'knots' referred to in §6. Transition to turbulence in which the vortex cores are composed of fluid in turbulent motion commences at Re somewhat greater than 140 and is due to mixing of fluid in the induced transverse flow. At this stage the vortices closest to the cylinder are laminar. Transition close to the cylinder occurs in the range of Re in which transition waves are present and it is at these Re that the vortices are turbulent when they first roll up.

The approach adopted in this work has been to cover a wide range of Re because by so doing, it is easier to appreciate the main changes which take place and so divide the phenomena into flow régimes in contiguous Re ranges. This philosophy has resulted in spending less time on the investigation of particular flow regions. Several investigations are still necessary for the construction of a more complete description of the flow. Formation region length at low Re needs to be properly defined and investigated. The understanding of the transition at $Re = 100$ would profit from measurement of base pressure and also of vortex strength, neither of which is simple at these Re . A subject with many unexplained features is the occurrence and phase relation of transition waves and their interference with vortex shedding. The whole of this work could be repeated with a slender cylinder as well as with cylinders of different cross sectional shapes. Inevitably we conclude with as many questions as answers!

It is my pleasant duty to gratefully acknowledge the assistance of the Science Research Council whose research grant financed the setting up of the apparatus.

REFERENCES

- Anagnostopoulos, E. & Gerrard, J. H. 1976 A towing tank with minimal background motion. *J. Phys. E Instrum.* **9**, 951.
- Berger, E. 1964a Transition of the laminar vortex flow to the turbulent state of the Karman vortex street behind an oscillating cylinder at low Reynolds number. *Jber. wiss. Ges. L. R.*, p. 164.
- Berger, E. 1964b The determination of the hydrodynamic parameters of a Karman vortex street from hot wire measurements at low Reynolds number. *Z. Flug.* **12**, 41.
- Berger, E. & Wille, R. 1972 Periodic flow phenomena. *A. Rev. Fluid Mech.* **4**, 313.
- Bloor, M. S. 1964 The transition to turbulence in the wake of a circular cylinder. *J. Fluid Mech.* **19**, 290.
- Bloor, M. S. & Gerrard, J. H. 1966 Measurements on turbulent vortices in a cylinder wake. *Proc. R. Soc. Lond. A* **294**, 319.
- Coutanceau, M. & Bouard, R. 1977 Experimental determination of the main features of the viscous hydrodynamic field in the wake of a circular cylinder in a uniform stream. I. Steady flow. *J. Fluid Mech.* **79**, 231.
- Dennis, S. C. R. & Chang, G. 1970 Numerical solutions for steady flow past a circular cylinder at Reynolds numbers up to 100. *J. Fluid Mech.* **42**, 471.
- Gaster, M. 1969 Vortex shedding from slender cones at low Reynolds numbers. *J. Fluid Mech.* **38**, 565.
- Gaster, M. 1971 Vortex shedding from circular cylinders at low Reynolds numbers. *J. Fluid Mech.* **46**, 749.
- Gerrard, J. H. 1965 A disturbance-sensitive Reynolds number range of the flow past a circular cylinder. *J. Fluid Mech.* **22**, 187.
- Gerrard, J. H. 1966a The three-dimensional structure of the wake of a circular cylinder. *J. Fluid Mech.* **25**, 143.
- Gerrard, J. H. 1966b The mechanics of the formation region of vortices behind bluff bodies. *J. Fluid Mech.* **25**, 401.
- Gerrard, J. H. 1967 Numerical computation of the magnitude and frequency of the lift on a circular cylinder. *Phil. Trans. R. Soc. Lond. A* **761**, 137.
- Griffin, O. M. & Votaw, C. W. 1972 The vortex street in the wake of a vibrating cylinder. *J. Fluid Mech.* **51**, 31.
- Griffin, O. M. & Ramberg, S. E. 1974 The vortex street wakes of vibrating cylinders. *J. Fluid Mech.* **66**, 553.
- Hama, F. R. 1957 Three-dimensional vortex pattern behind a circular cylinder. *J. Aeronaut. Sci.* **24**, 156.
- Hama, F. R. 1962 Streaklines in a perturbed shear flow. *Phys. Fluids* **5**, 644.
- Honji, H. & Taneda, S. 1969 Unsteady flow past a circular cylinder. *J. Phys. Soc. Japan* **27**, 1668.
- Hussain, A. K. M. F. & Ramjee, V. 1976 Periodic wake behind a circular cylinder at low Reynolds number. *Aeronaut. Q.* **27**, 123.

- Kohan, S. & Schwarz, W. H. 1973 Low speed calibration formula for vortex shedding from cylinders. *Phys. Fluids* **16**, 1528.
- Koopman, G. H. 1967 The vortex wake of vibrating cylinders at low Reynolds number. *J. Fluid Mech.* **28**, 501.
- Masliyah, J. H. & Epstein, N. 1971 Steady symmetric flow past elliptical cylinders. *Am. Chem. Soc. I.A.E.C. Fundam.* **10**, 293.
- Morkovin, M. 1964 Flow around circular cylinders – A kaleidoscope of challenging fluid phenomena. *Am. Soc. Mech. Engrs Symp.* Fully separated flows, p. 102.
- Nayler, J. L. & Frazer, R. A. 1917 Vortex motion. I. Preliminary report on an experimental method of investigating by the aid of kinematograph photography, the history of eddying flow past a model immersed in water. Aeronaut. Res. Coun. Rep. Memo. p. 332.
- Nishioka, M. & Sato, H. 1974 Measurements of velocity distribution in the wake of a circular cylinder at low Reynolds number. *J. Fluid Mech.* **65**, 97.
- Papailou, D. D. & Lykoudis, P. S. 1974 Turbulent vortex streets and the entrainment mechanism of the turbulent wake. *J. Fluid Mech.* **62**, 11.
- Roshko, A. 1954*a* On the development of turbulent wakes from vortex streets. N.A.C.A. Report 1191.
- Roshko, A. 1954*b* On the drag and shedding frequency of two-dimensional bluff bodies. N.A.C.A. Technical note 3169.
- Sato, H. 1956 Experimental investigation of the transition of laminar separated layer. *J. Phys. Soc. Japan* **11**, 702.
- Taneda, S. 1955 Studies on wake vortices. II. Experimental investigation of the wakes behind cylinders and plates at low Reynolds numbers. *Rep. Res. Inst. appl. Mech. Kyushu Univ.* **4**, 29.
- Taneda, S. 1956 Experimental investigation of the wakes behind cylinders and plates at low Reynolds numbers. *J. Phys. Soc. Japan* **11**, 302.
- Taneda, S. 1963 The stability of two-dimensional laminar wakes at low Reynolds number. *J. Phys. Soc. Japan* **18**, 288.
- Toebes, G. H. 1969 The unsteady flow and wake of an oscillating aerofoil. *Trans. Am. Soc. mech. Engrs D J. Basic Engng* **91**, 493.
- Tritton, D. J. 1959 Experiments on the flow past a circular cylinder at low Reynolds numbers. *J. Fluid Mech.* **6**, 547.
- Tritton, D. J. 1971 A note on vortex streets behind circular cylinders at low Reynolds number. *J. Fluid Mech.* **45**, 203.
- Zdravkovich, M. M. 1967 Note on transition to turbulence in vortex-street wakes. *J. R. Aero. Soc.* **71**, 866.
- Zdravkovich, M. M. 1969 Smoke observations of the formation of a Karman vortex street. *J. Fluid Mech.* **37**, 491.

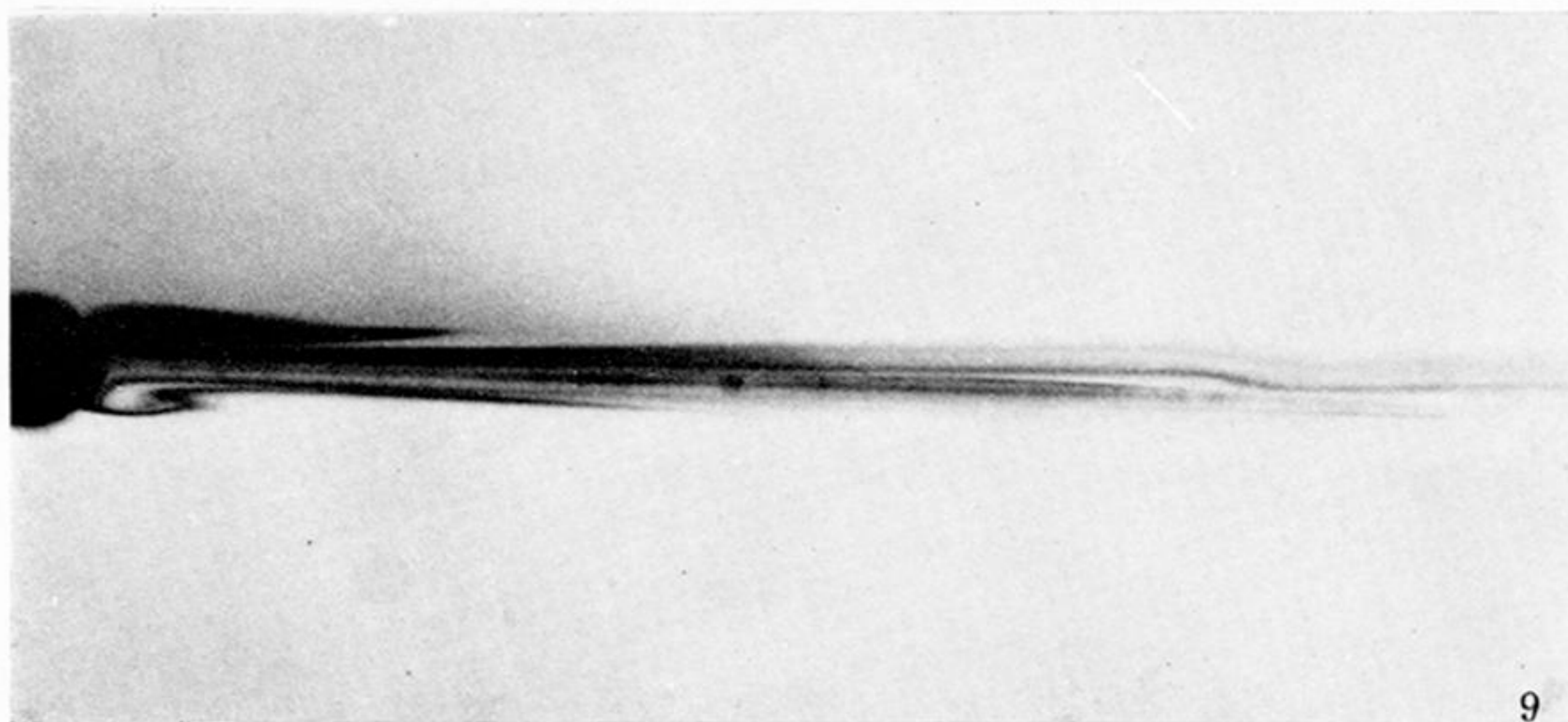
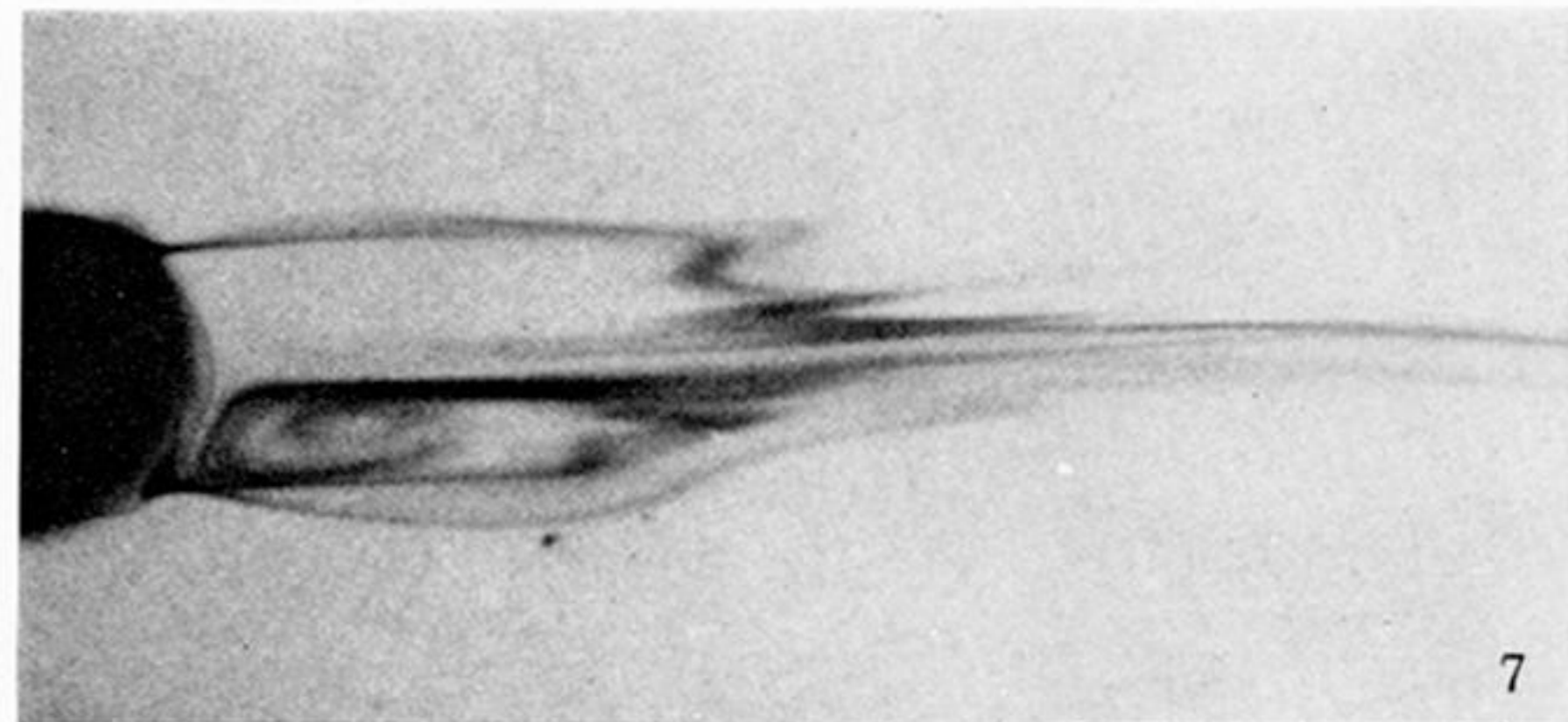
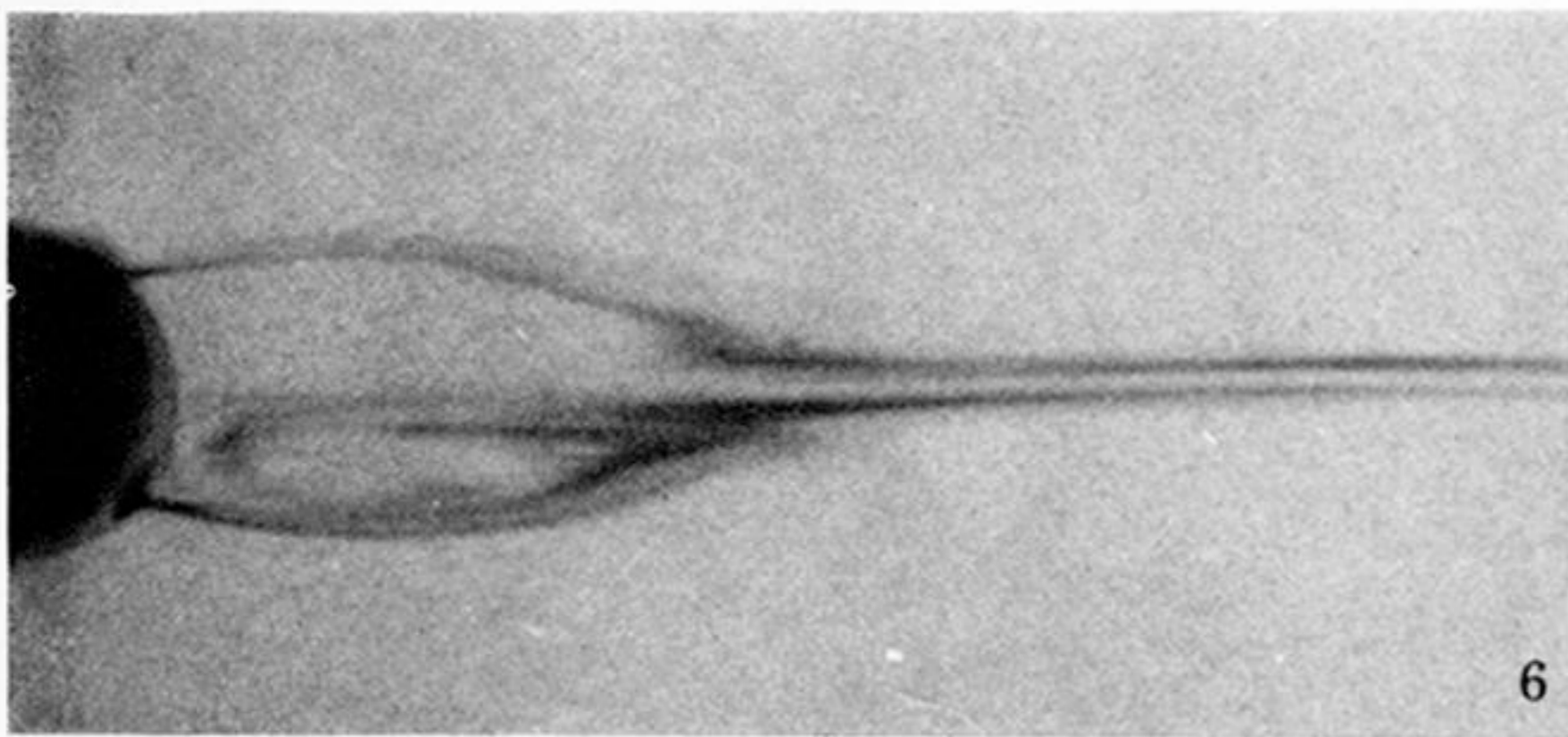


FIGURE 6. Wake of a circular cylinder at $Re = 37.8$.

FIGURE 7. Wake of a circular cylinder at $Re = 44.4$.

FIGURE 8. Wake of a circular cylinder at $Re = 39.6$ showing gathers folding on to sinuous wake.

FIGURE 9. Wake of a circular cylinder with a splitter plate 10.8 diameters in length. $Re = 40.2$.

FIGURE 11. Elongated gathers and a sinuous wake at $Re = 52.5$. Dye injected into the wake.

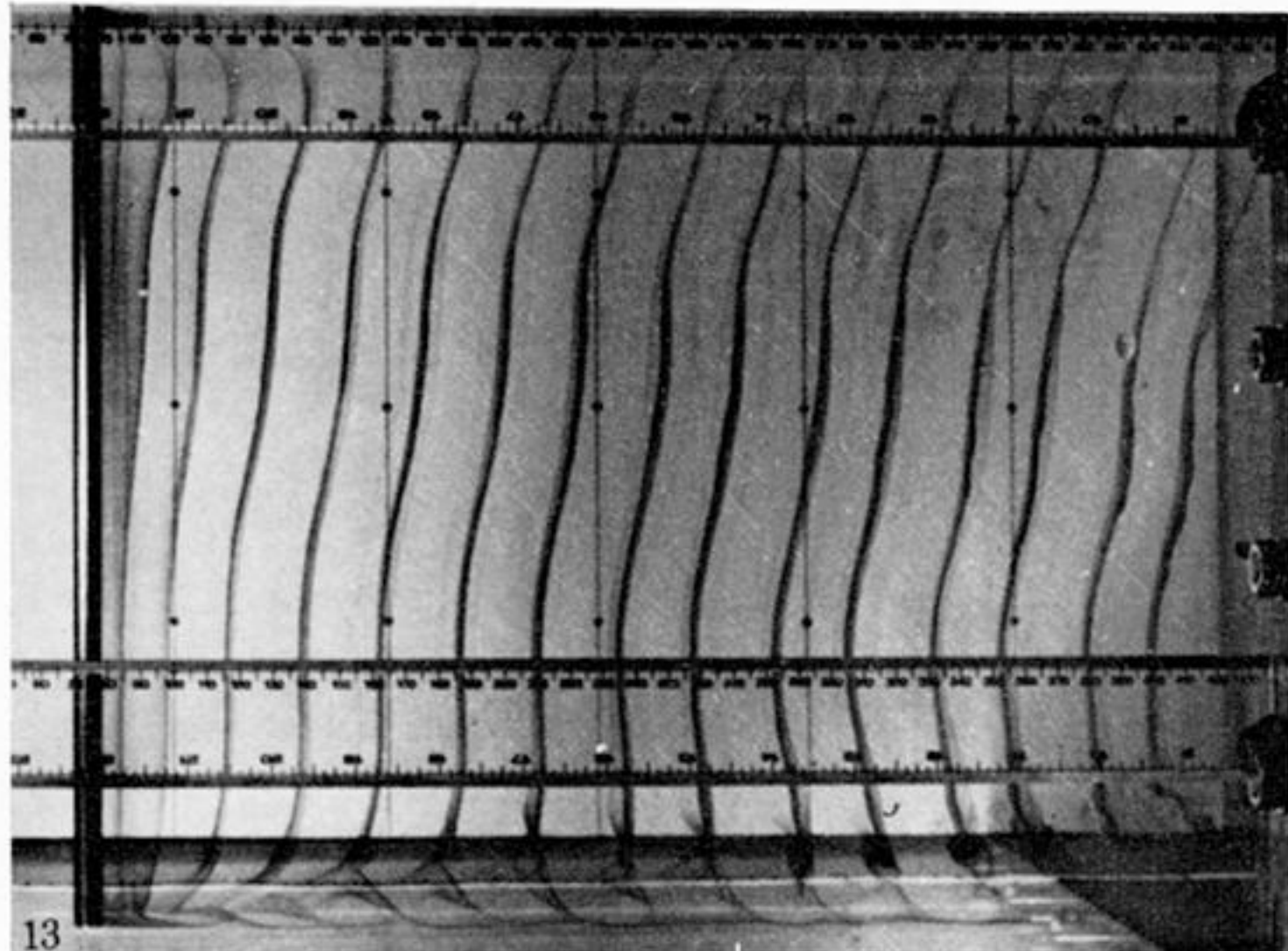


FIGURE 13. Vortex street in its most regular appearance $Re = 75$.

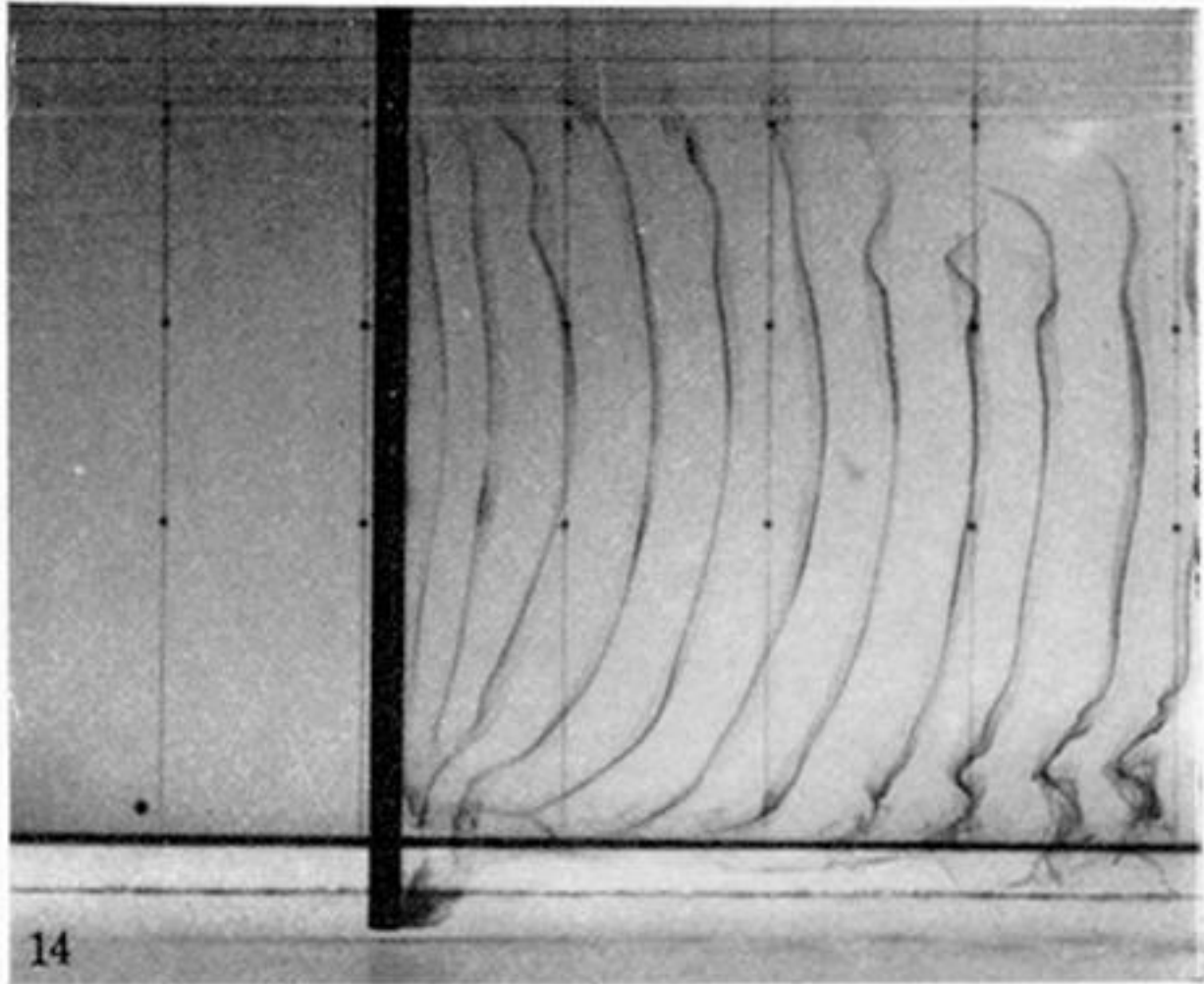


FIGURE 14. The usual bowed appearance of vortices when they attain their established form.

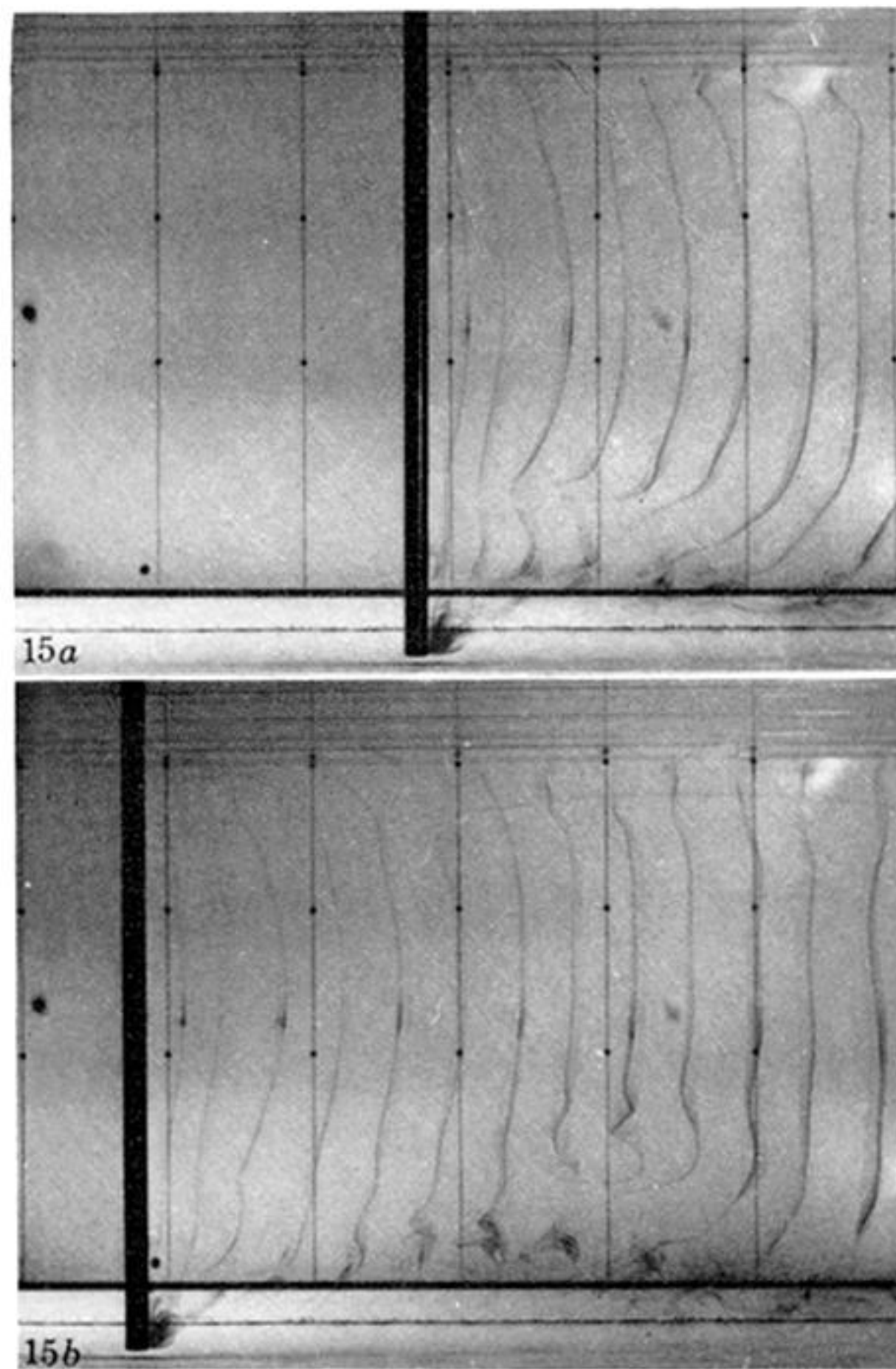


FIGURE 15. Two photographs obtained in the same run showing the appearance of a 'knot' near to the lower end. The water in the tank has minimal background motion. $Re = 120$.

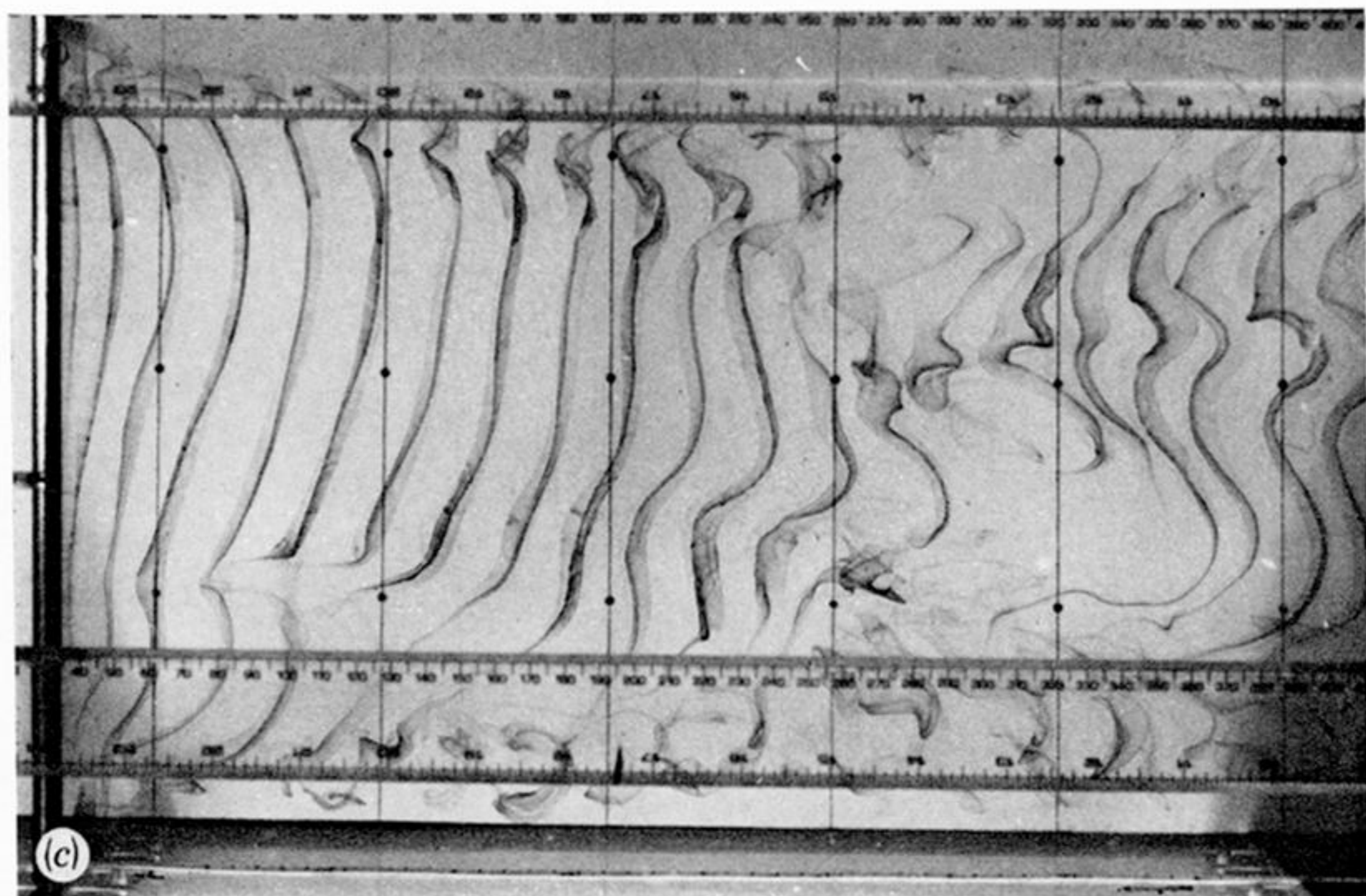
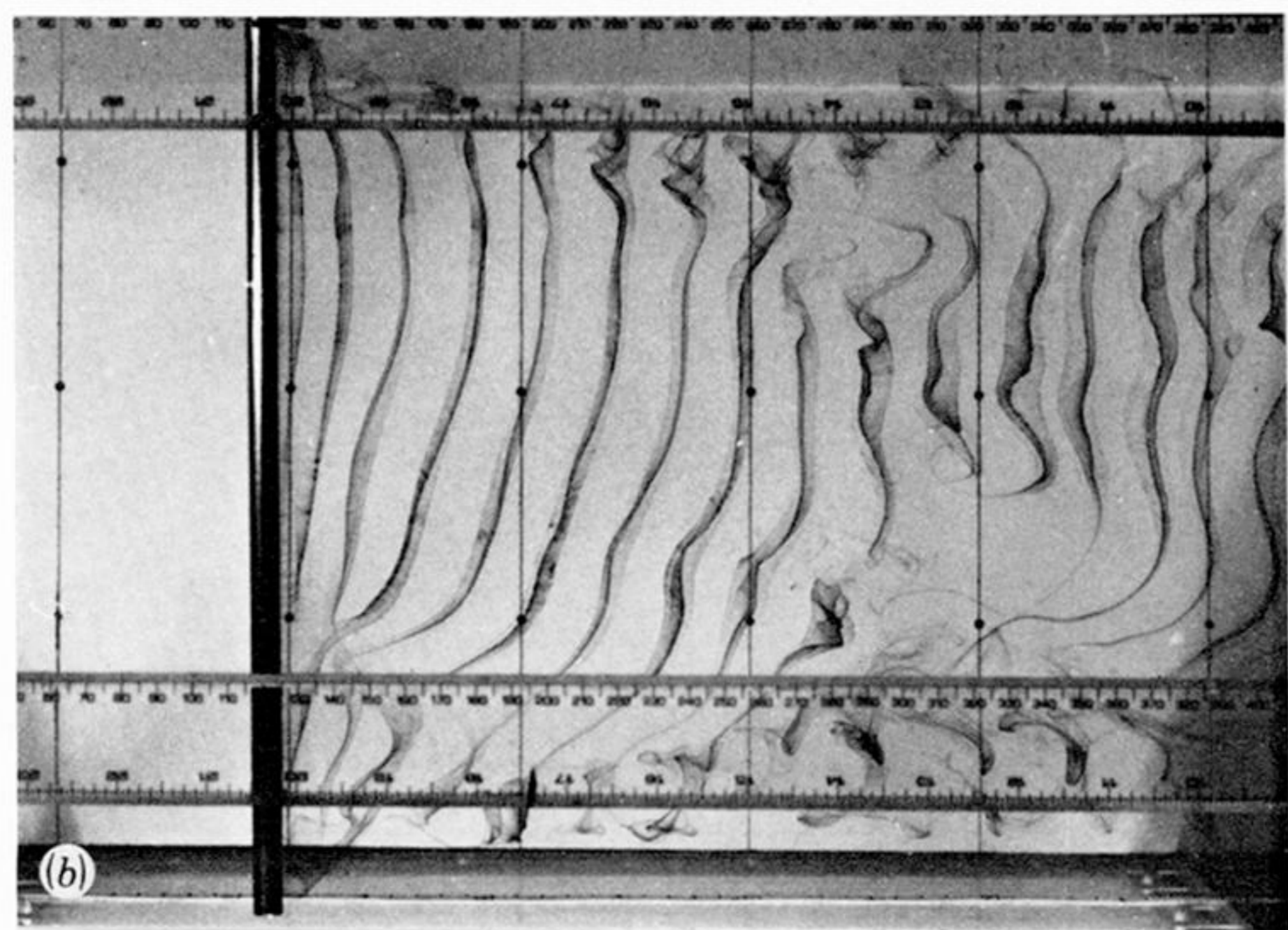
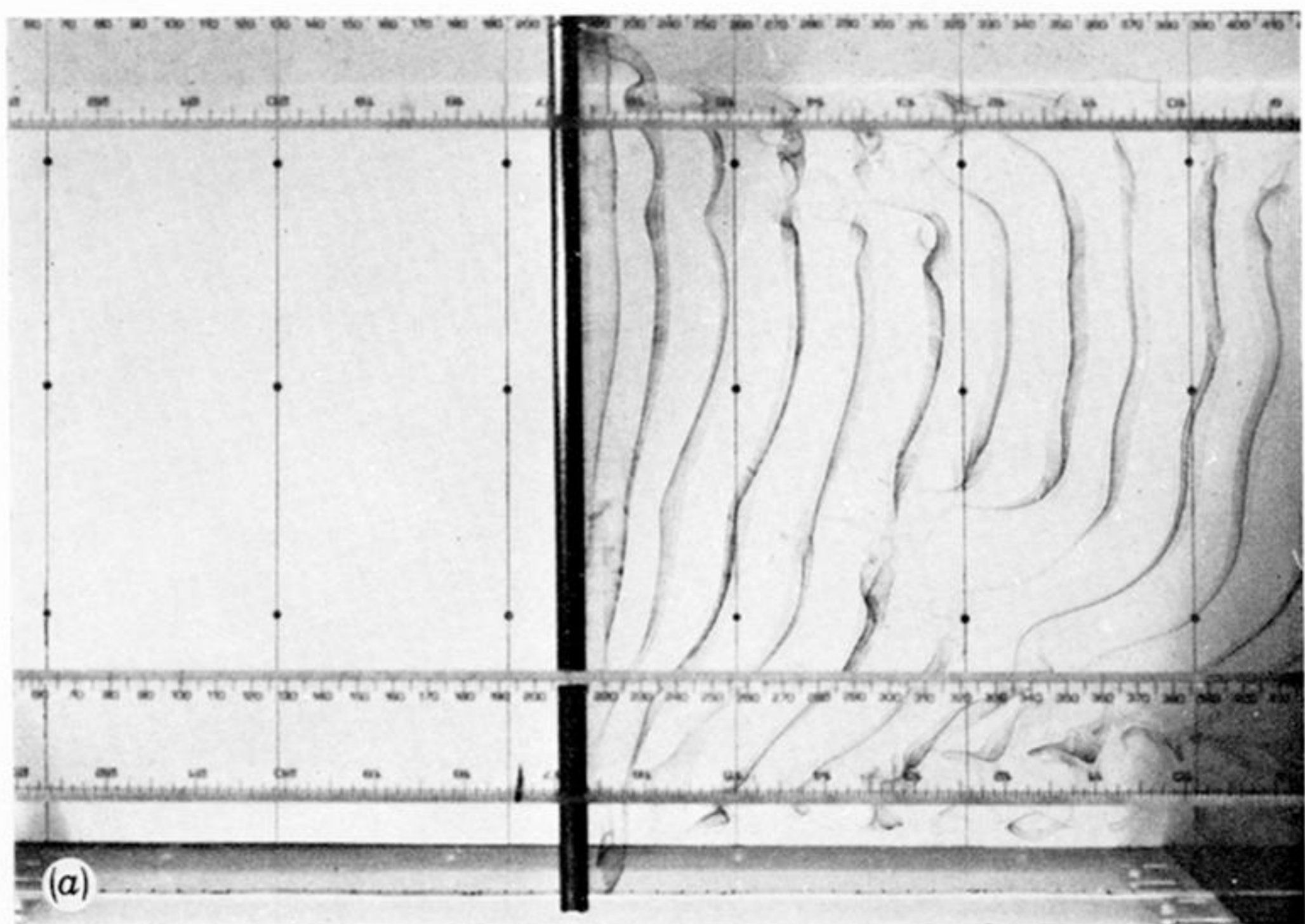


FIGURE 16. The appearance of knots when there are background motions of about 0.2 mm/s. Knots appear at regular intervals. $Re = 129$.

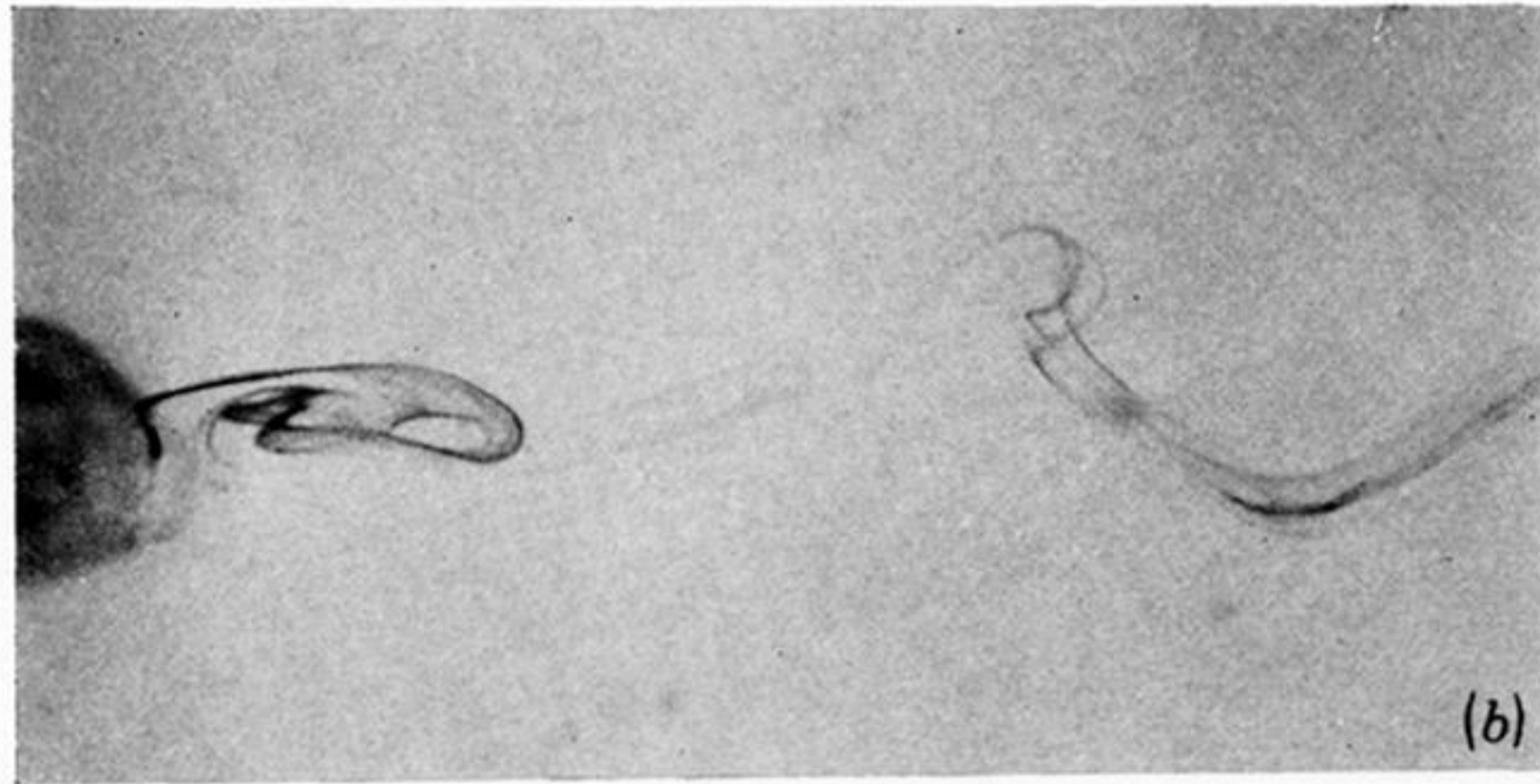
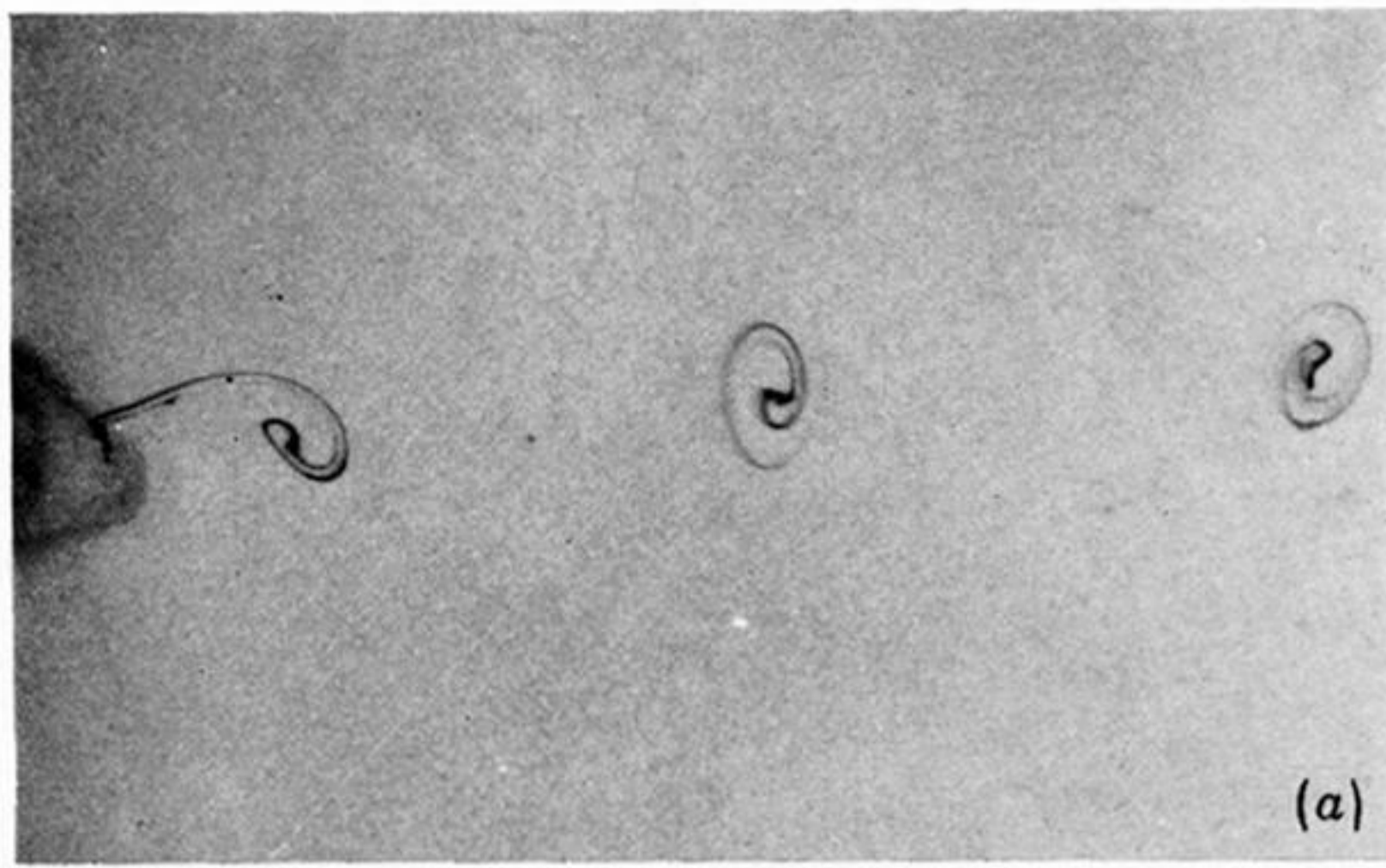


FIGURE 17. The appearance of a knot from above. Wake of a flat plate with a 2% step in its width. Re above and below the step 73.1 and 71.7. Dye on one side of the cylinder only. (a) Wake appearance with no knot present; (b), (c) and (d) Consecutive photographs showing the vortext core linking with the next vortex of the same sign.

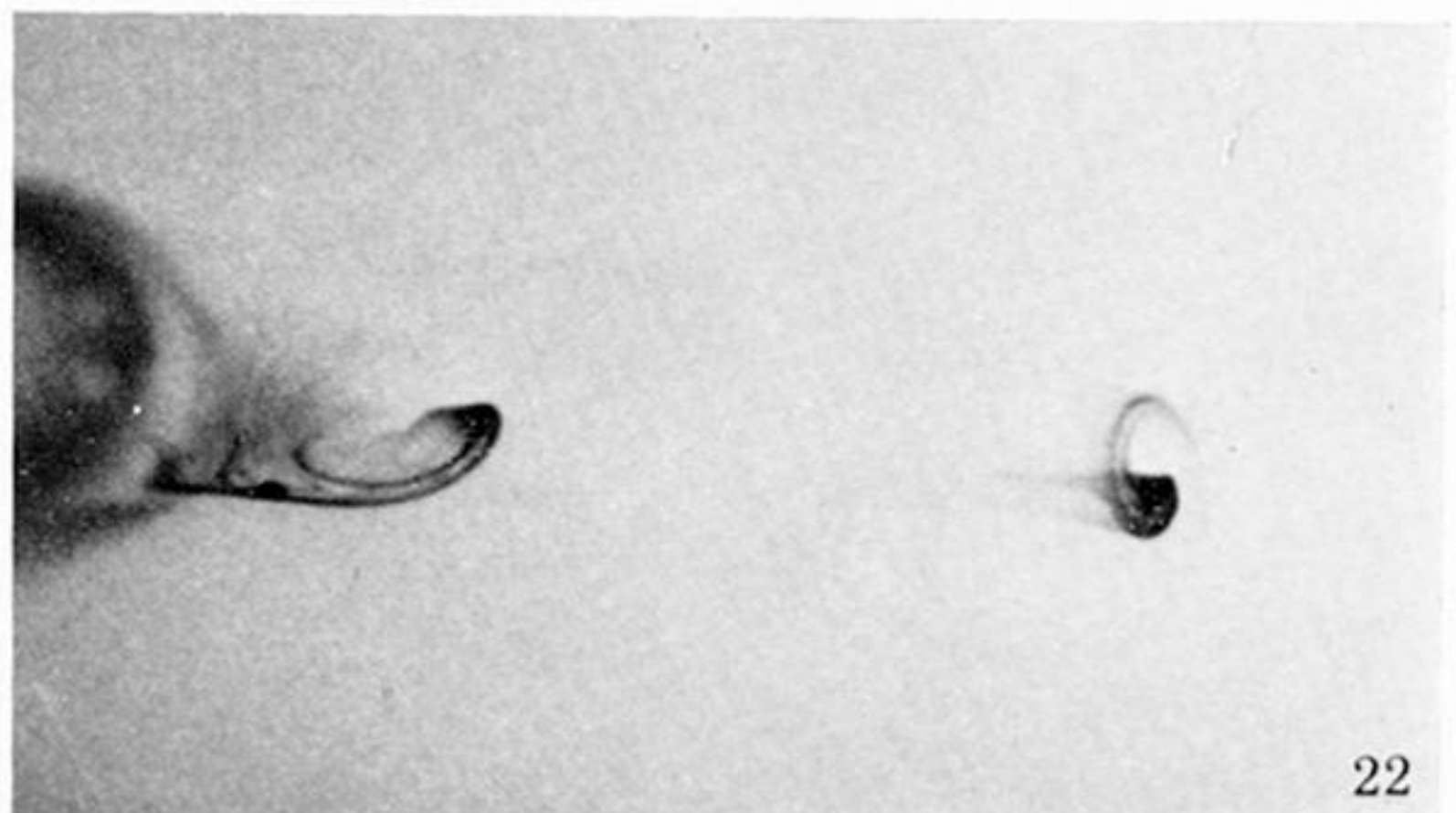
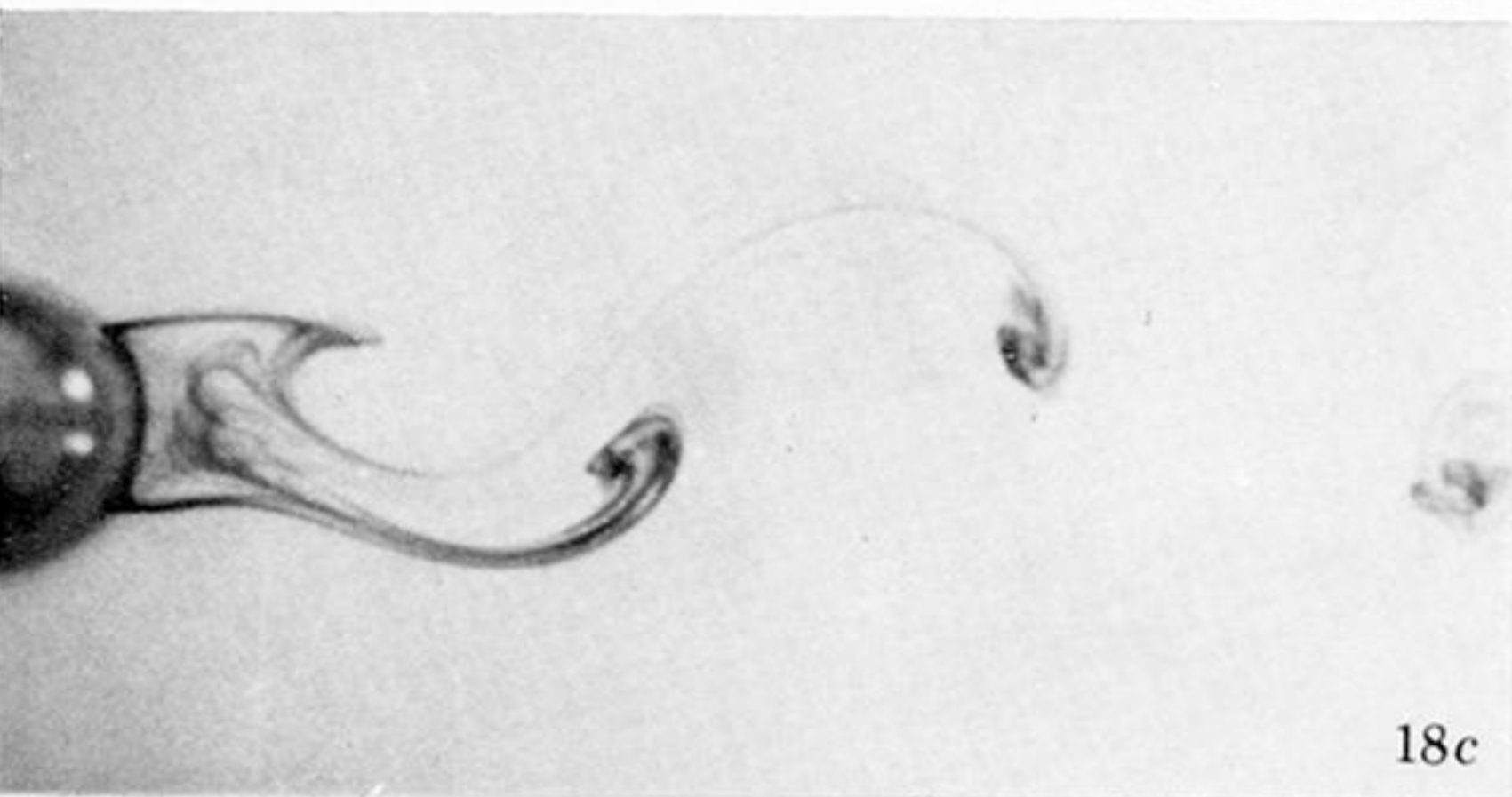
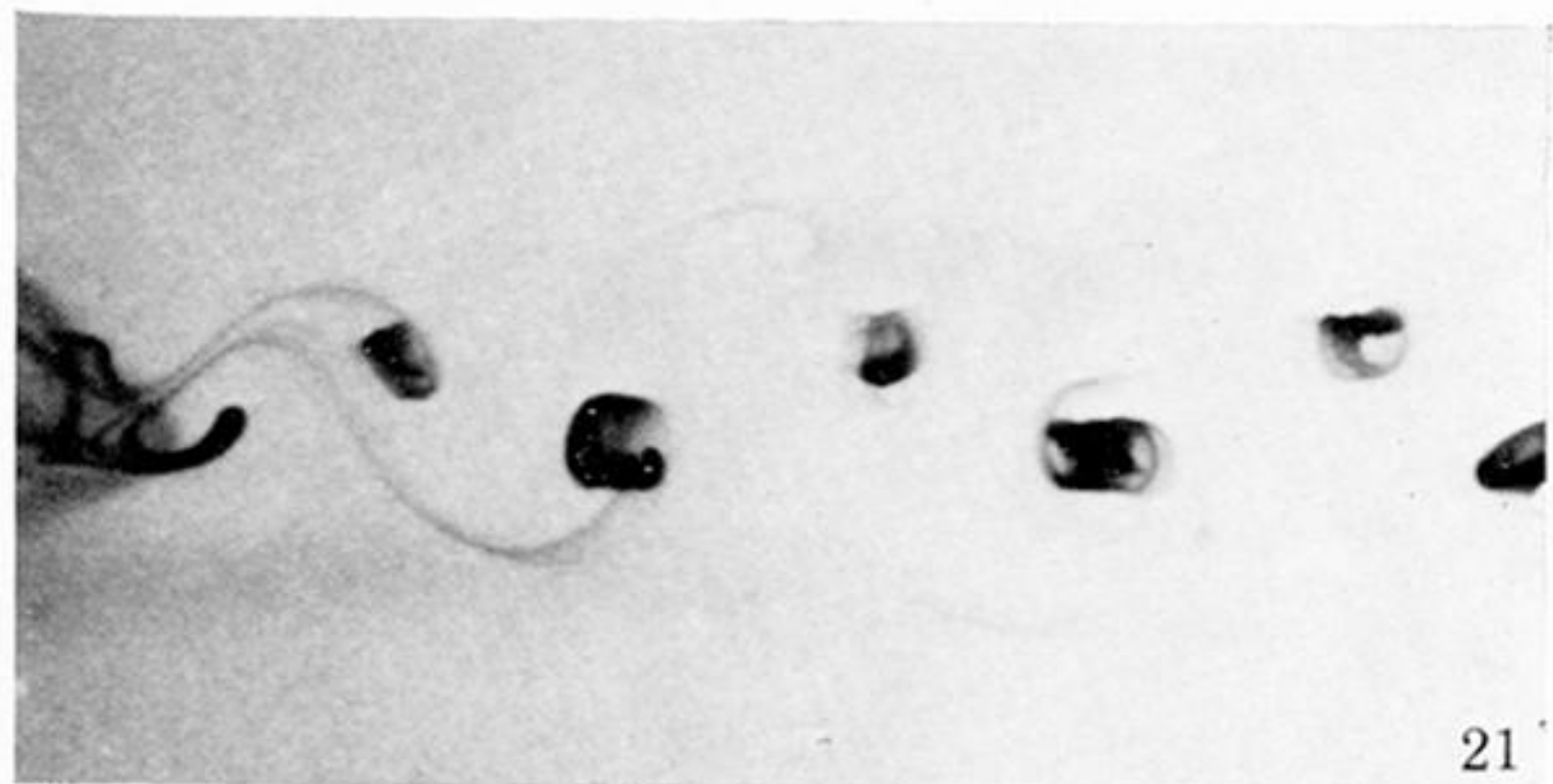
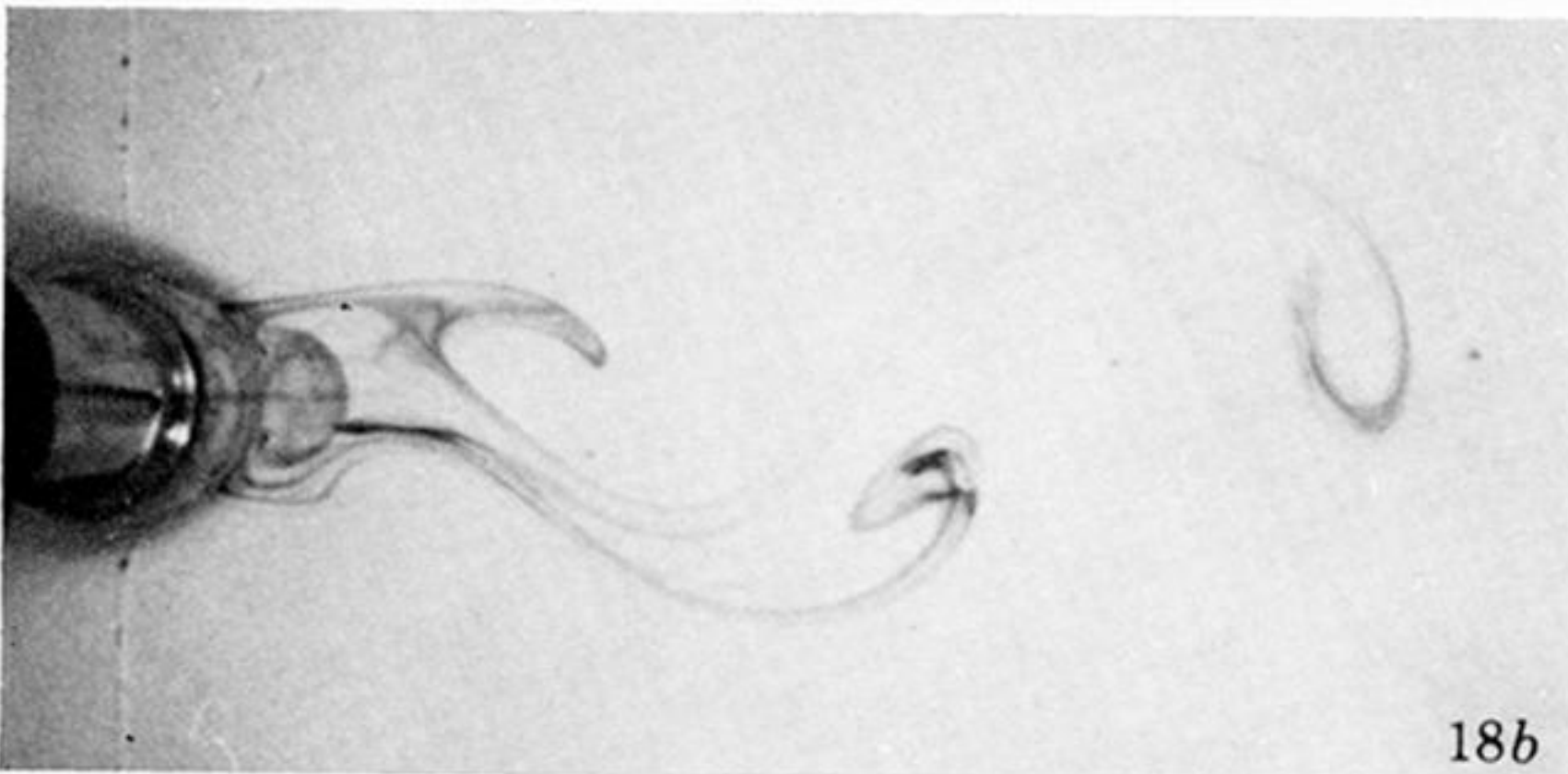
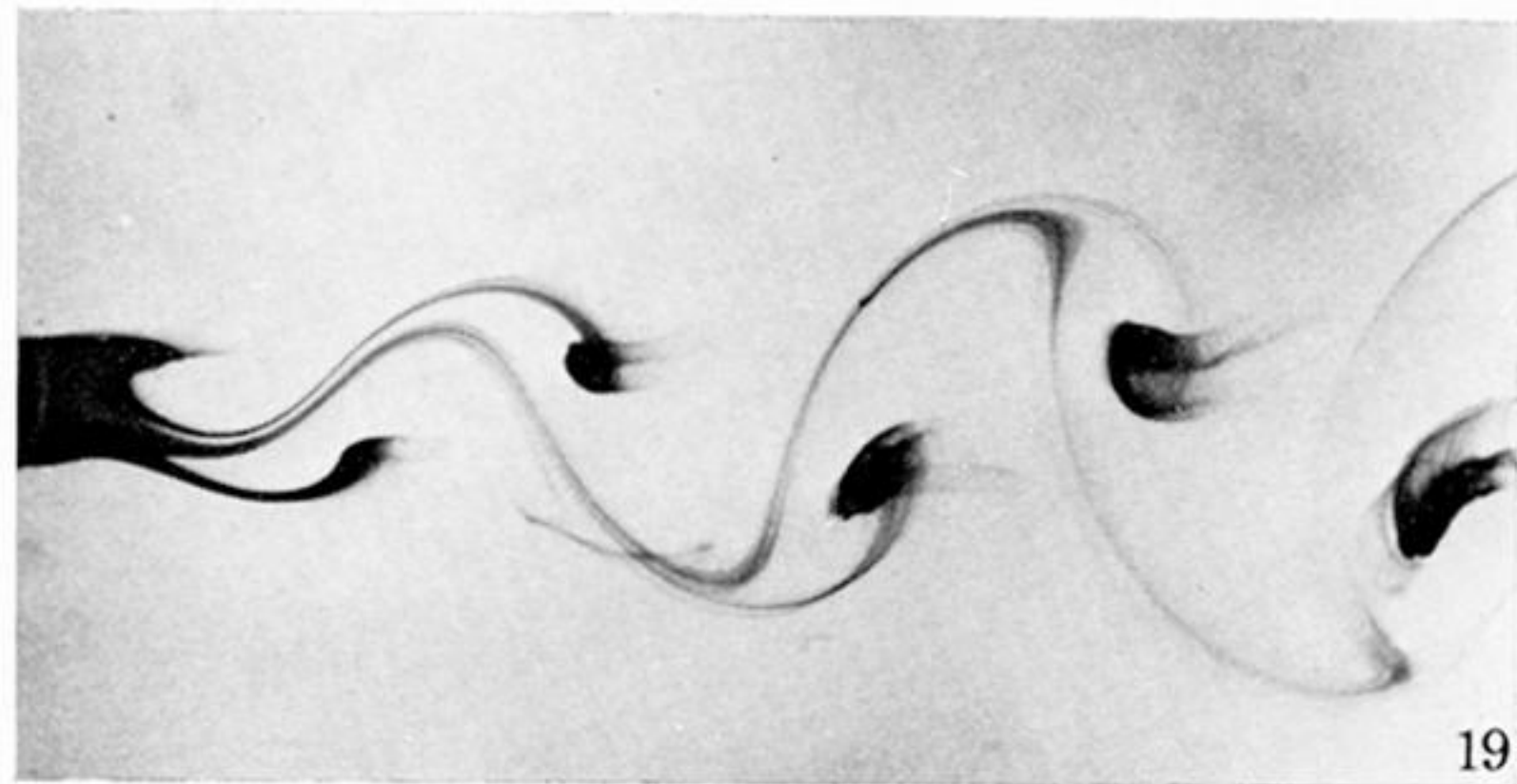


FIGURE 18. Views of the wake produced by injection of dyed water into the wake showing the steadily oscillating pattern resulting after the cloud of dye has been left behind. (a) $Re = 91$, (b) $Re = 124$, (c) $Re = 150$.

FIGURE 19. Circular cylinder wake at $Re = 77$. The region behind the body is filled with dyed fluid.

FIGURE 21. Circular cylinder wake at $Re = 106$. The absence of an accumulation of dyed fluid behind the body is apparent.

FIGURE 22. Circular cylinder wake at $Re = 109$. Dye on one side of the rear of the body. Two filaments of dye are visible close behind the body.

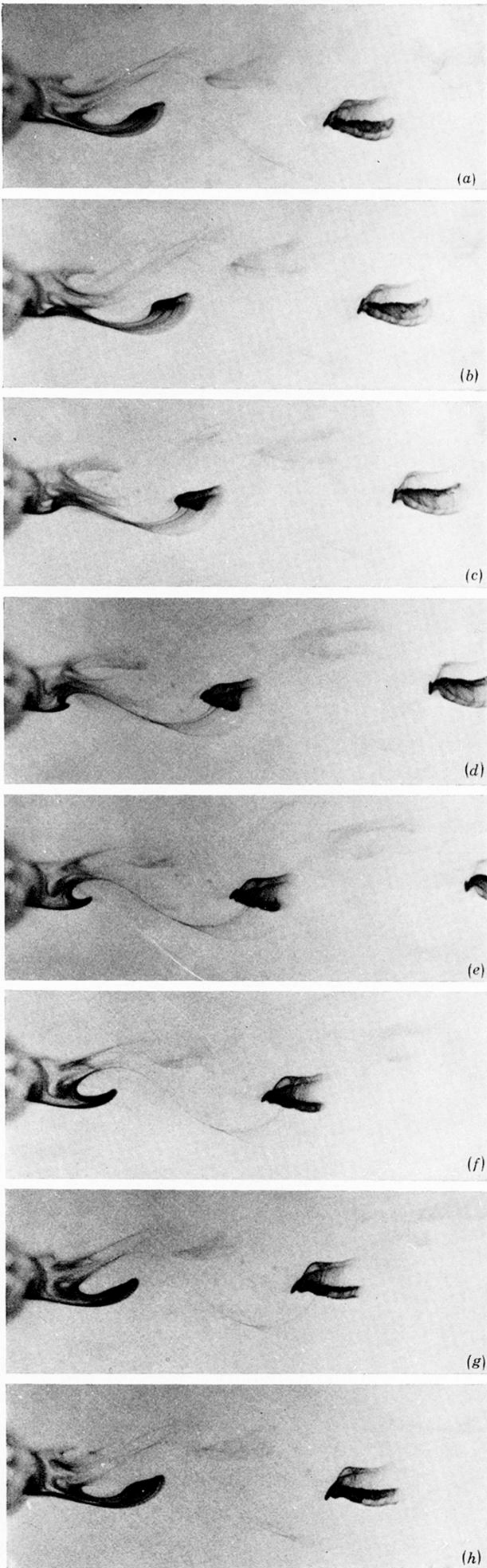


FIGURE 20. Consecutive views of the wake of a circular cylinder at $Re = 93$. Time intervals between exposures = 0.135 period.

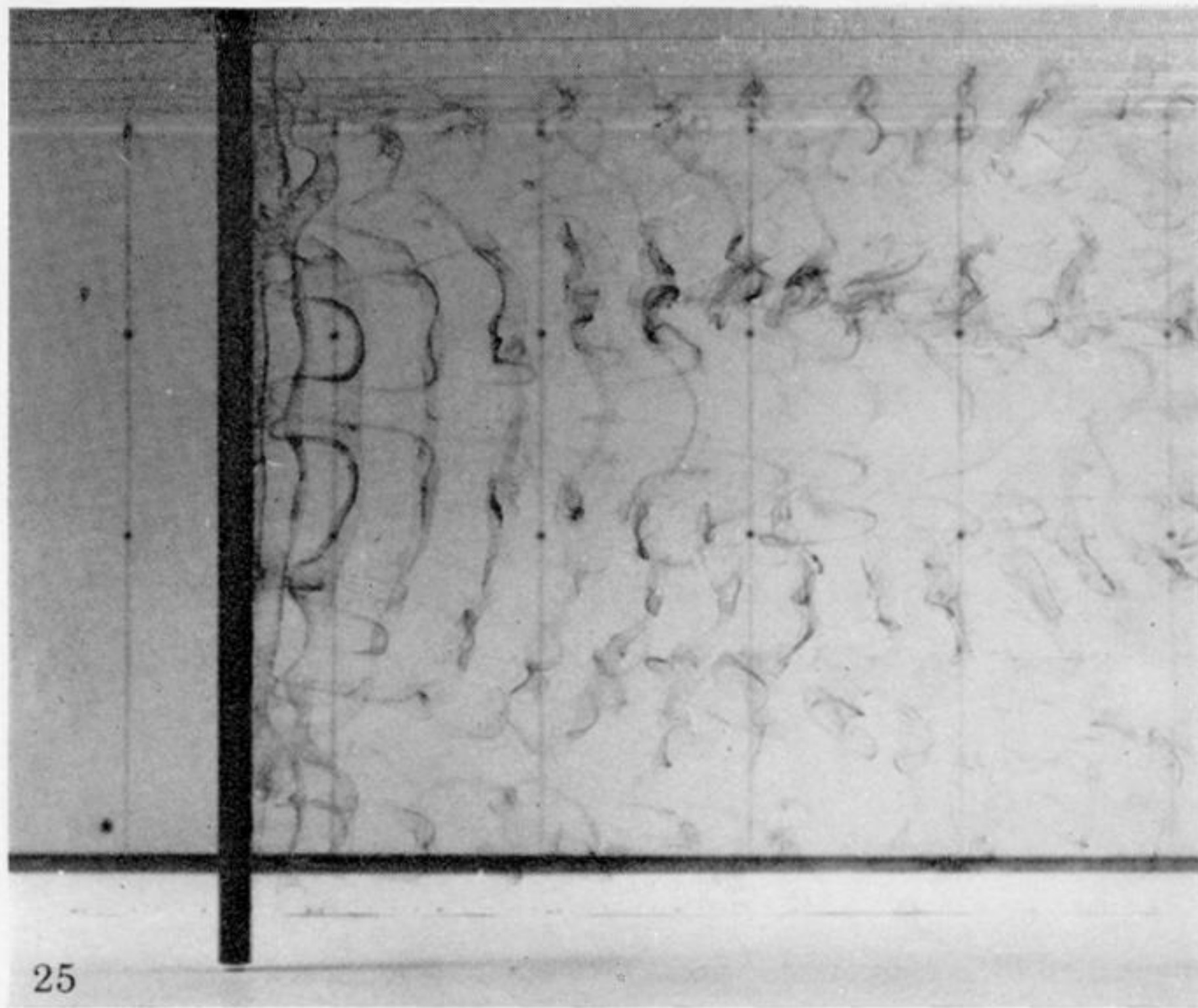


FIGURE 25. Side view of the wake of a circular cylinder at $Re = 200$.

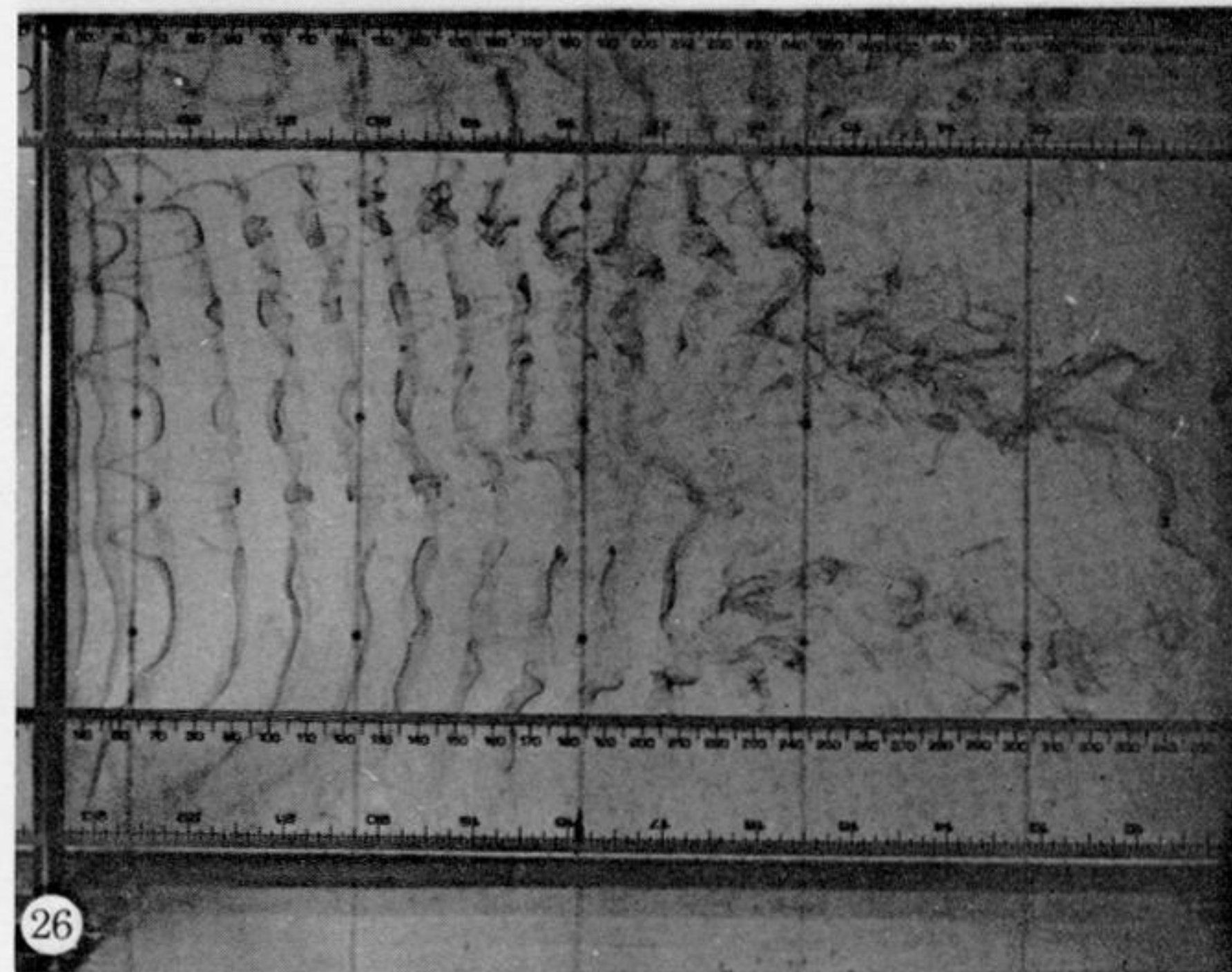


FIGURE 26. Side view of the wake of a circular cylinder at $Re = 217$.

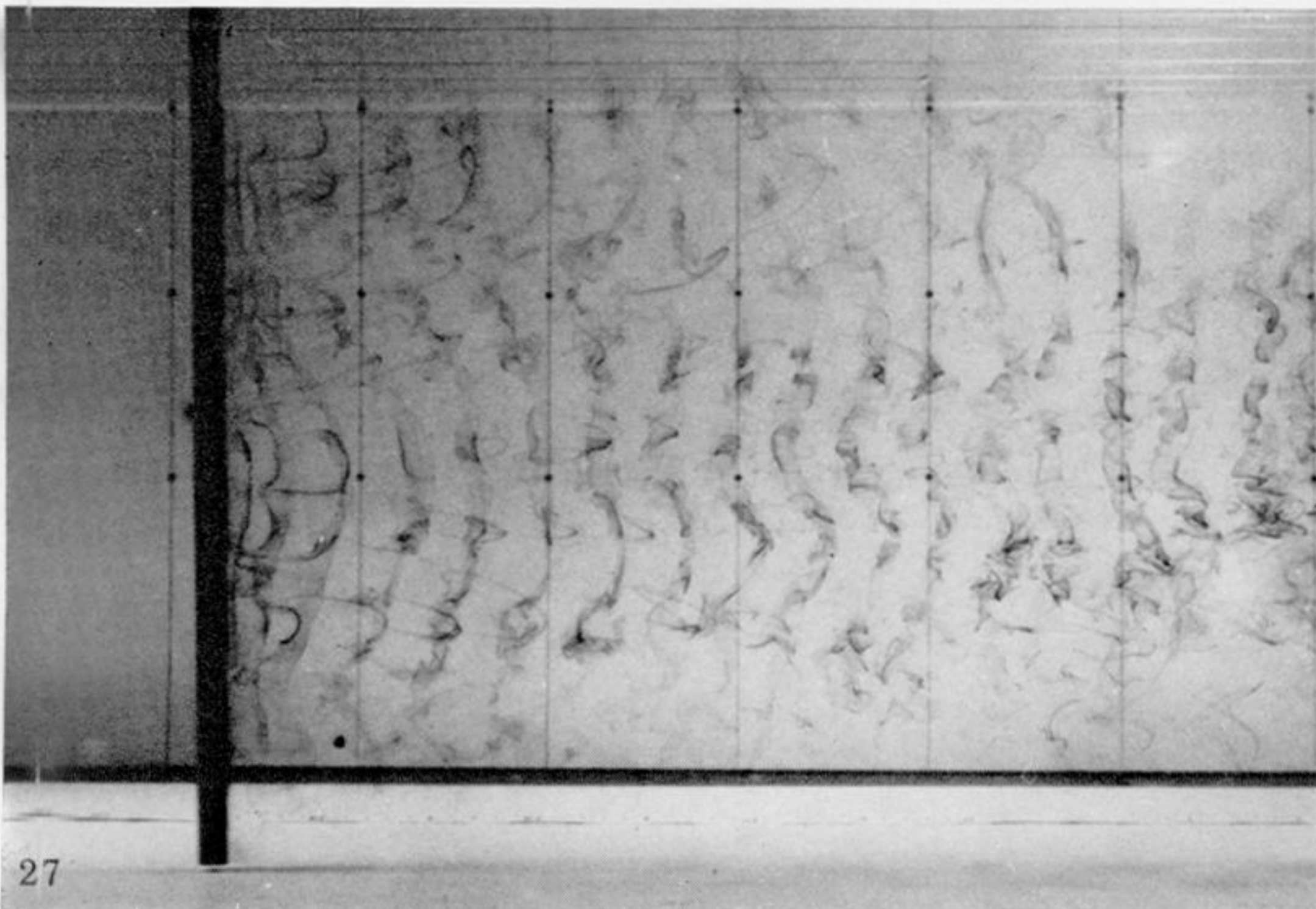


FIGURE 27. Side view of the wake of a circular cylinder at $Re = 232$.

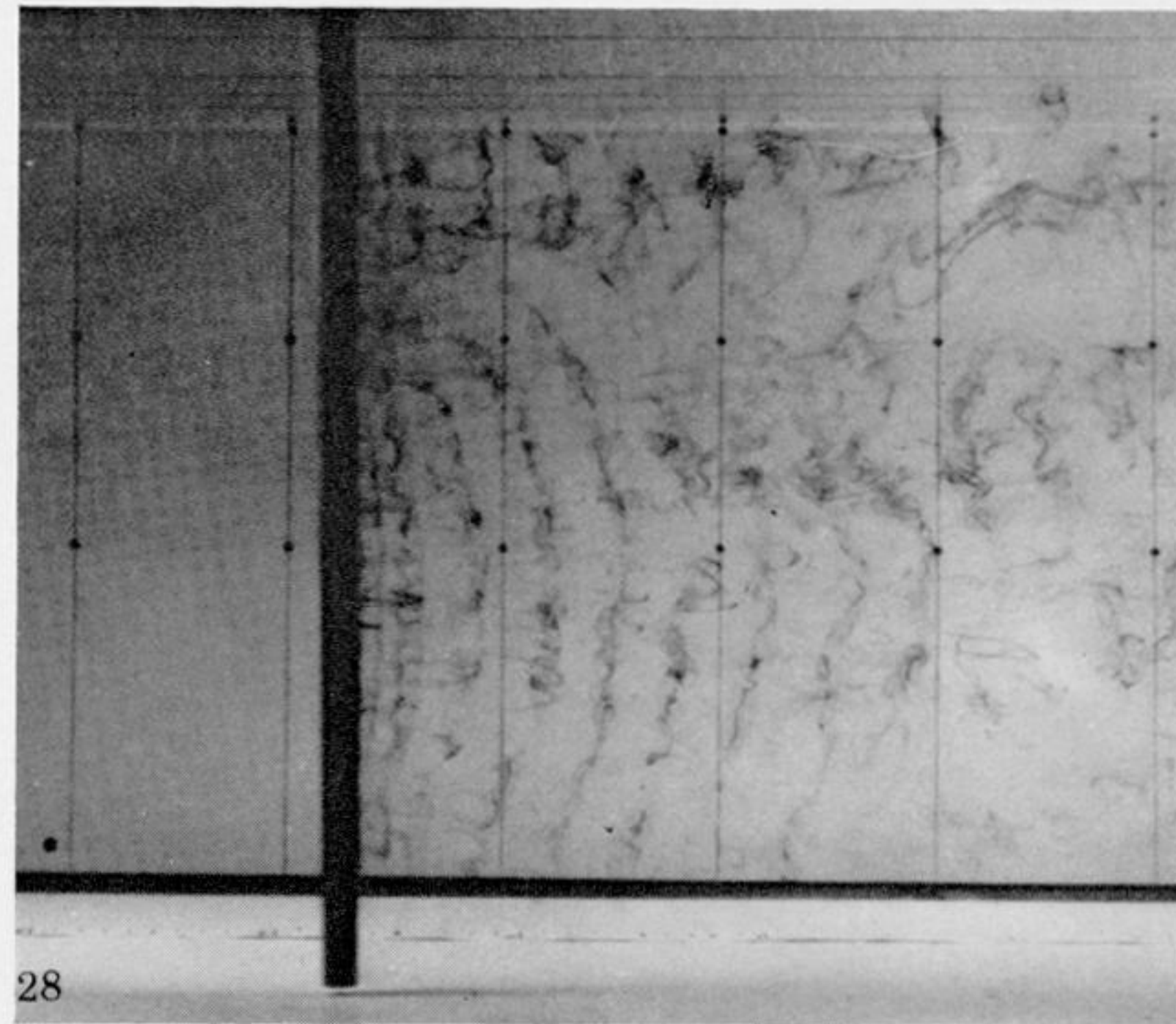


FIGURE 28. Side view of the wake of a circular cylinder at $Re = 344$.



26

FIGURE 26. Side view of the wake of a circular cylinder at $Re = 217$.

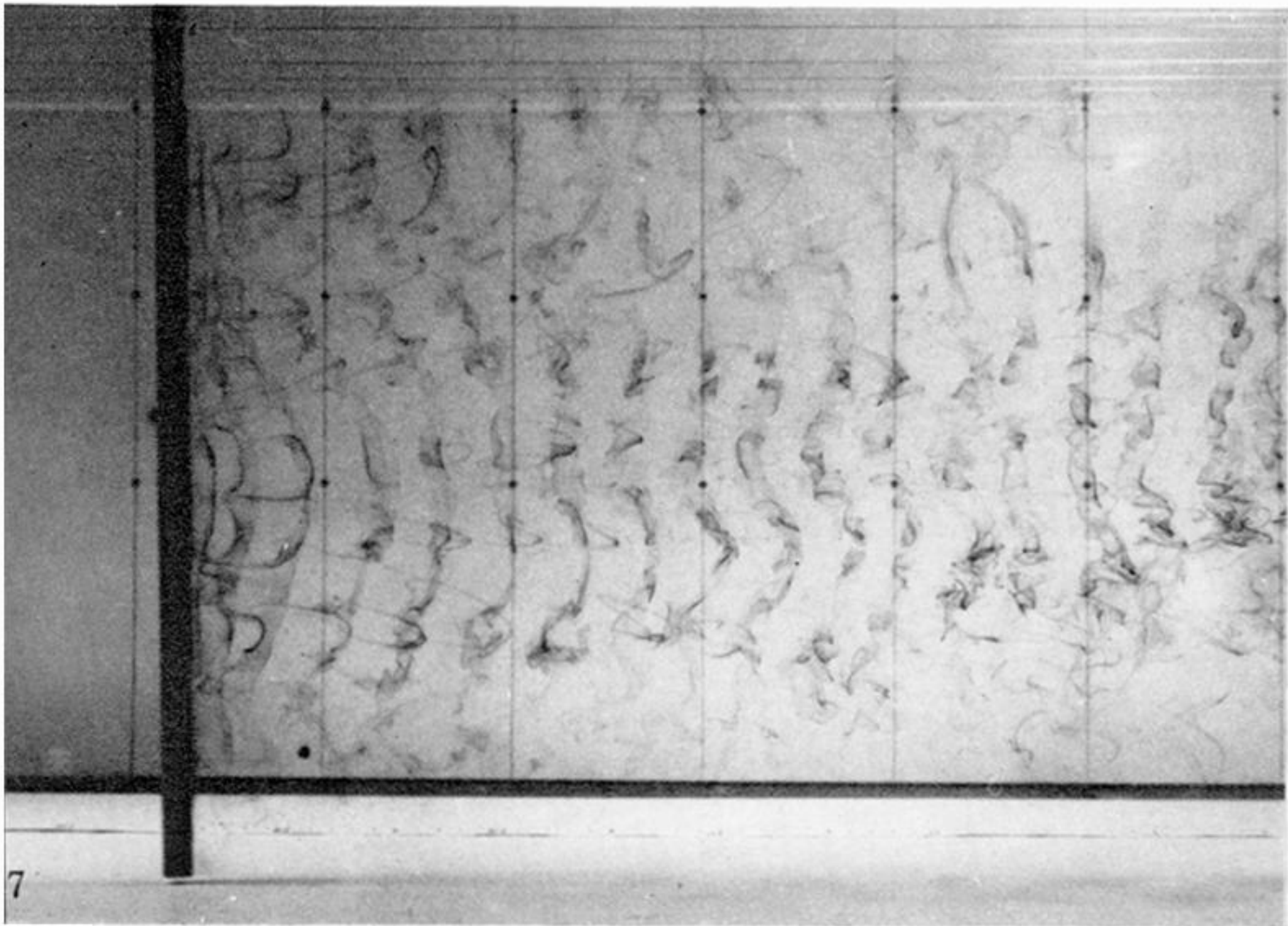
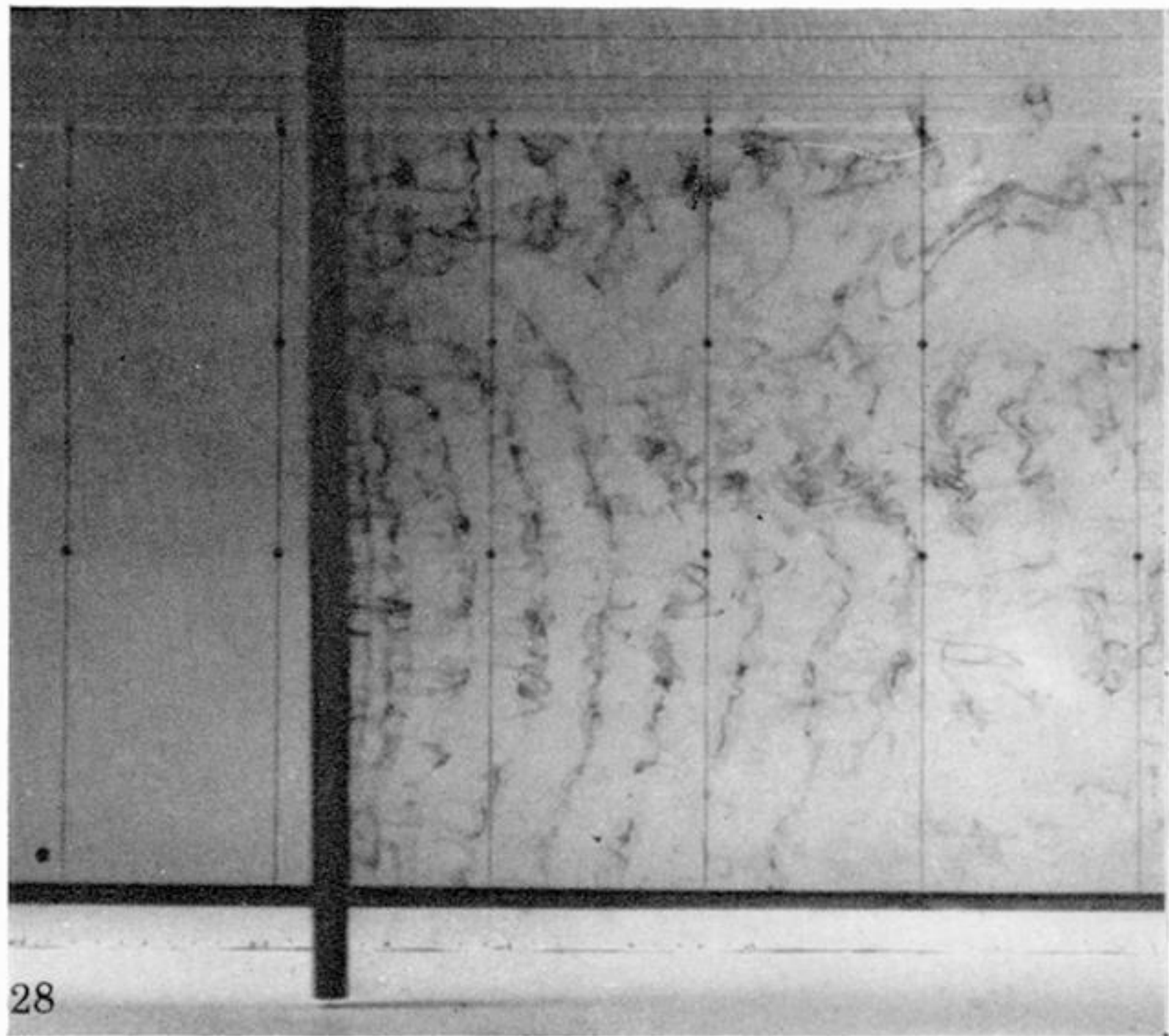


FIGURE 27. Side view of the wake of a circular cylinder at $Re = 232$.



28

FIGURE 28. Side view of the wake of a circular cylinder at $Re = 344$.

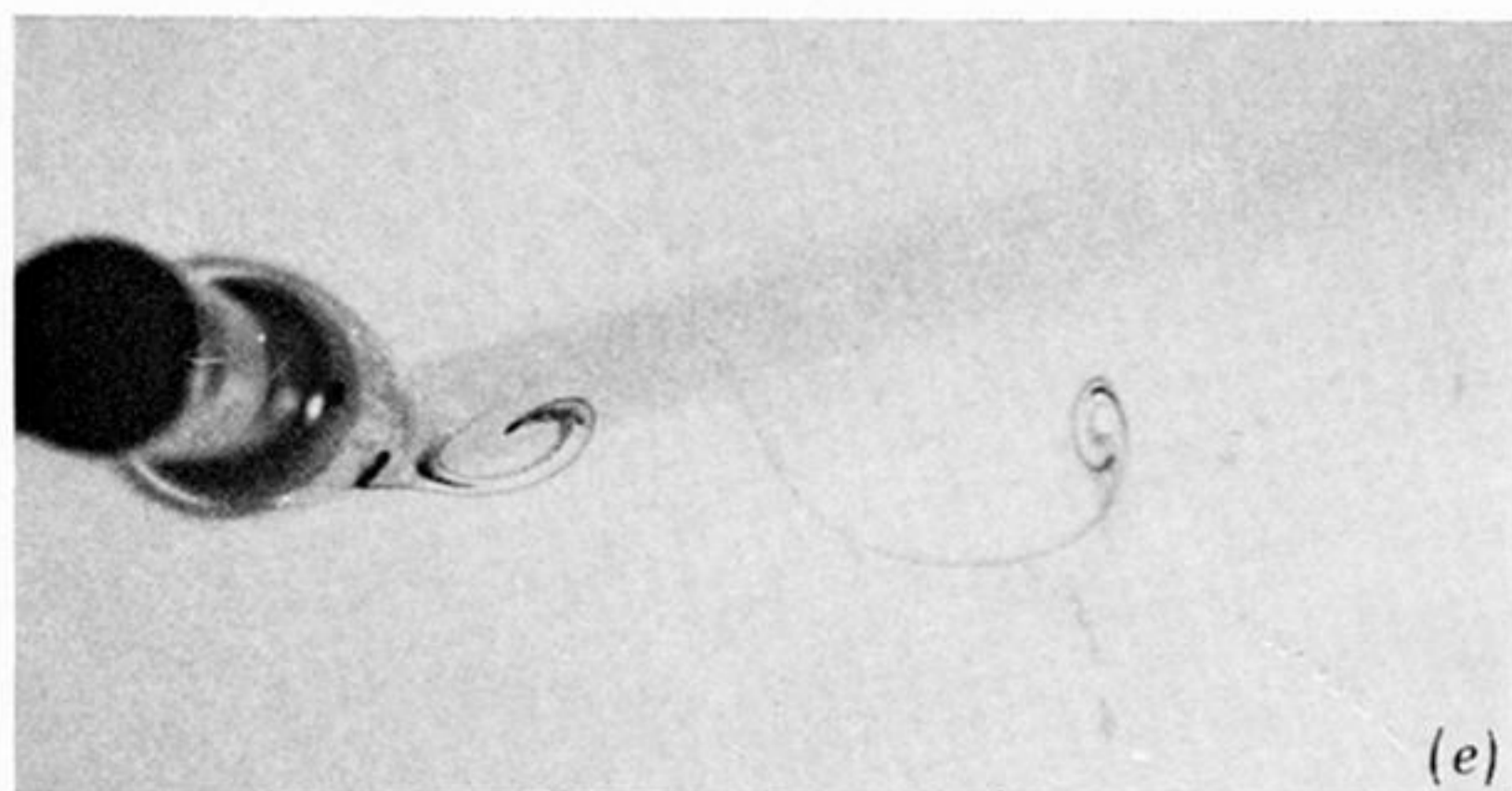
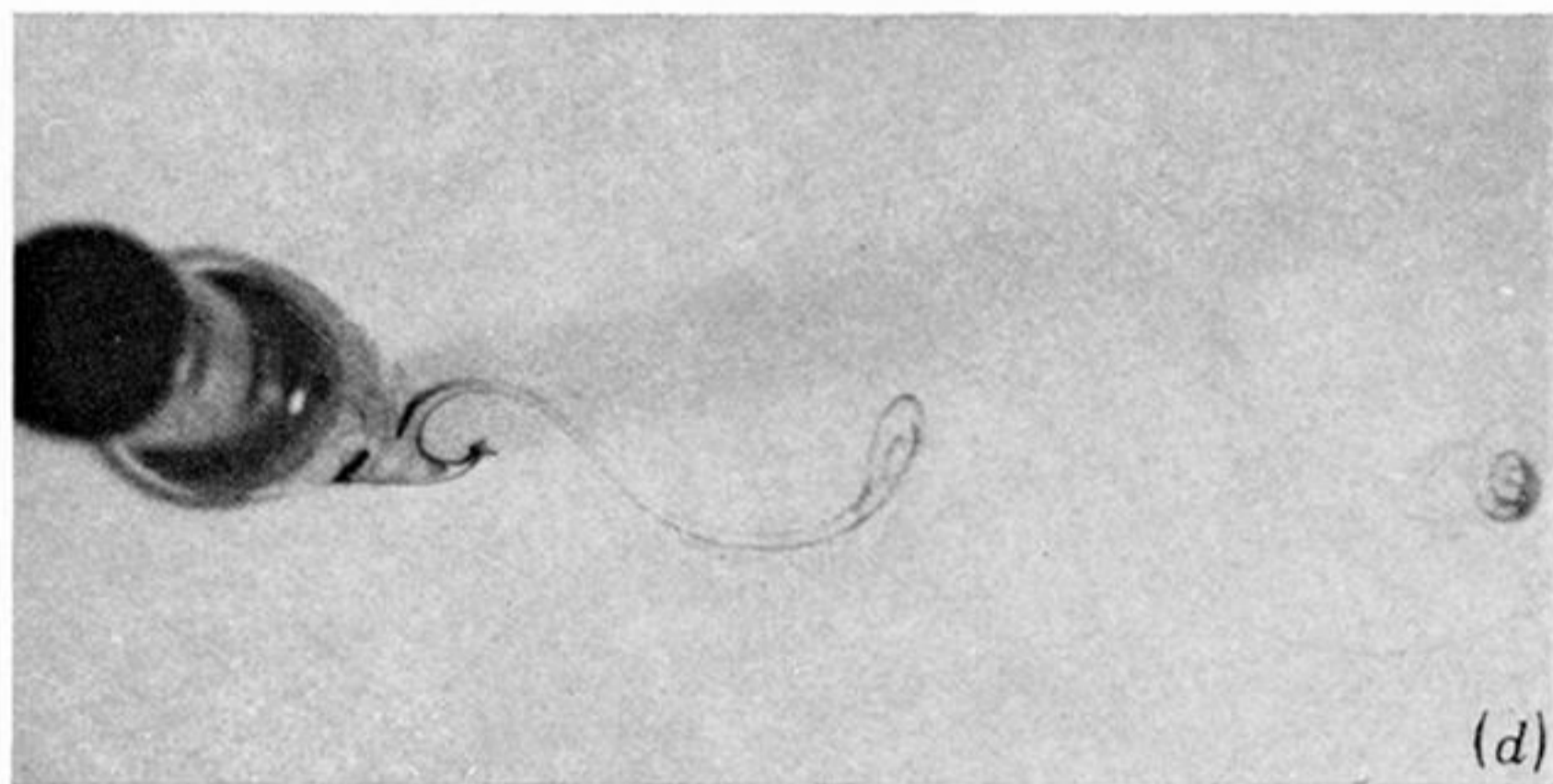
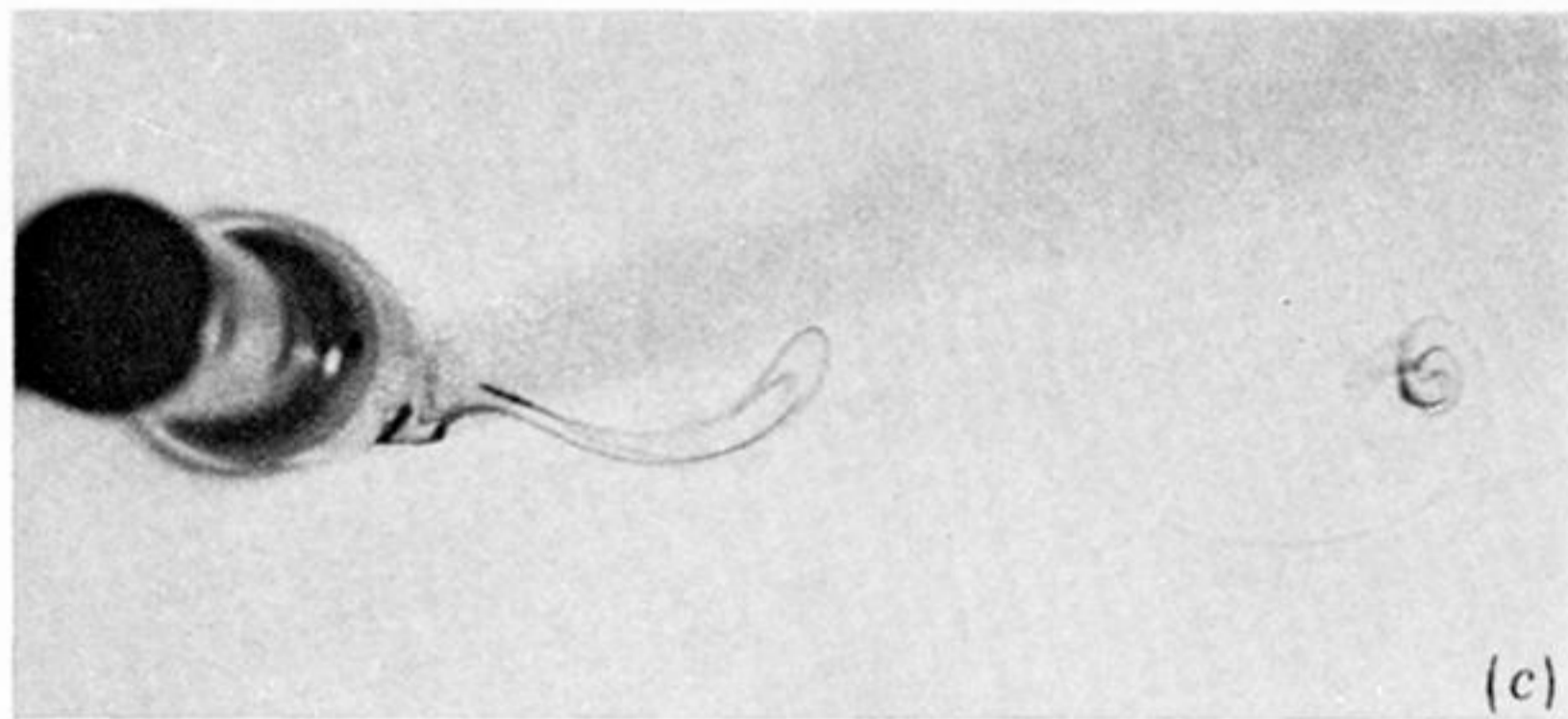
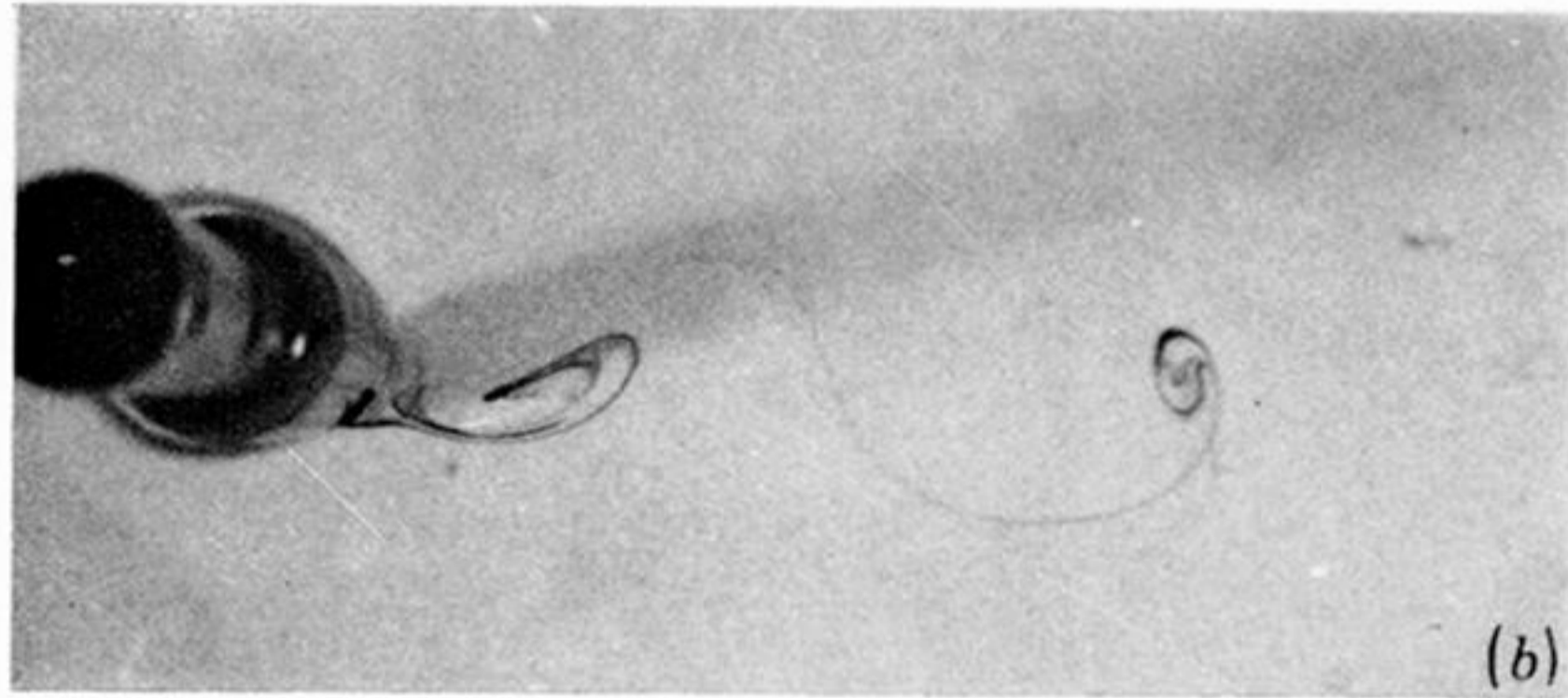
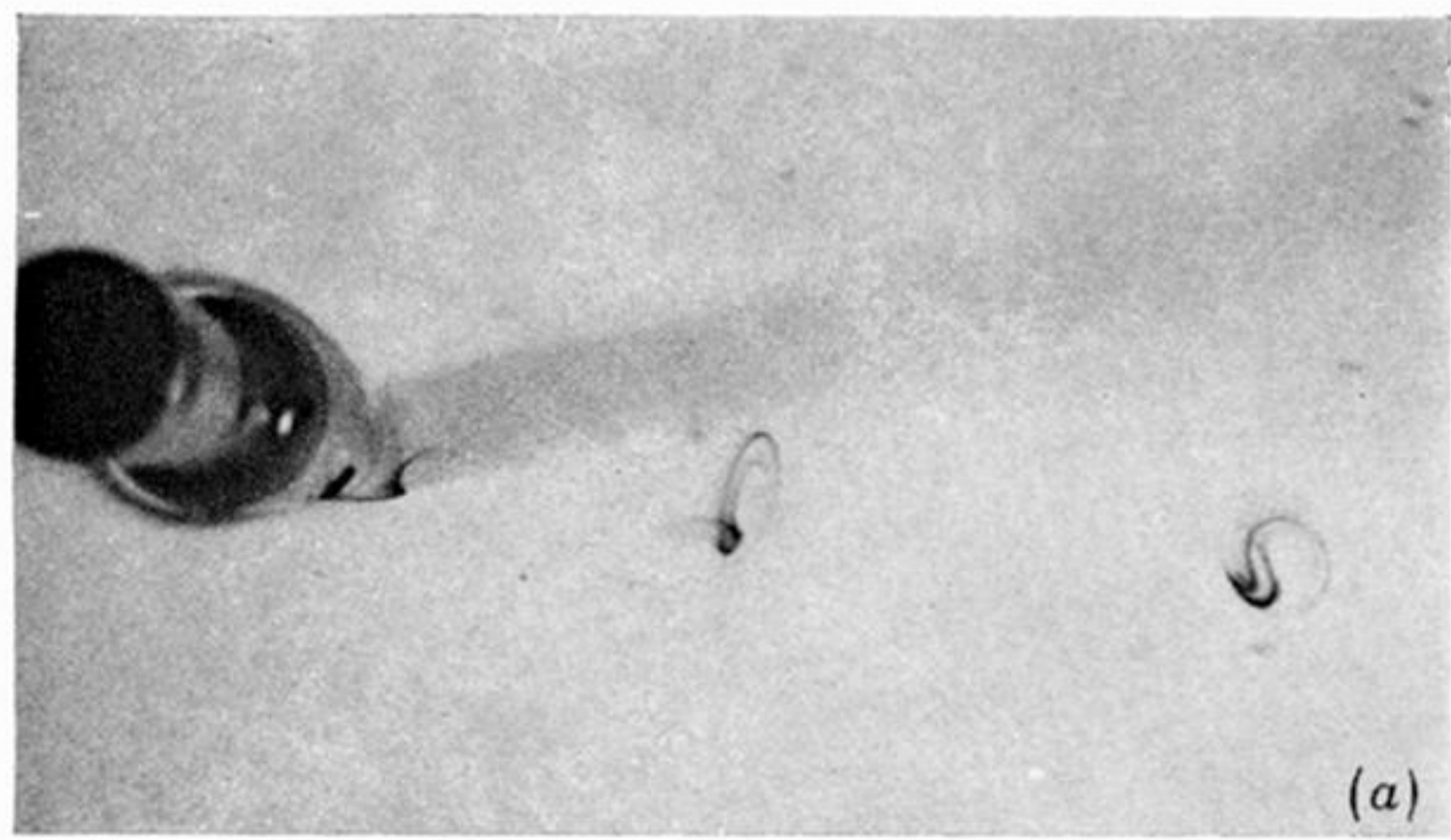


FIGURE 29. Wake of a circular cylinder at $Re = 180$ showing a minor form of finger. Dye on one side only of the rear of the body. (a) Appearance in the absence of a finger. (b)–(e) Consecutive instants during which dye is drawn back from a vortex into the next vortex on the same side of the wake.

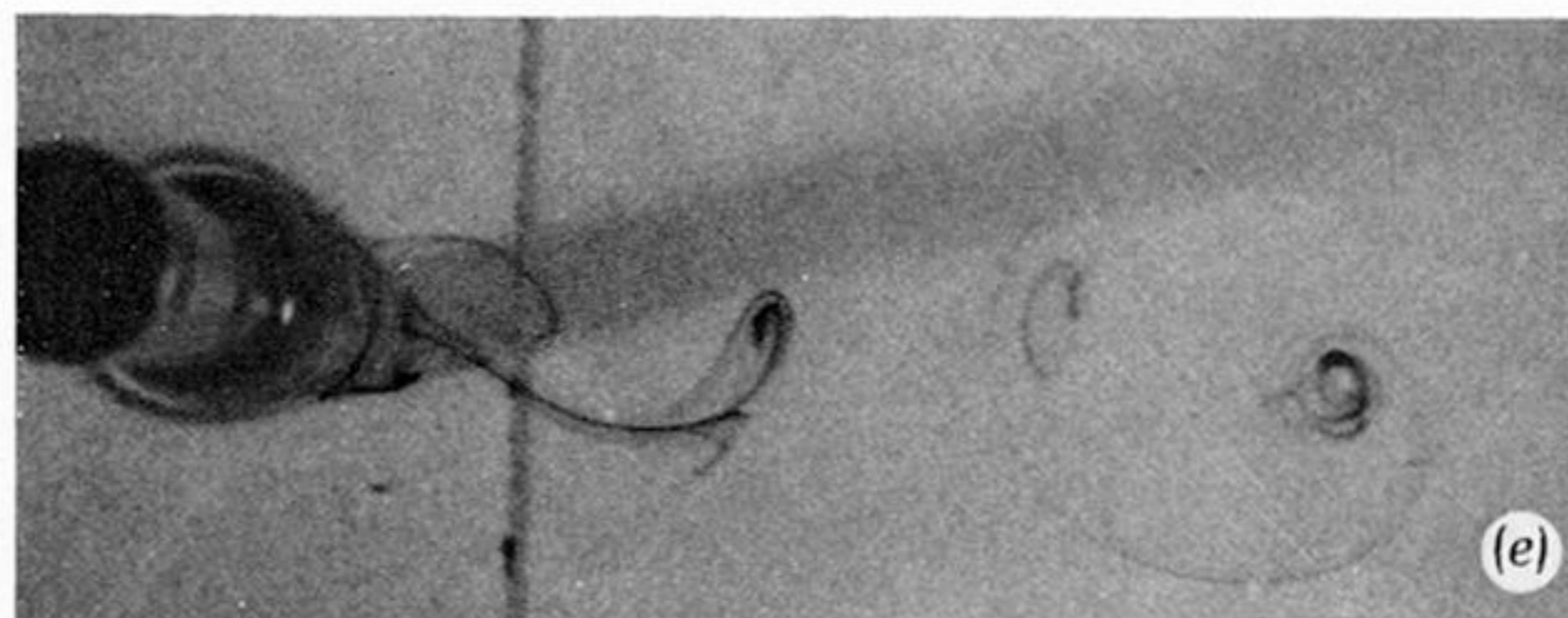
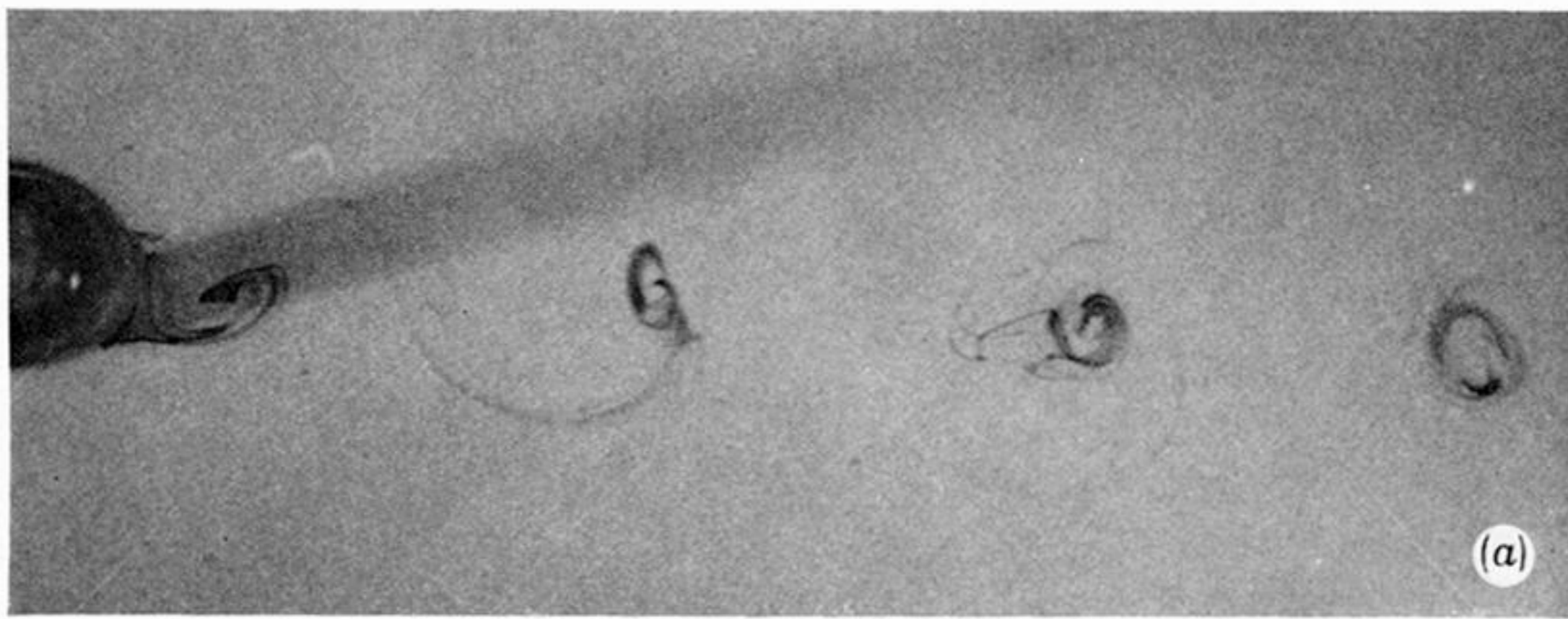


FIGURE 30. Wake of a circular cylinder at $Re = 230$ showing the sequence of events in the formation of a finger. Dye is drawn back from a vortex to the rear of the body and thence into the opposite side of the vortex street.

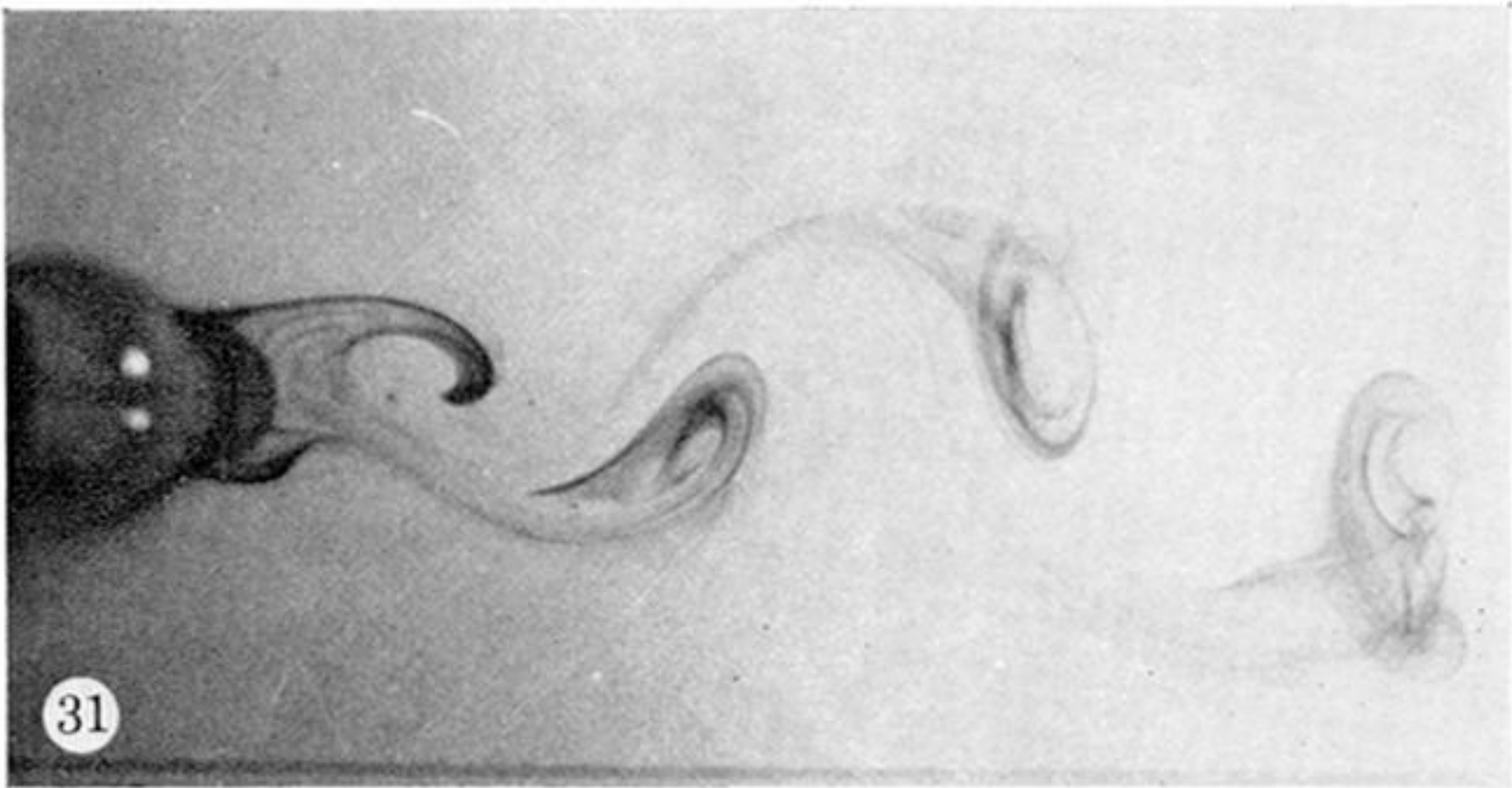


FIGURE 31. Wake of a circular cylinder at $Re = 188$.

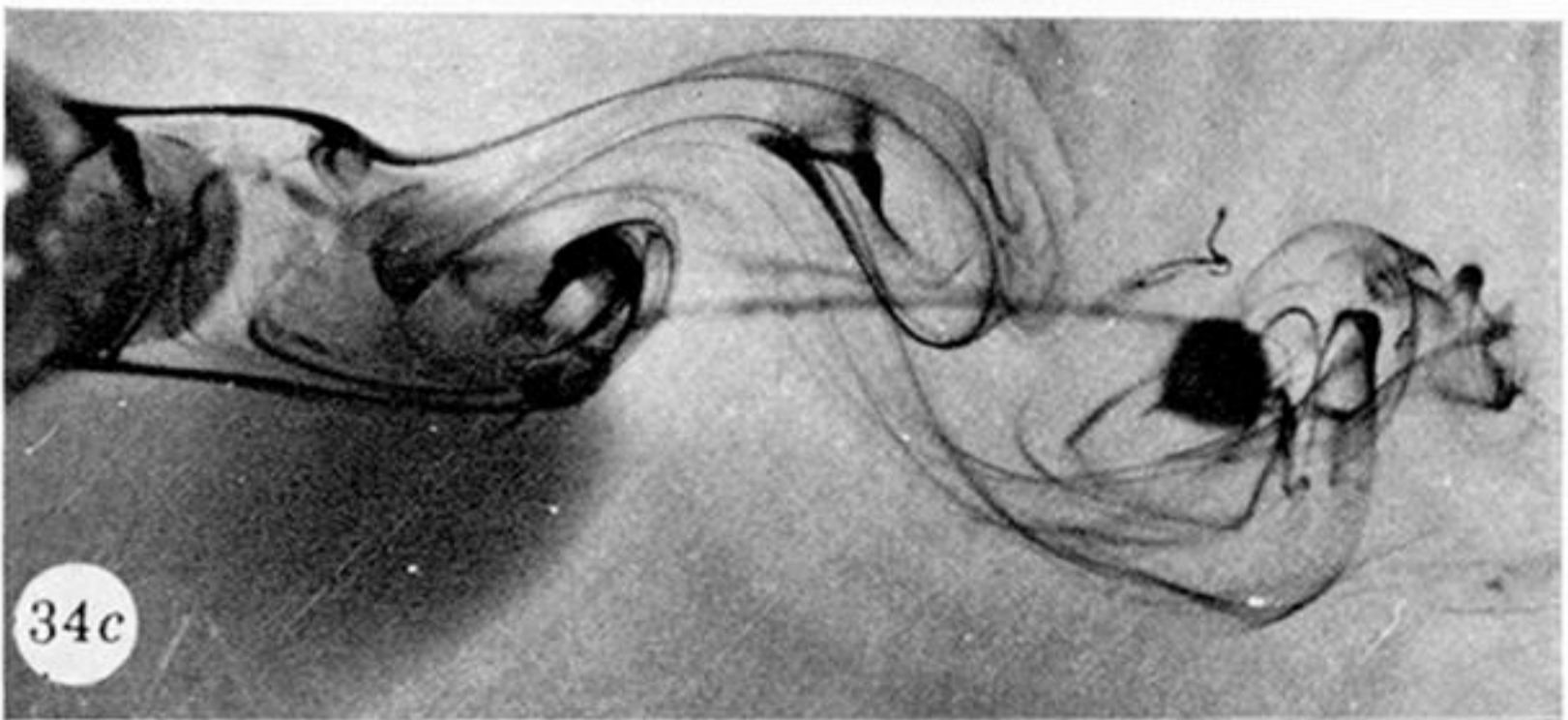
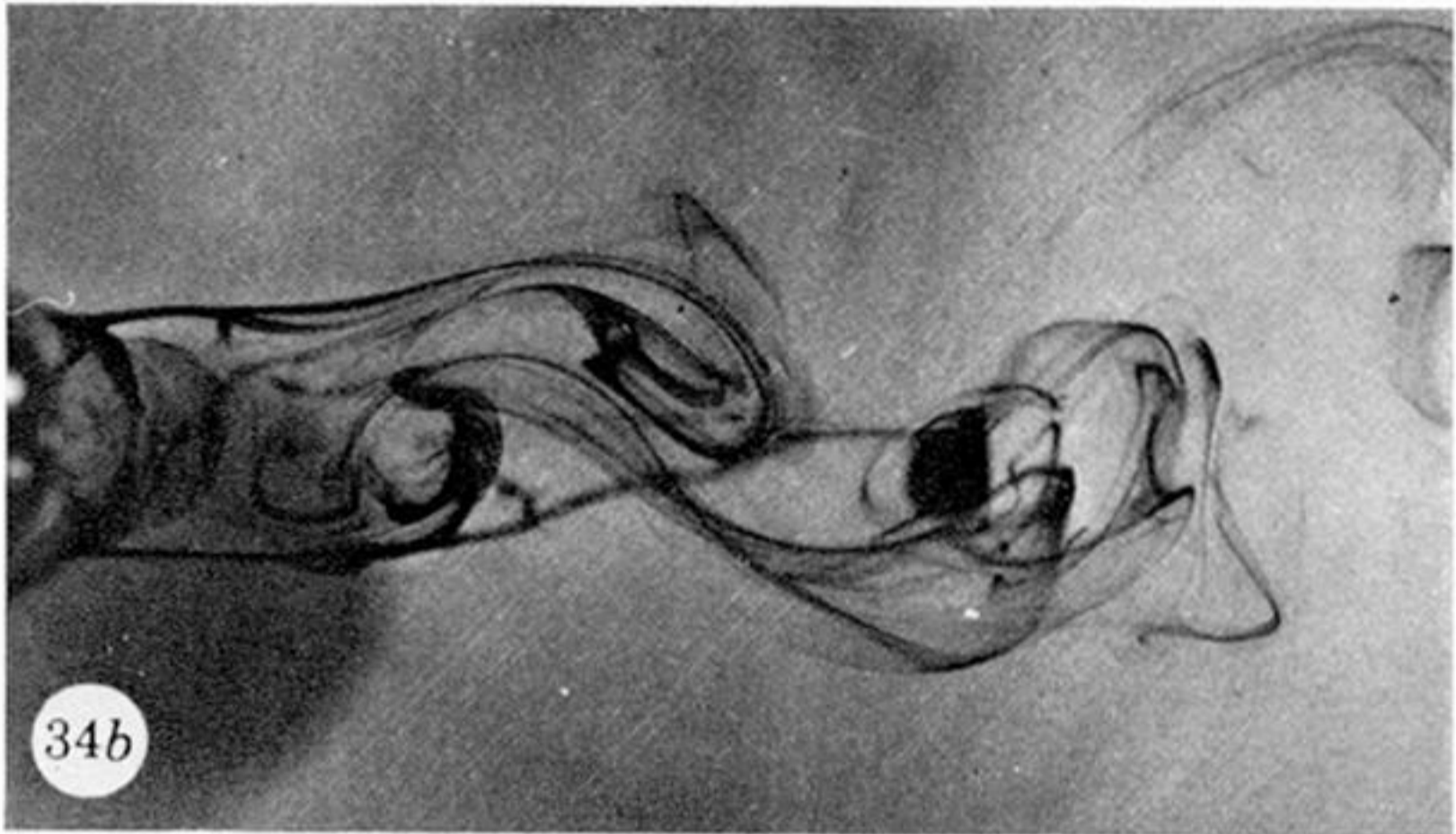
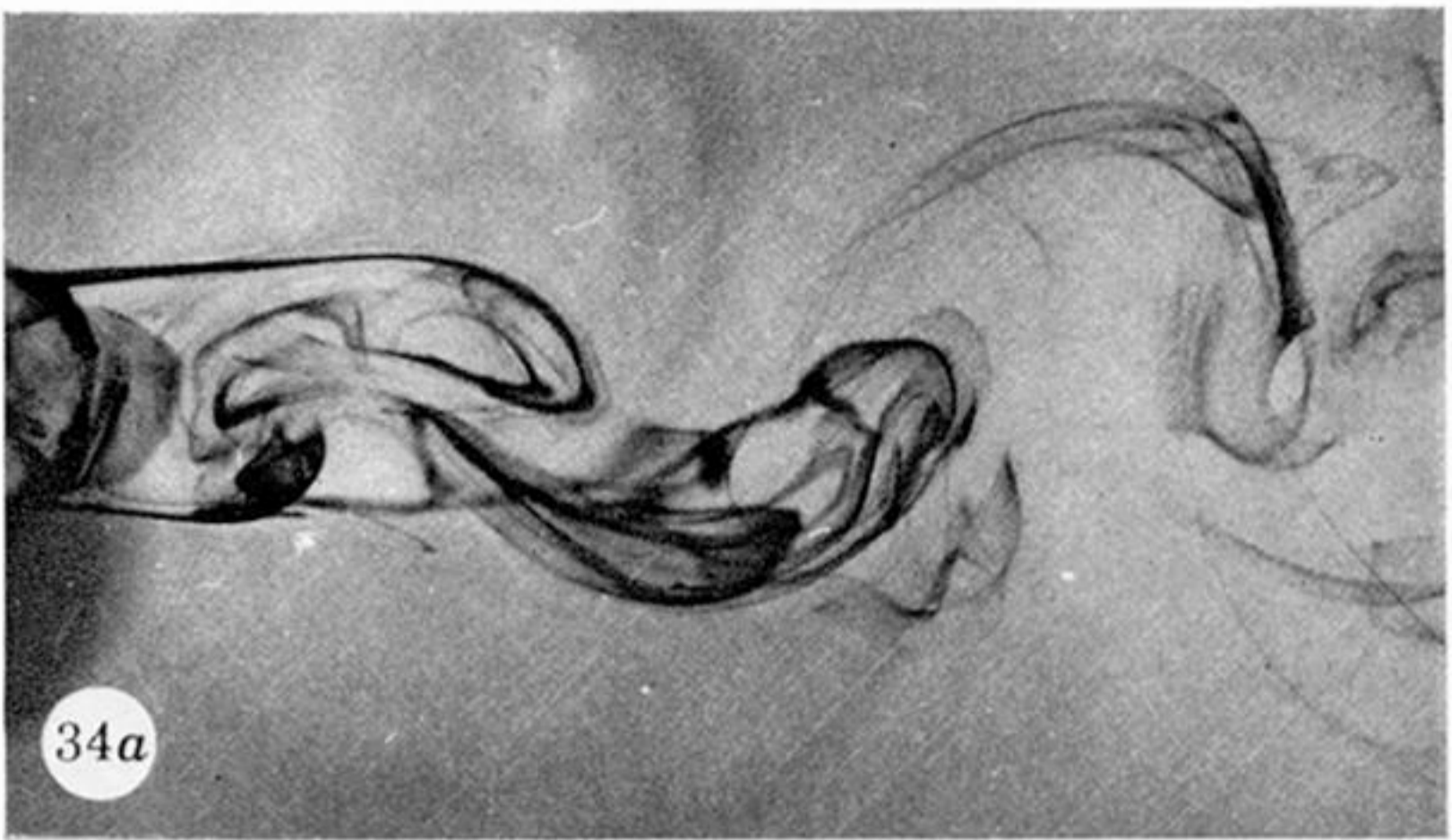


FIGURE 34. The wake of a circular cylinder at $Re = 334$. Consecutive views at separation 0.22 period of oscillation.

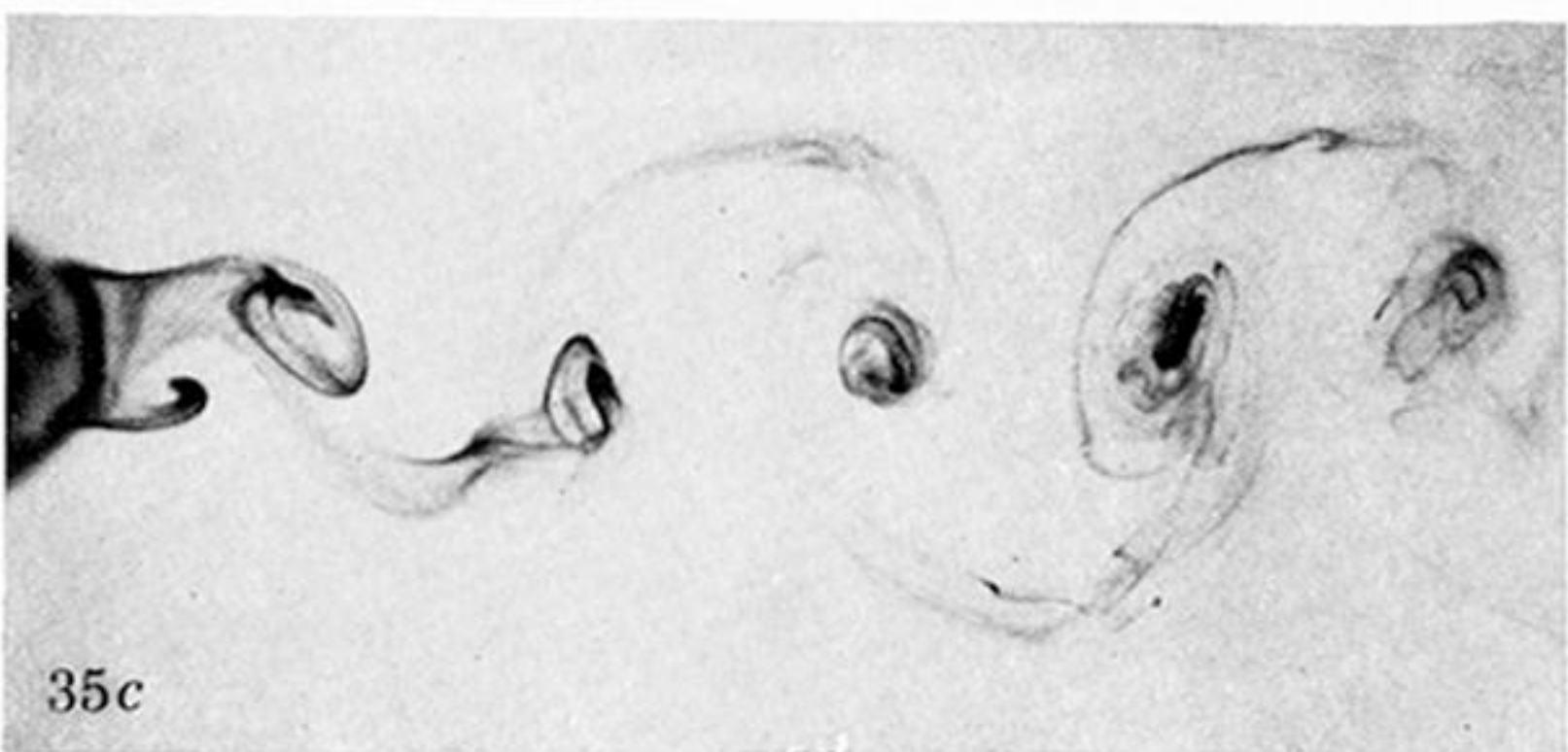
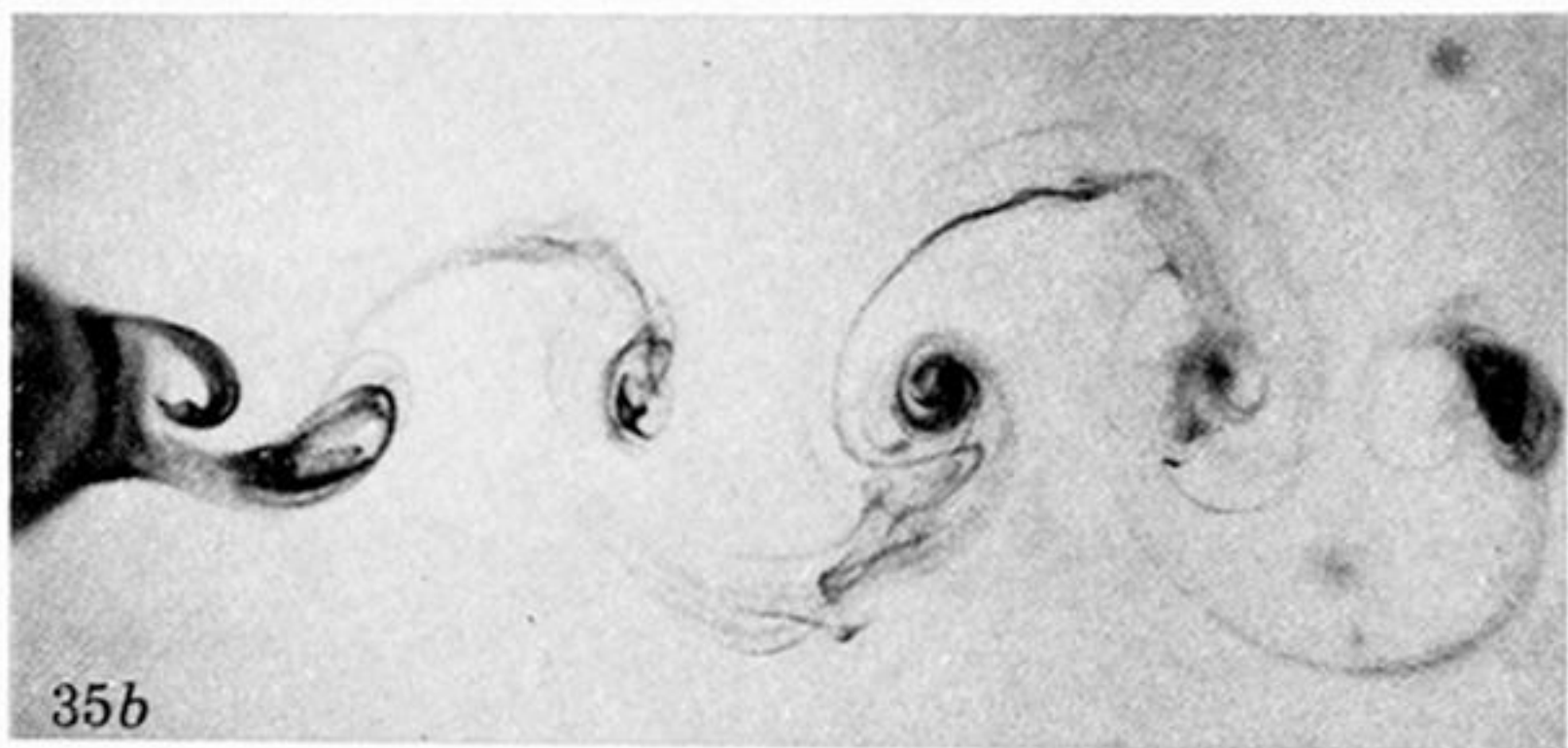
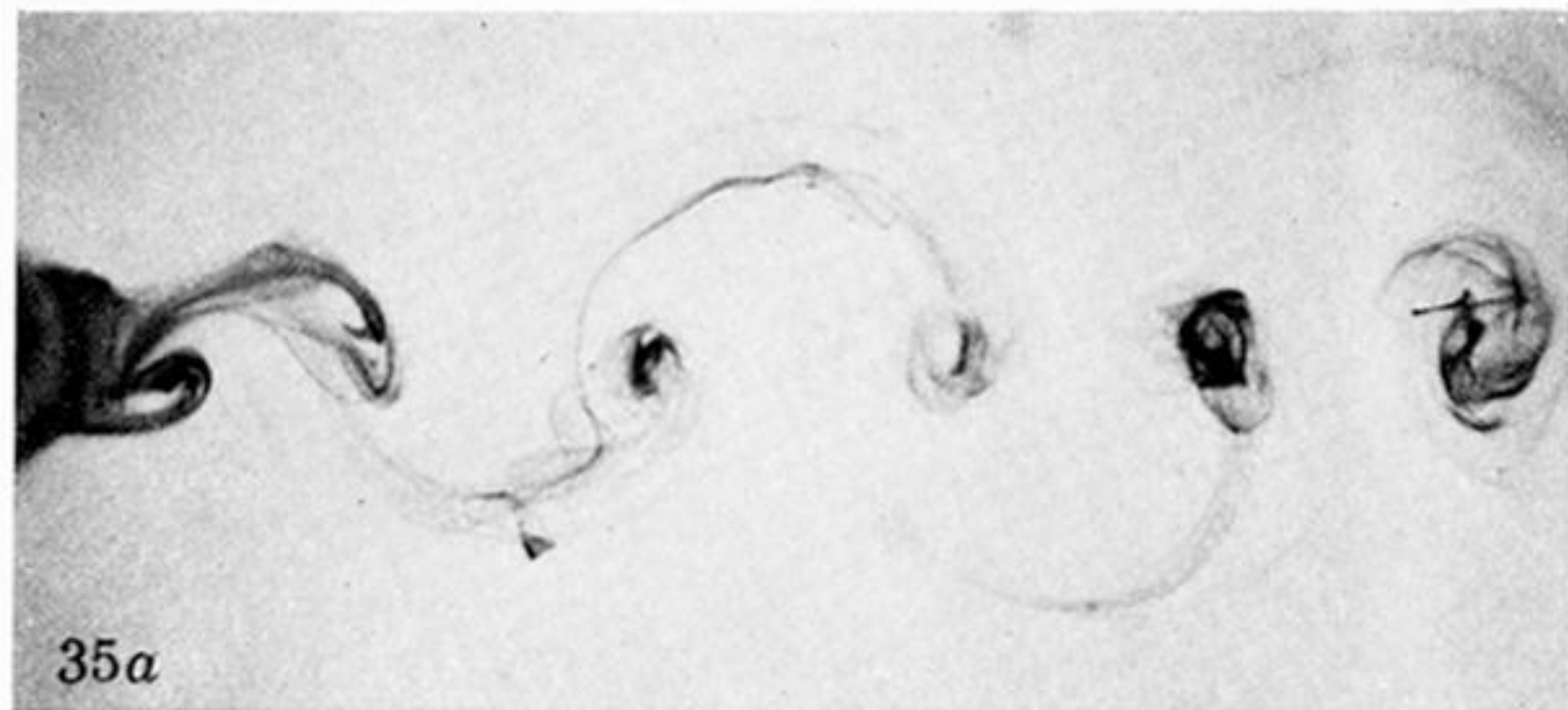


FIGURE 35. The wake of a circular cylinder at $Re = 340$. Consecutive views separated by 0.41 period.

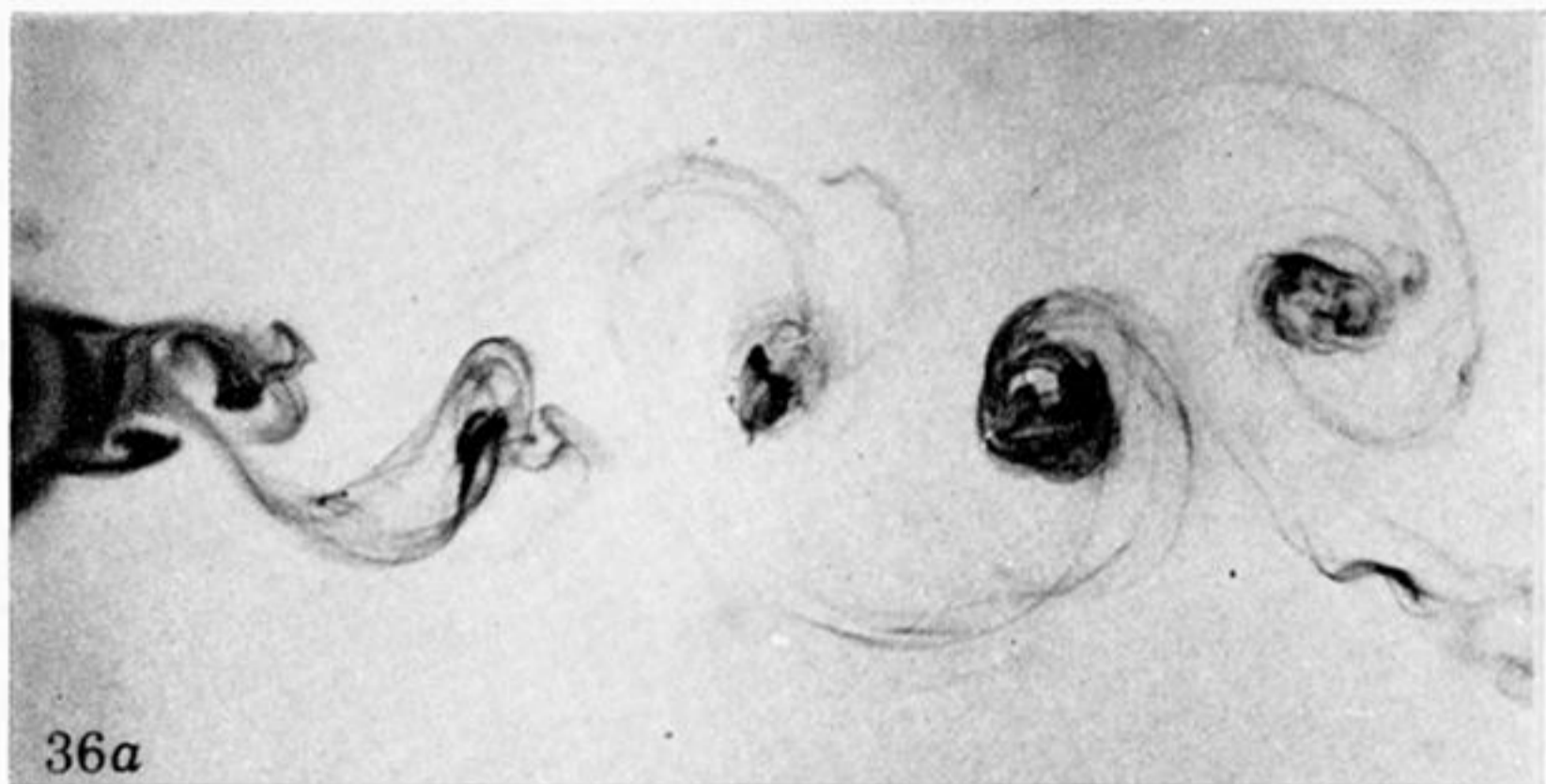


FIGURE 36. The wake of a circular cylinder at $Re = 407$. Consecutive views separated by 0.55 period.

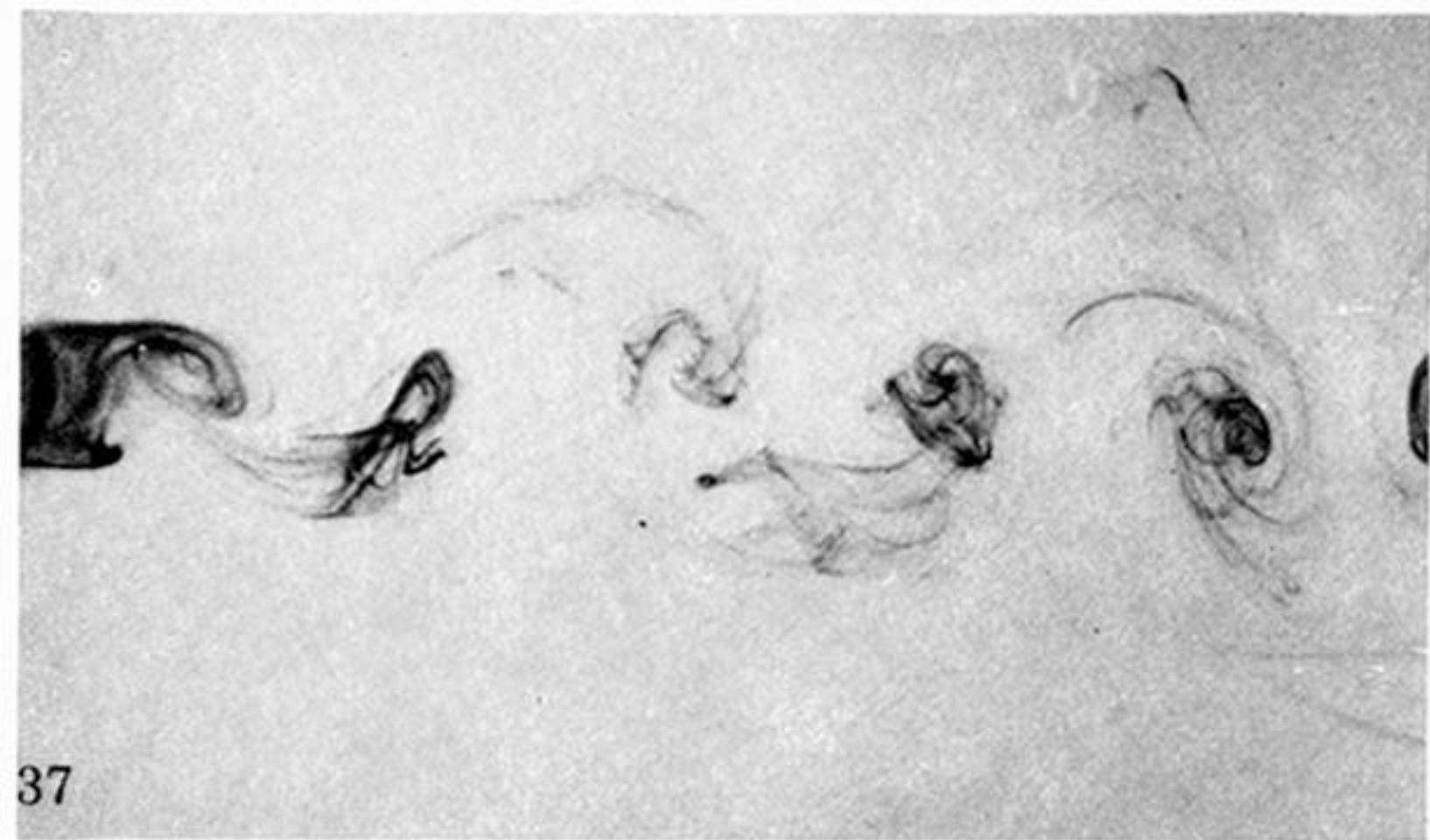


FIGURE 37. The wake of a circular cylinder at $Re = 464$.

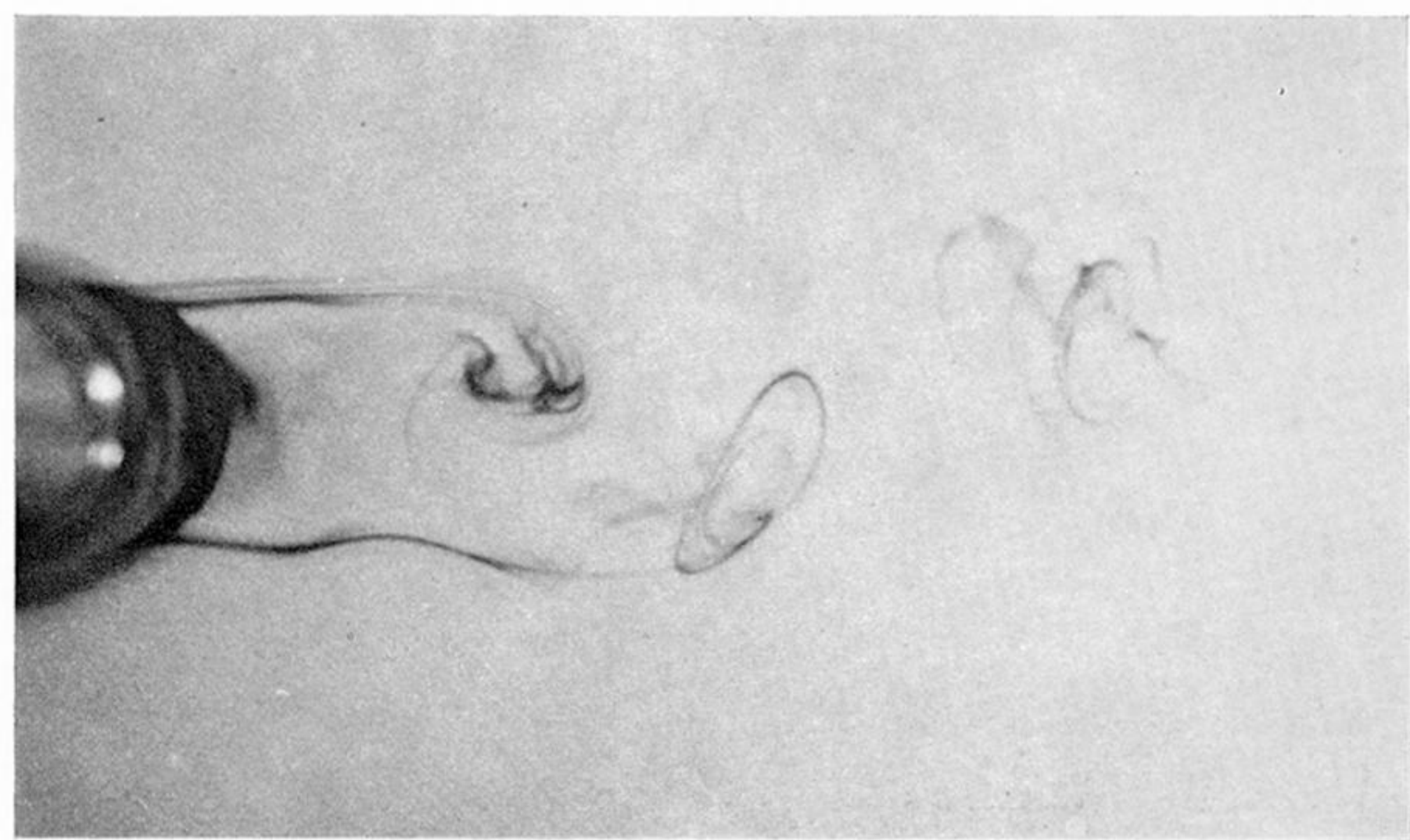


FIGURE 38. Transition waves at $Re = 488$.

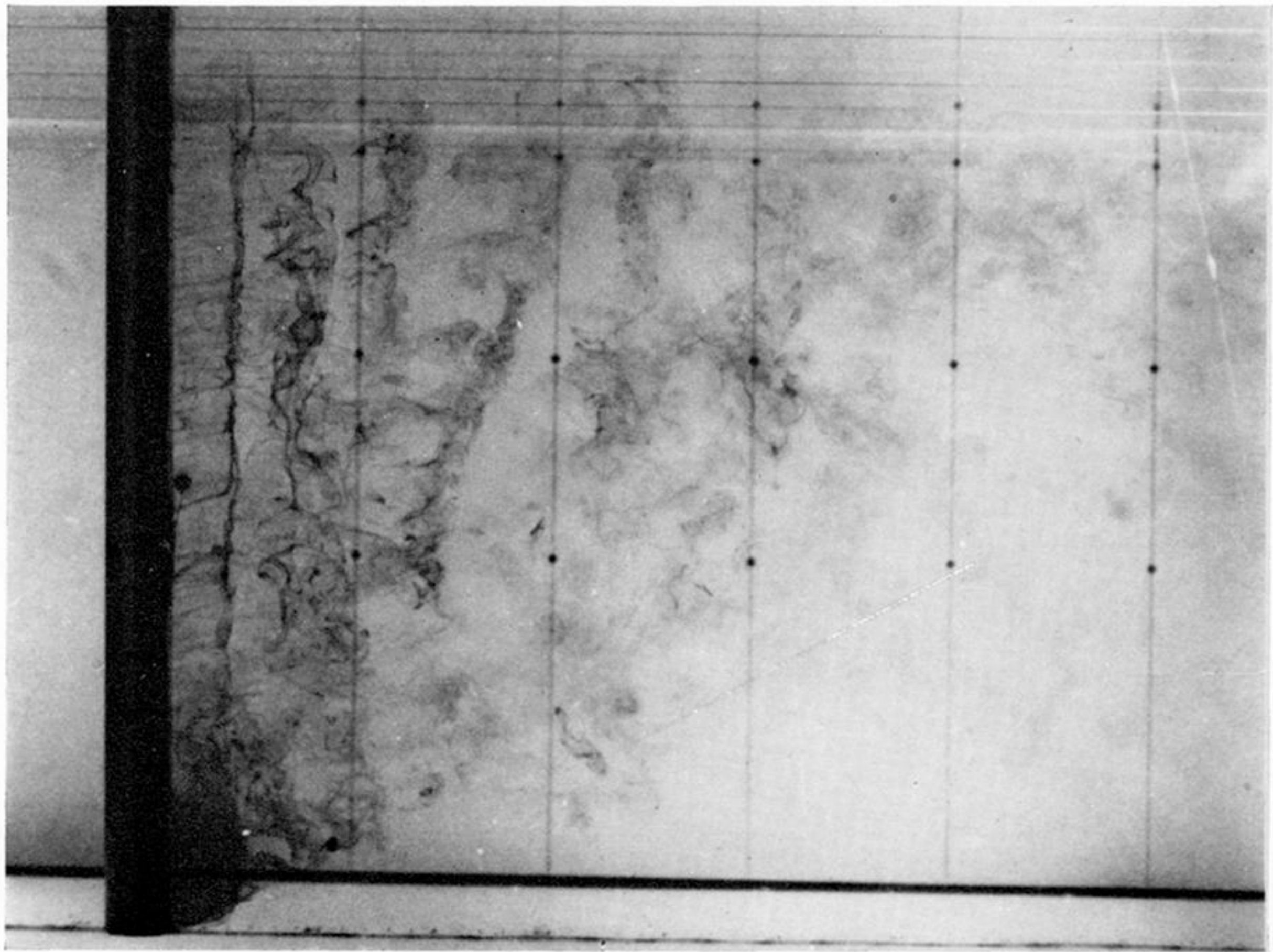


FIGURE 42. Side view of the wake at $Re = 1116$ showing the transition waves in phase along the span.

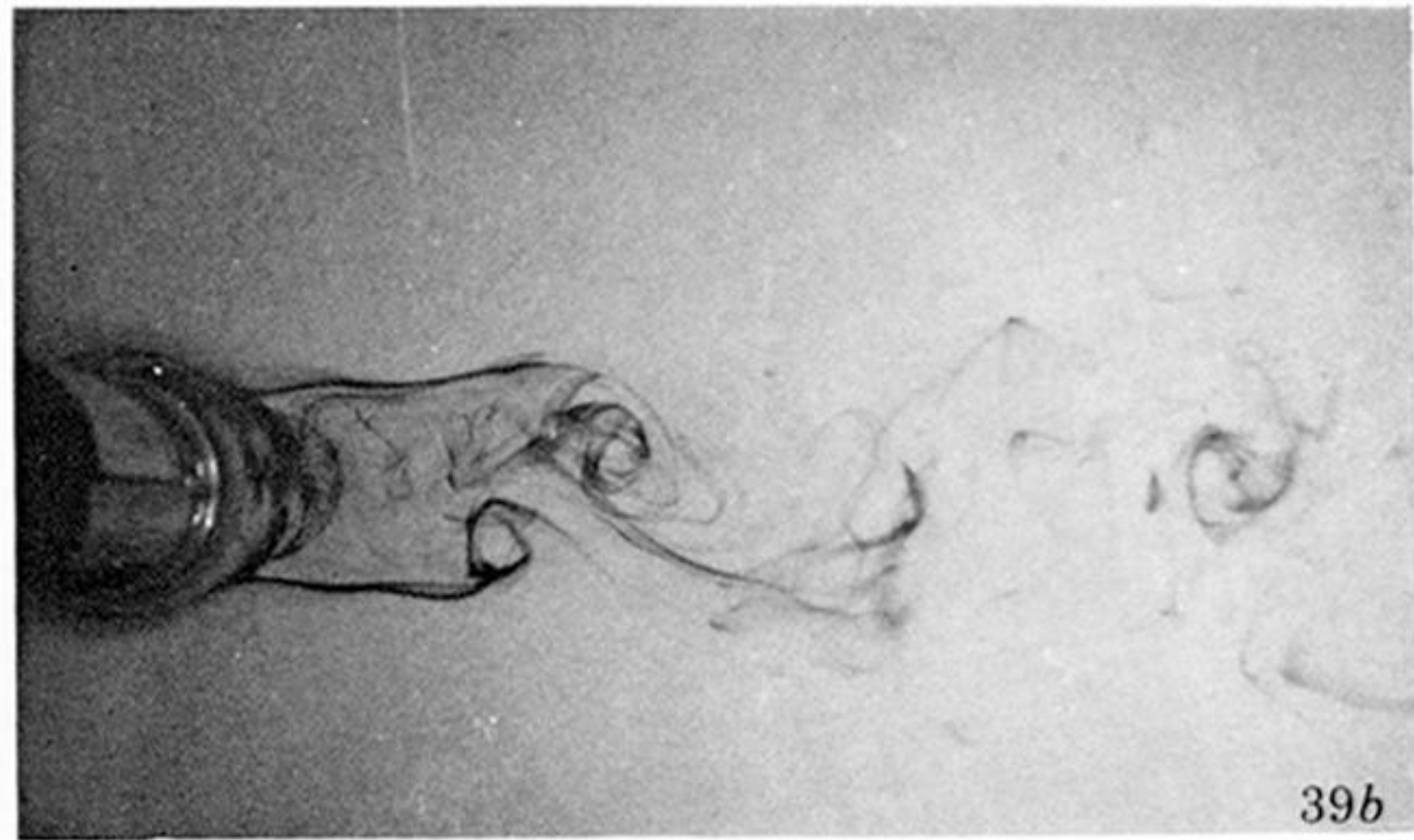
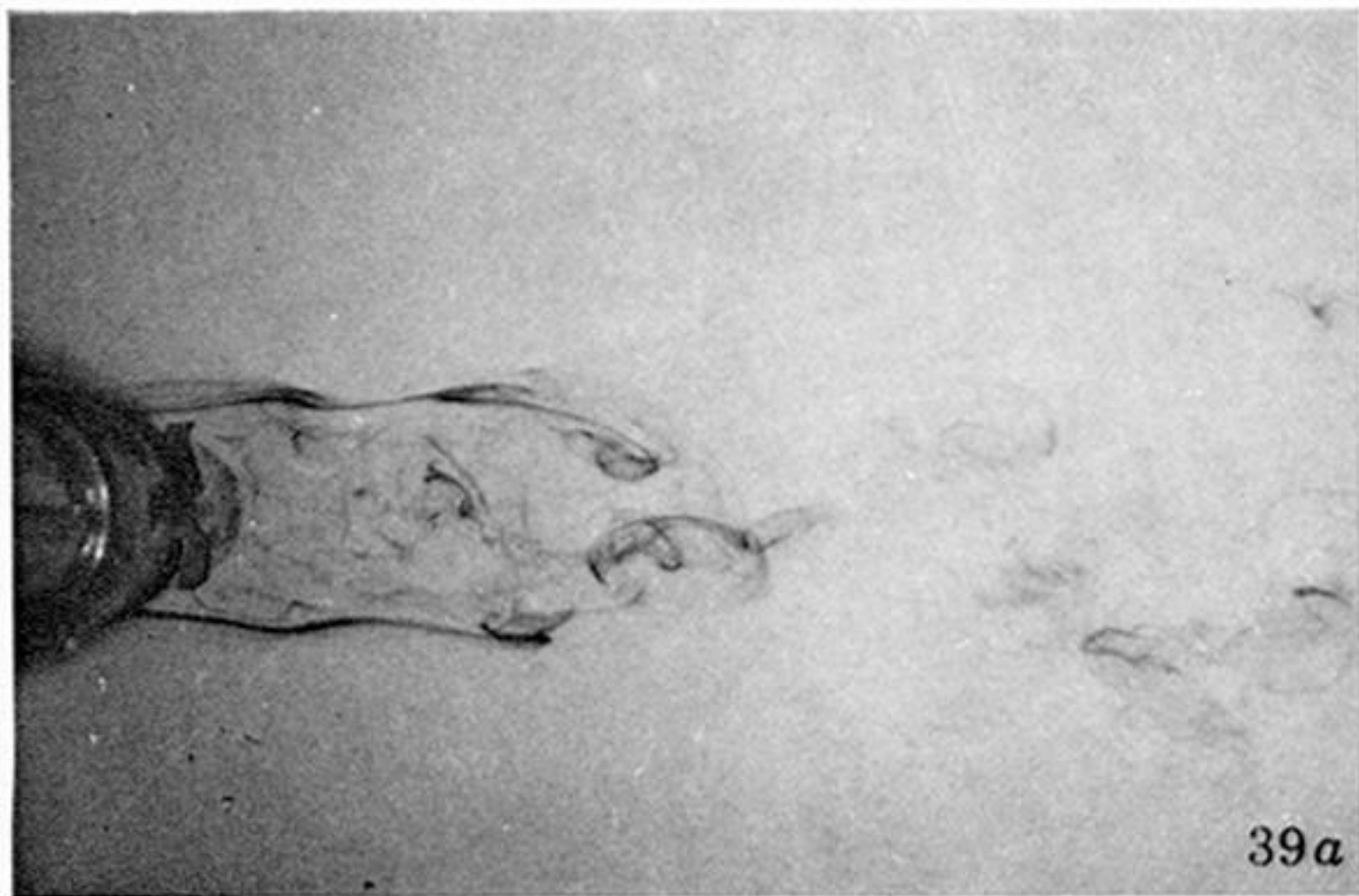


FIGURE 39. Transition waves at $Re = 682$.

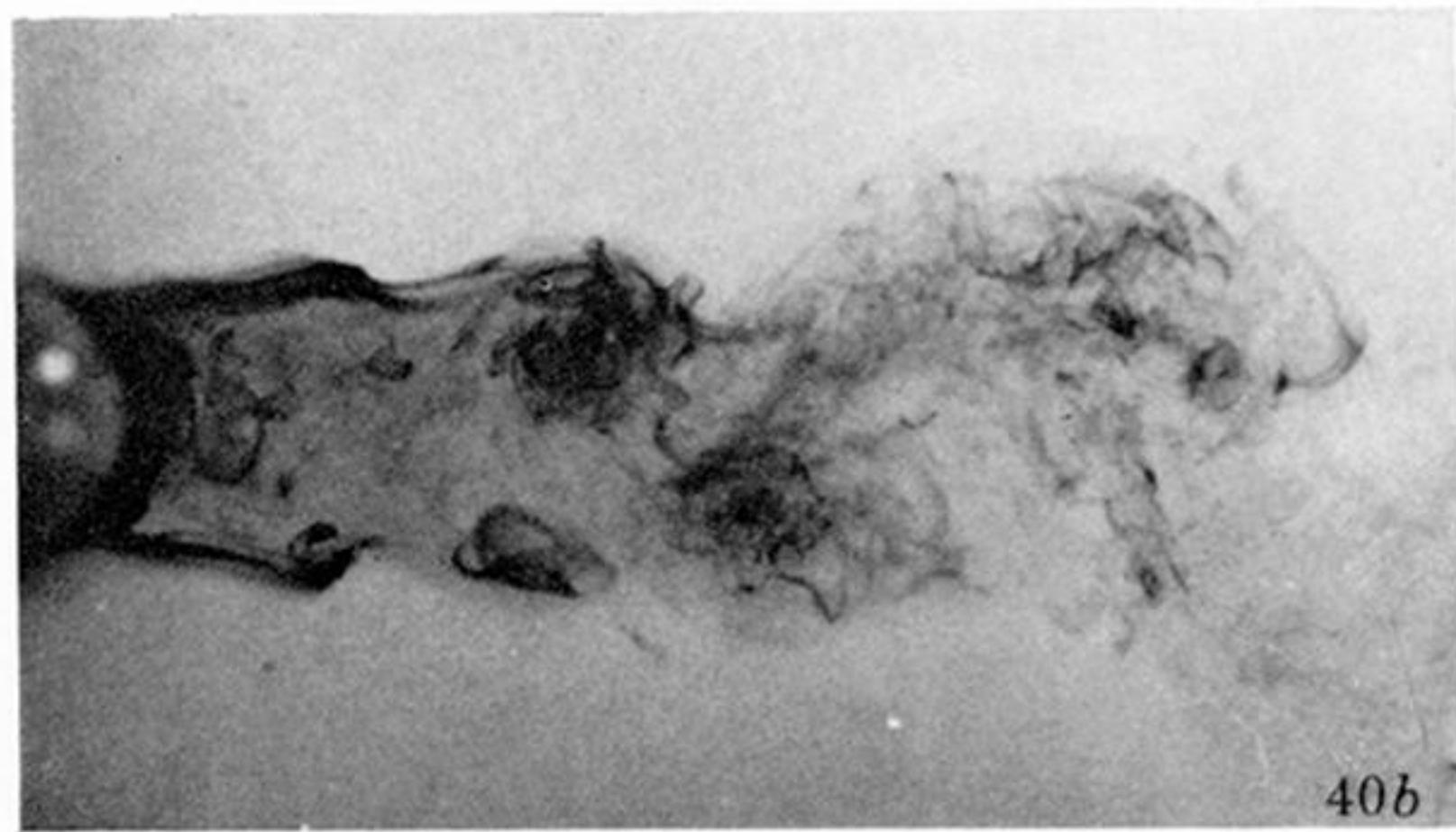
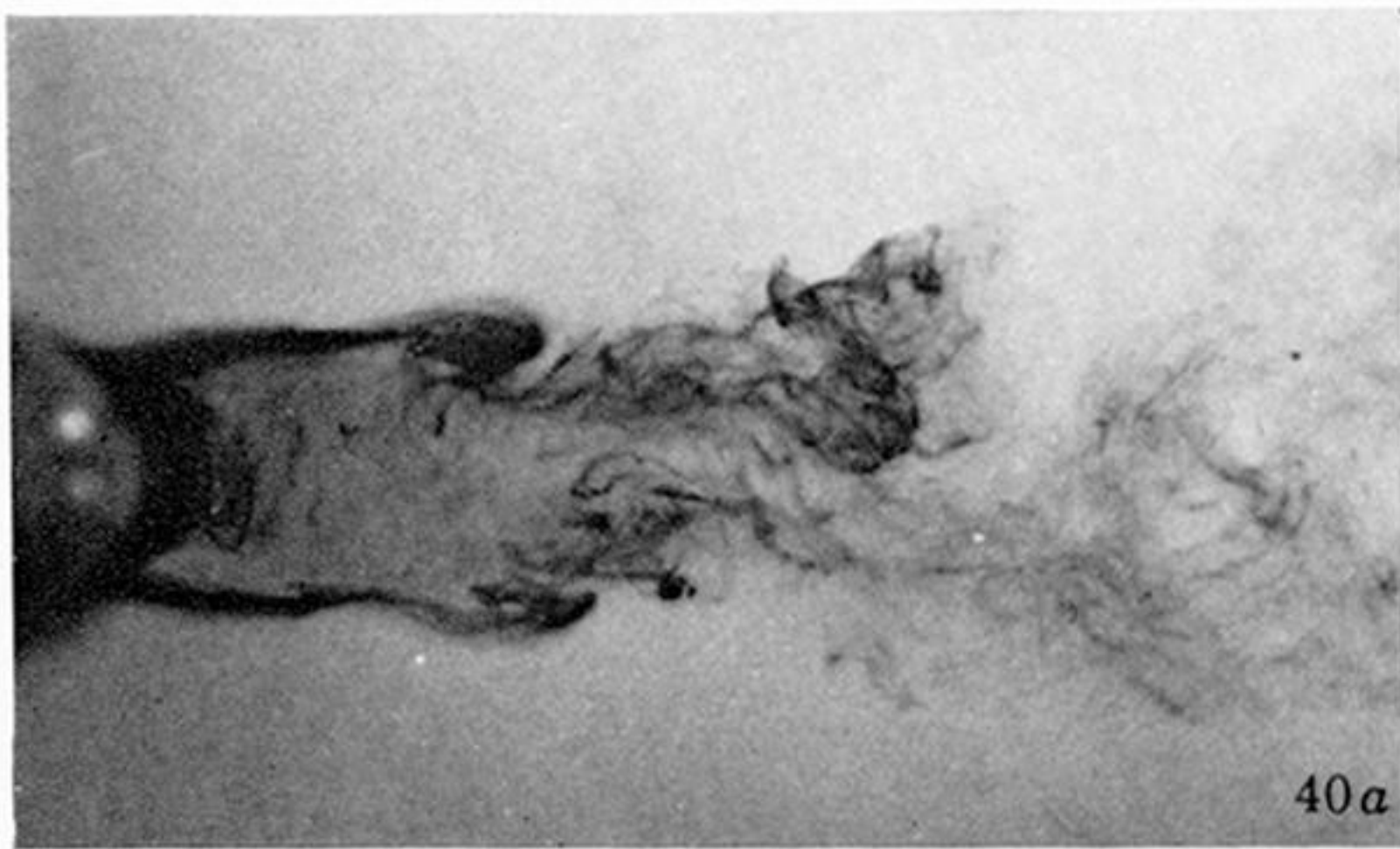


FIGURE 40. Transition waves at $Re = 1083$.

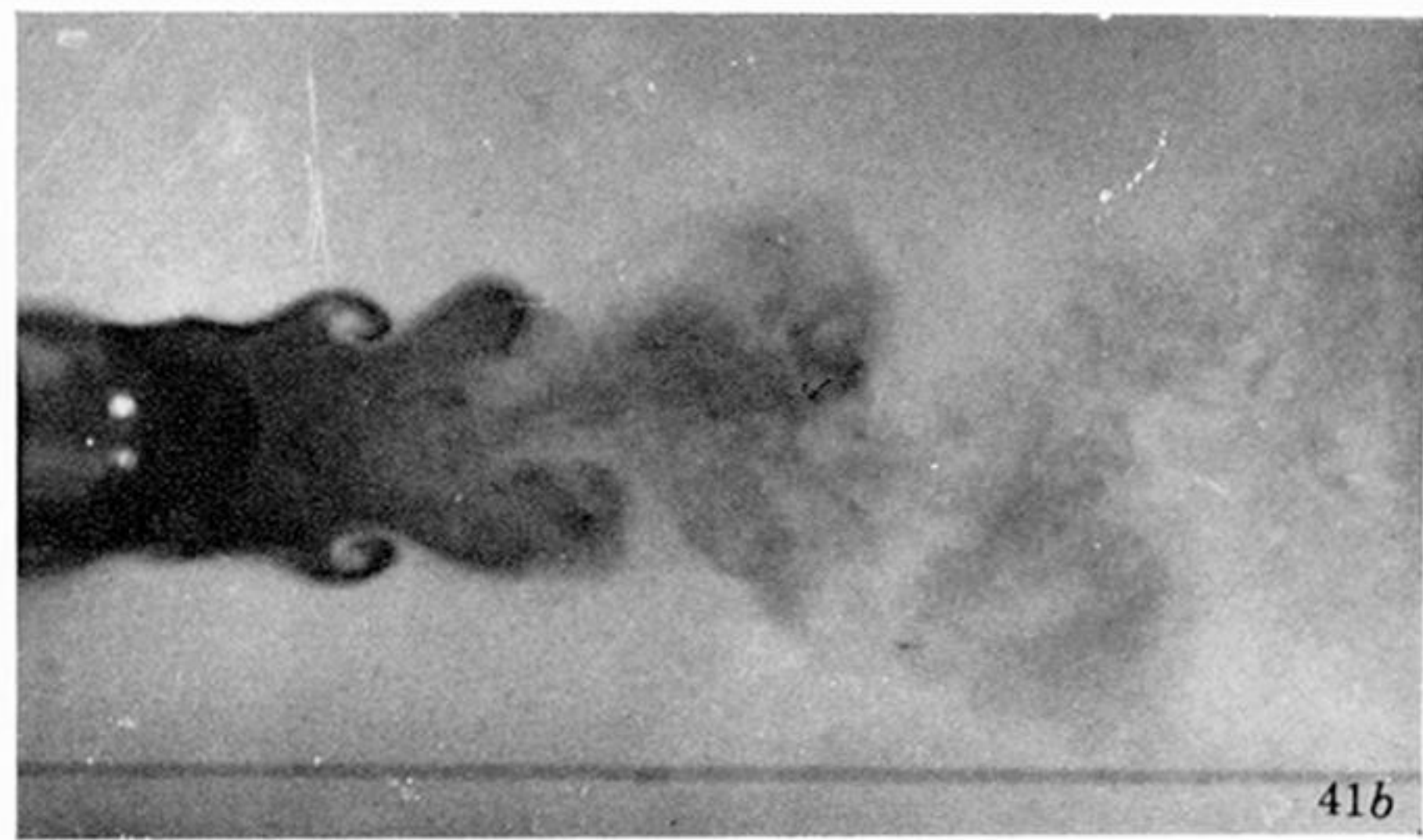
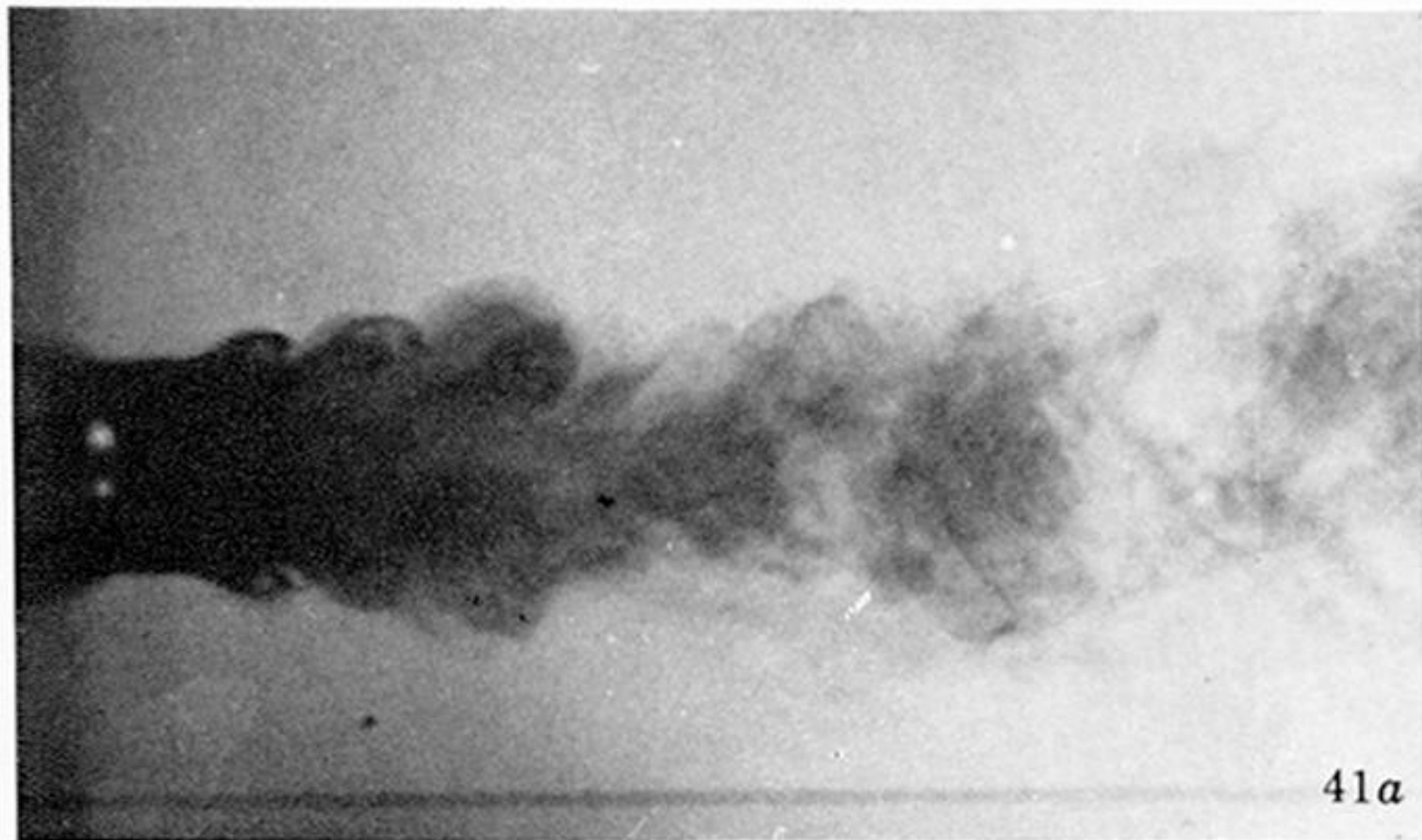


FIGURE 41. Transition waves at $Re = 1968$.

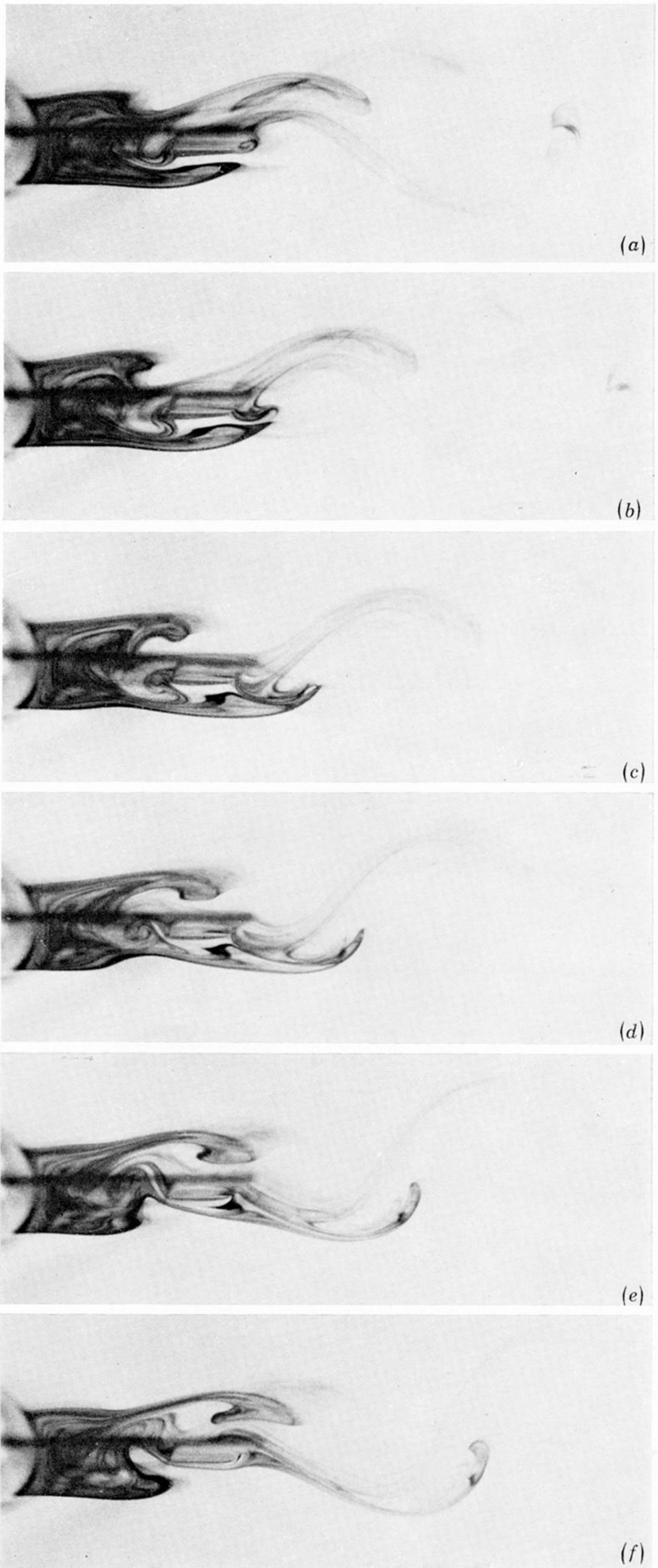


FIGURE 48. Consecutive equally spaced views of the wake of a circular cylinder with splitter plate with $g/d = 1.265$ at $Re = 166$.